

Lehrstuhl für Fluidmechanik und Prozeßautomation
der Technischen Universität München

State Detection and Feedback Control of the Anaerobic Wastewater Treatment Using Fuzzy Logic

Ernst Murnleitner

Vollständiger Abdruck der von der Fakultät Wissenschaftszentrum Weihenstephan für Ernährung, Landnutzung und Umwelt der Technischen Universität München zur Erlangung des akademischen Grades eines

Doktor-Ingenieurs (Dr.-Ing.)

genehmigten Dissertation.

Vorsitzender: Univ.-Prof. Dr.-Ing. K. Sommer

Prüfer der Dissertation: 1. Univ.-Prof. Dr.-Ing. habil. Antonio Delgado
2. Univ.-Prof. Dr.-Ing. Roland Meyer-Pittroff
3. Univ.-Prof. Dr.-Ing., Dr. h.c. Peter A. Wilderer

Die Dissertation wurde am 22. 11. 2001 bei der Technischen Universität München eingereicht und durch die Fakultät Wissenschaftszentrum Weihenstephan für Ernährung, Landnutzung und Umwelt am 21. 12. 2001 angenommen.

This thesis was published with the same title in the series 15, number 237 of the “VDI Fortschrittsberichte” (VDI proceedings) by VDI Verlag, Düsseldorf.

ISBN 3-18-323715-6

ACKNOWLEDGEMENTS

This thesis was made from 1997 to 2001 at the “Lehrstuhl für Fluidmechanik und Prozessautomation” at the “Technische Universität München”. My thank goes to all, who have supported me in this time.

Especially, I wish to thank my “Doktorvater” Prof. Dr.-Ing. Antonio Delgado, who made this work possible and who allowed me wide academic freedom. I also want to thank Dr.-Ing. Thomas Becker for the productive discussions and disputes. He also developed the core of the fuzzy logic system, which was used as basis in this work. I had also a lot of productive discussions with my colleague, Dipl.-Ing. Tomas Kurz.

I also wish to thank Walter Seidl and Sepp Rohrer who supported me in construction of the pilot plant, as well as Hans Bauer and Ralph Schmidt, who supported me in electrical affairs.

The pH controllers presented in this work follow directly from the master thesis of Dipl.-Ing. Tobias König. I also thank him for assistance in the PLC programming.

Special thank goes to Dipl.-Ing. Martin Grepmeier for cooperation in the experiments and for the COD analytics. I also wish to thank Dr.-Ing. Uwe Behmel, who suggested the controlling of a biogas plant by the use of Fuzzy logic.

I wish to thank Nicole Weber for the correction concerning the English language.

Further, I wish to thank Prof. Dr.-Ing. Meier-Pittroff and Prof. Dr.-Ing., Dr. hc. Peter Wilderer for their interest in my work and for their audit, as well as Prof. Dr.-Ing. Karl Sommer for taking the chair of the examination board.

This work would not have been possible without the knowledge about modelling, which I learned from Prof. Dr.ir. Sef Heijnen and Prof. Dr.ir. Mark van Loosdrecht at the Technical University Delft in the course of my master thesis.

Parts of this work were supported by the Bayerische Forschungsstiftung (AZ 216/96).

Last, but not least, I wish to thank all my colleagues at the LFP for the friendly climate I could experience there.

Freising, December 2001

Ernst Murnleitner

Meinen Eltern gewidmet.

For my parents.

TABLE OF CONTENTS

<i>Acknowledgements</i>	<i>III</i>
<i>Table of Contents</i>	<i>V</i>
<i>Nomenclature</i>	<i>VIII</i>
Units	VIII
Appreviations	VIII
Symbols	IX
Subscripts for Flows	X
Subscripts for Balances	XI
<i>Abstract</i>	<i>XII</i>
<i>Zusammenfassung</i>	<i>XIV</i>
<i>Publications</i>	<i>XVI</i>
1 Introduction and Conceptual Formulation	1
1.1 Initial Situation	1
1.2 State of the Art	3
1.3 The Scope of the Thesis	4
1.4 Reference to Other Theses	5
2 Relevant Aspects with Regard to the Thesis	6
2.1 Microbial Considerations	6
2.1.1 Hydrolysis and Acidogenesis	8
2.1.2 Acetogenesis and Methanogenesis	11
2.1.3 Sulphate Reducing Bacteria	13
2.1.4 Temperature and pH value	13
2.2 Process engineering aspects	15
2.2.1 One or Two Stage Process	15
2.2.2 Reactor types	16
2.3 Control Aspects	17
2.3.1 pH Control	18
2.3.2 Alternative Control Methods	19
2.3.3 Fuzzy Rulebase	20
2.4 Experimental Setup	25
3 Presentation and Discussion of the Results	28

3.1 Overall Concept	28
3.1.1 Sequential Controls and Subcontrollers on the PLC	29
3.1.2 Tasks on the PC	39
3.1.3 Conclusions	40
3.2 Development of the gas measurement system	41
3.2.1 Choice of Sensors	42
3.2.2 Integration of the Sensors	43
3.2.3 Validation of the Gas Test System	44
3.2.4 Conclusions	46
3.3 Development of the pH Controllers	46
3.3.1 Requirements for the pH controllers	46
3.3.2 Adaptive Controller for the Acidificaton Buffer Tank	47
3.3.3 PID Controller for the Methane Reactor	51
3.3.4 Conclusions	53
3.4 Development of the Fuzzy Logic Expert System	54
3.4.1 Structure of the Fuzzy System	54
3.4.2 Input values	60
3.4.3 Fermentation states	61
3.4.4 Global strategies	63
3.4.5 Output values	63
3.4.6 Conclusions	64
3.5 Experimental Validation of the Whole System	65
3.5.1 Conclusions	73
3.6 Modelling and Simulation	73
3.6.1 Requirements for the Simulation Model	73
3.6.2 Existing Models	74
3.6.3 General Strategy and Choice of Base Models	75
3.6.4 Development and Details of the Model	77
3.6.5 Validation of the Model	96
3.6.6 Conclusions	102
3.7 Validation by Simulation	103
3.7.1 Simulation of the Overload Experiment	103
3.7.2 Prediction of More Extreme Process Variations	107
3.7.3 Conclusions	110
4 Conclusions and Outlook	111
5 Materials and Methods	112
5.1 Reactor	112
5.2 Fixed Bed	114

5.3 Analytical Methods	114
5.4 Experiments and Simulations	115
5.4.1 Experiment E0	115
5.4.2 Experiments E1, E2, E3	115
5.4.3 Simulations S0, S1 and Substrate Peaks	115
5.4.4 Experiments K5, K7 and Simulations SK5, SK7	116
5.5 Online-Measurements and Data Logging	116
5.5.1 Calibration	116
5.5.2 Measurement Value Processing and Logging	117
5.6 Implementation of the Human Machine Interface	117
5.7 Implementation of the Fuzzy Logic Software	118
5.7.1 Rule parser	119
5.7.2 Fuzzy inference	120
5.8 Implementation and Tuning of the Controllers	122
5.8.1 Adaptive pH Controller for the Acidification Buffer Tank	122
5.8.2 PID Controller for the pH of the Methane Reactor	123
5.8.3 PID Controllers for the Temperature	124
Appendix	126
Derivation of the modified PID controller	126
Additional Figures	127
Simulation of pH-Step Function-Response of the Methane Reactor	130
Investigations about Replacement Methods for TOC or COD	131
Conductivity, pH and Volatile Fatty Acid Concentrations	133
Conversion of units	136
Volatile Fatty Acid Concentrations of Experiment E0	137
References	138

NOMENCLATURE

Units

If not mentioned otherwise, SI units are used, except for time and temperature where h and $^{\circ}C$ are used.

Gas concentrations in % or ppm are meant as volume/volume.

Appreviations

A/D	analogue to digital conversion
AF	anaerobic filter reactor (fixed bed reactor)
ANN	artificial neural net
ATP	adenosin triphosphate
BOD₅	biological oxygen demand (5 days)
C1	chemical or biological reactor 1 = acidification reactor
C2	chemical or biological reactor 2 = methane reactor
COD	chemical oxygen demand
COG	center of gravity
CSTR	continuous stirred tank reactor (ideally mixed reactor)
D/A	digital to analogue conversion
DC	direct current
DLL	dynamic link library (compiled computer code)
FB	function block
FBBR	fluidised bed biofilm reactor
Fd	ferredoxin, oxydised
FdH	ferredoxin, reduced
HMI	human/machine interface
KOP	ladder diagram (Kontaktplan)
IC	internal circuit reactor
IL	instruction list
LAD, LD	ladder diagram
MO	microorganism(s)
NAD	nicotinamide adenine dinucleotide, oxydised
NADH₂	nicotinamide adenine dinucleotide, reduced
OLE	object linking and embedding (a data exchange method)
ORP	oxido/reductivo potential
P&ID	piping and installation diagram
PC	personal computer
PCS	process control system
PFR	plug flow reactor
PD	proportional – differential controller
PI	proportional – integral controller
PID	proportional – integral – differential controller
PLC	programmable logic controller

QF	liquid test point for quality measurands
QG	gas test point for quality measureands
RIP	rulebased interpolation controller
SAK	spectral absorbance coefficient
STL	instruction list (statement list)
TOC	total organic carbon
UASB	upflow anaerobic sludge bed reactor

Symbols

a	specific surface	$\text{m}^2 \text{m}^{-3}$
A	surface	m^2
C_i	total concentration of component i	mol m^{-3}
$C_{i,c}$	total concentration of component i in compartment c	mol m^{-3}
$C_{in,i}$	concentration of component i in the inflow	mol m^{-3}
$C_{ini,i}$	initial concentration of component i	mol m^{-3}
$C_{in,i,c}$	concentration of component i in the inflow of compartment c	mol m^{-3}
$C_{ini,i,c}$	initial concentration of component i in compartment c	mol m^{-3}
$C_{X,i}$	concentration of component i degrading bacteria	mol m^{-3}
$C_{X,in,i}$	concentration of component i degrading bacteria in inflow	mol m^{-3}
$C_{X,ini,i}$	initial concentration of component i degrading bacteria	mol m^{-3}
$D_{f,i}$	diffusion coefficient of component i in the biofilm matrix	$\text{m}^2 \text{h}^{-1}$
d_h	hydraulic diameter	m
D_i	diffusion coefficient of component i in water	$\text{m}^2 \text{h}^{-1}$
$d_{X,i}$	decay/maintenance rate for component i degrading bacteria	h^{-1}
e	control deviation	
$f_{pH,i}$	pH dependency function	
f_{puffer}	factor for relative puffer capacity (pH controller)	
f_T	temperature dependency term	
h	reactor liquid level (fraction of filling level to full volume)	
H	height of reactor liquid level	m
H_i	partition coefficient according to henry's law	
I_j	non-competitive inhibition term	
$I_{nh4,pH}$	inhibition term for $\text{pH} > 7$ including ammonia toxicity	
$K_{a,i}$	dissociation constant of component i	mol m^{-3}
k_i	kinetic constant for degradation of component i	$\text{mol mol}^{-1} \text{h}^{-1}$
$K_{I,i,j}$	half inhibition concentration of component j on the degradation of component i	mol m^{-3}
$k_{Lg,i}$	liquid to gas mass transfer coefficient	m h^{-1}
$k_{Ls,i}$	liquid to solid mass transfer coefficient	m h^{-1}
K_i	Monod half velocity constant of component i	mol m^{-3}
K_p	proportional action coefficient (for PID controller)	
K'_p	proportional action coefficient, normalized for flow and concentration	mol h m^{-2}
K_w	ion product of water	mol m^{-3}
L	length	m
M_i	monod substrate limitation term	
$MI_{i,j}$	substrate limitation term of component i with competitive	

	inhibition of component j	
p	absolute pressure	bar
pH	pH value	
pH_{act}	actual pH value	
ΔpH_{inc}	expected increase of pH value due to control action	
pH_m	pH value, where maximum growth occurs	
pH_l	lower pH value, where inhibition is total	
p_i	partial pressure of component i	bar
Q	water or gas flow	$m^3 h^{-1}$
Re_h	dimensionless Reynold number using the hydraulic diameter	
s	thickness	m
Sc_i	dimensionless Schmidt number for component i	
Sh	dimensionless Sherwood number	
t	time	h
T	temperature	$^{\circ}C$
T_n	integral action time for PI and PID controller	h
T_u	dead time	h
T_v	derivative action time for PD and PID controller	h
u	hydraulic velocity	$m h^{-1}$
V	volume of liquid (plus bed) in the reactor or compartment	m^3
\dot{V}	circulation rate	$m^3 h^{-1}$
V_{lye_abs}	amount of lye which is added in a pH control action	m^3
V_{lye_rel}	amount of lye which is needed to increase pH of full reactor for 1 unit from current pH value	m^3
$Y_{e,i}$	yield enzyme per component i	$mol mol^{-1}$
Y_i	yield biomass per component i	$mol mol^{-1}$
z_{h2}	term, used for hydrogen inhibition	
$z_{h2factor}$	term, used for hydrogen inhibition	
α_i	enzyme saturation constant for degradation of component i	$mol m^{-3}$
ν	kinematic viscosity	$h m^{-2}$
ΔG°	reaction enthalpy at pH 7, 25 $^{\circ}C$ and molar concentrations.	$J mol^{-1}$
\emptyset	diameter	m
\emptyset_i	inner diameter	m
\emptyset_o	outer diameter	m

Subscripts for Flows

1	acidification buffer tank
2	methane reactor
circ	circulation
G	head space of reactor
L	lye vessel
l	lower compartment
m	medium compartment
O	outside reactors
u	upper compartment

Subscripts for Balances

in	liquid flow into the bulk liquid
out	liquid or gas flow out of a compartment
film	mass transfer between the bulk liquid and the biofilm
gas	mass transfer between the bulk liquid and the head space
hydrol	hydrolysis of complex substrate
growth	biomass formation
decay	decay and maintenance of biomass
form	formation of enzymes
conv	conversion of substrate

ABSTRACT

Anaerobic treatment of wastewater offers the advantage of the elimination of the main part of pollutants, which saves disposal charges. Compared to the aerobic technology, less sludge is formed, and energy is produced in the form of biogas. However, anaerobic treatment has also several drawbacks. These are the more difficult handling and the extreme long characteristic times, whereby particularly an overload can lead to a complete break-down of the plant. A restart takes weeks to months, which has restricted the user's acceptance compared to conventional aerobic plants. But using intelligent control systems can circumvent this problem. Up to now comparatively few control engineering is applied in the wastewater treatment. The controlled variables are mostly regarded in isolation, e.g. temperature and pH are held constant and controlled by a local controller. Connecting the particular measurands and manipulated variables, one can essentially increase the efficiency of wastewater treatment systems as well as the stability. Even though such controllers would be possible by using classical control engineering, the effort would be considerable due to its high complexity.

Therefore, Fuzzy logic (the classical Mamdani-type fuzzy rulebase) was chosen for state detection and control of the two-stage anaerobic wastewater treatment. A two-stage anaerobic wastewater treatment reactor system was modelled and controlled the way the biological state of the reactors could be predicted. Based upon this, proper control actions were enacted automatically. Even very strong fluctuations in the loading of both, concentration and volumetric flow rate, could thereby be handled successfully. Moreover, effluent concentrations could be kept relatively low without using TOC, COD or equivalent measurements.

In concrete, the engineering should be developed and tested on a lab scale plant using wastewater from the potato processing industry. As no existing plant meeting the requirements was available, particularly in consideration of the automation, a new lab scale plant was developed and constructed.

For further testing of the control system developed, a dynamic mathematical simulation model was used. For this, an existing model for an anaerobic digester was extended in order to be able to simulate the two-stage anaerobic wastewater treatment reactor system with biofilm. All the relevant measurands, like pH, hydrogen, methane, as well as the manipulated variables (flows, pH, temperature) of the controller are covered by the new simulation model. The model was validated with both sensitivity analysis and with experimental data. Sensitivity analysis points out the important parameters of the model. Connected with the fuzzy logic controller software, dynamic simulations were performed where the command variables were altered by the output of the fuzzy logic. Data from controlled and uncontrolled experiments could be reproduced satisfactorily by the use of the dynamic model.

XIII

Moreover, effluent quality could be improved by changing several fuzzy sets. Simulating different overload scenarios, the control system was able to detect overloads and thus to execute proper control actions.

ZUSAMMENFASSUNG

Die anaerobe Abwasserreinigung wird hauptsächlich eingesetzt, um den Hauptanteil der organischen Schmutzfracht aus Abwässern zu entfernen, wobei die Einleitergebühren gesenkt werden können. Im Vergleich mit der aeroben Abwasserbehandlung fällt weniger Überschuss-Schlamm an und zudem wird Energie, in der Form von Biogas, gewonnen. Jedoch weist die anaerobe Behandlung auch Nachteile auf, wie die schwierigere Handhabung und die sehr langen charakteristischen Zeiten. Insbesondere kann eine Überladung mit Nährstoffen zu einem Zusammenbruch des Systems führen. Ein Neuanfahren der Anlage dauert einige Wochen bis zu mehreren Monaten, was die Akzeptanz dieses Systems bei den Betreibern einschränkt. Dieses Problem kann jedoch gelöst werden, wenn intelligente Regelsysteme eingesetzt werden. Bisher wird noch relativ wenig Regelungstechnik in Abwasserreinigungsanlagen eingesetzt. Die Regelgrößen werden meist isoliert betrachtet, so werden zum Beispiel die Temperatur und der pH-Wert mit Hilfe eines lokalen Reglers konstant gehalten. Wenn die entsprechenden Meß- und Stellgrößen auf geeignete Weise verbunden werden, dann kann sowohl die Effektivität als auch die Stabilität von anaeroben Abwasserbehandlungsanlagen gesteigert werden. Obwohl solche Regelsysteme auch mit klassischer Regelungstechnik realisiert werden könnten, wäre der Aufwand auf Grund der großen Komplexität beträchtlich.

Deshalb wurde Fuzzy-Logik (die klassische Fuzzy-Regelbasis nach Mamdani) sowohl für die Zustandserkennung als auch für die Regelung für die zweistufige anaerobe Abwasserreinigung eingesetzt. Ein zweistufiges Abwasserreinigungssystem wurde in der Weise modelliert und geregelt, daß der biologische Zustand in den Reaktoren abgeschätzt werden konnte. Darauf aufbauend wurden geeignete Stelleingriffe automatisch durchgeführt. Sogar sehr große Schwankungen in der Konzentration und der volumetrischen Belastung konnten damit erfolgreich gehandhabt werden. Ausserdem konnte die Auslauf-Konzentration relativ niedrig gehalten werden, ohne daß Größen wie der chemische Sauerstoffbedarf (CSB) oder der gesamte organische Kohlenstoff (TOC) gemessen worden wären.

Konkret sollte die Technik an einer Anlage im Labormaßstab entwickelt und getestet werden. Da aber auf keine geeignete Anlage zugegriffen werden konnte, besonders in Bezug auf die Automation, wurde eine neue Anlage entwickelt und konstruiert.

Für weitere Tests des Regelungssystems wurde ein dynamisches mathematisches Simulationsmodell verwendet. Dafür wurde ein existierendes Modell für einen anaeroben Reaktor erweitert, um ein zweistufiges System mit Biofilm simulieren zu können. Alle relevanten Messgrößen, wie der pH-Wert, die Wasserstoff- und Methankonzentration, wie auch die Stellgrößen des Regelsystems (Durchflußraten, pH-Wert, Temperatur) wurden durch das neue Modell abgedeckt. Das Modell wurde

mittels einer Sensitivitätsanalyse und mit Hilfe von Daten aus Experimenten validiert. Die Sensitivitätsanalyse hebt die wichtigen Modell-Parameter hervor. Mit der Simulation, die mit der Fuzzy-Logik-Software verbunden wurde, konnten dynamische Simulationen durchgeführt werden, wobei die Führungsgrößen des Prozesses durch die Ausgangswerte der Fuzzy-Logik dynamisch festgelegt wurden. Daten von sowohl unregelmäßigen als auch von regelmäßigen Versuchen konnten mit dem Modell zufriedenstellend simuliert werden. Ausserdem konnte die Ablaufqualität in der Simulation verbessert werden, indem einige Fuzzy-Sets geändert wurden. Bei der Simulation von verschiedenen Überlastungs-Szenarien konnte das System die Überlastungs-Zustände erkennen und geeignete Stellmaßnahmen durchführen.

PUBLICATIONS

Paper in Refereed Journal:

Murnleitner, E., Becker, T., Delgado, A.: State Detection and Control of Overloads in the Anaerobic Wastewater Treatment using Fuzzy Logic. *Water Research* (2001), Vol. 36 (1), 201 - 211

Paper Submitted to Refereed Journal:

Optimisation and Validation of a Fuzzy-Based Closed-Loop Control Strategy Using a Dynamic Simulation Model. *Biotechnology and Bioengineering*. submitted.

Conference Papers:

Kurz T., Becker T., Fellner M., Schmitz M., Delgado A., Murnleitner E.: Cognitive Computing in Brewing Technology. - In: 7th European Congress on Intelligent Techniques & Soft Computing (EUFIT), Aachen, Germany, 13 -16 September 1999, 235 - 236.

Murnleitner, E., Becker T., Delgado, A.: Modelling and Control of the anaerobic wastewater treatment with fuzzy-logic. *Bioprocess Systems '99*, Sophia, Bulgaria, 18 - 20 October 1999, I45-I48.

Murnleitner, E.; Becker, T.; Delgado, A.: State detection and control of overloads in the anaerobic treatment of brewery wastewater using fuzzy logic. 28th International Congress European Brewery Convention, Budapest, Hungary, 12.-17.05.2001.

Other:

Murnleitner, E.; Becker, T.; Delgado A.: Verhinderung von Überlastungen bei der anaeroben Abwasserreinigung. *Der Weihenstephaner*, 68 (2000) Nr. 4, 97-100.

1 Introduction and Conceptual Formulation

The objective of this work is the development and control of an anaerobic wastewater treatment plant for the treatment of heavily polluted wastewater from the food processing industry. Through developing and using a Fuzzy logic expert system (fuzzy logic rulebase), the state is determined and proper automatic control actions are carried out subsequently. Hence it is possible to utilise wastewater (in order to clean it or to gain energy) with highly variable composition, concentration and volume. The new control system was validated by means of laboratory scale experiments and a dynamic simulation model. Hence also an extensive simulation model, which was able to simulate all the relevant state variables of the fuzzy logic system, was developed.

1.1 Initial Situation

Due to on-going industrialisation and urbanisation, more and more wastewater is introduced into the waters, whereby the self-cleaning potential is often exceeded. Therefore, boundary values for introducing into the waters, which are tightened more and more, were released by the governments. Measures for wastewater treatment become even more difficult for complying with these regulations. Wastewater from industry is often polluted heavily, whereby the load can vary considerably over a period of time. In many cases, it is macro-economically advantageous to clean this special wastewater with a technology that is optimised for it instead of cleaning it in an urban wastewater treatment plant together with other sewage waters. Raising charges for polluted industrial effluents favour the installation of a pre-treatment for many plants. While the removal of the major part of the pollution is mostly economical and reasonable, this is not the case for cleaning to direct discharge levels, because the degradation is represented by a first order reaction. Thus, degradation of low concentrated wastewater takes a relatively long time.

Still, the pre-treatment and the final-treatment in urban wastewater plants is mostly made aerobically, which is due to the less difficult handling compared to anaerobic techniques. Yet the anaerobic treatment gains more and more importance. Advantages compared to the aerobic techniques are:

- Less need of energy, because no oxygen has to be introduced into the liquid.
- Usable energy is produced in the form of biogas.
- Substances which cannot be degraded aerobically can be decomposed, e. g. Pectin.
- Much less surplus sludge is produced (typically one tenth).

- Fewer nutrients are necessary, because less biomass is produced.

But there are also several drawbacks of the anaerobic treatment:

- Most of the time the concentration in the effluent is higher compared to the aerobic process.
- The process is less stable.
- Higher time constants due to the small growth rates.

Due to these characteristics, the anaerobic wastewater treatment is suitable best for the pre-treatment of heavily polluted industrial wastewater, whereby the amount of energy, which is produced from the biogas, can be much higher than what is needed for the process.

Thus, the production of energy is sometimes even the main motivation of building such plants. Particularly in recent times, biogas plants are sometimes only constructed in order to produce energy from organic waste or even from plants which are planted only for energy production, as in some countries of the European Union rather high prices can be achieved for the energy produced (e.g. EUR 0.10 per kWh in Germany).

Mostly a full treatment is not intended, because the effort for reaching very low effluent concentrations rises more than proportional, and moreover, the effluent is lead into a municipal sewage treatment plant. For direct discharge more limit values had to be adhered, e.g. phosphate and ammonia, which is not economic for individual undertakings.

If the process is running non-controlled, relevant variations of the load and subsequently also damage of the biomass is not detected, which can lead to a complete break-down of the anaerobic process. Sometimes overloaded reactors have to be emptied completely. The time span from the restart until the reaching of the full performance can last several weeks or even months, which is due to the low growth rates of the involved microorganisms. During this time not the full waste stream can be treated and therefore it flows into the sewer untreatedly. If the plant is mainly used for production of biogas, energy cannot be produced as usually and cannot be sold; it even has to be bought in addition.

Using of intelligent controllers or permanent support by qualified staff could circumvent the drawback of the lower process stability. For trained staff is often not available or the expenditures are too high for small companies, it is possible to make human expert knowledge effectively available by the use of cognitive methods in order to achieve the aims, which will be defined later (sub-chapter 1.3).

1.2 State of the Art

Compared to aerobic metabolism, microorganisms gain much less energy in anaerobic metabolism in relation to the amount of consumed substrate. Thus, growth of biomass occurs relatively slow, and generation times are long (e. g. maximal growth rate of butyrate degraders is 100 hours). In order to gain higher degrading rates, an accumulation of biomass is necessary, which is achieved by the use of several miscellaneous process concepts. These are the following:

- mixed reactor with phase separation and biomass recycling
- immobilisation of the microorganisms by means of a carrier (fixed bed reactor, floating bed reactor)
- aggregation of the microorganisms by formation of pellets or flocks (sludge bed reactor, internal circuit reactor)

Depending on the requirements, all these reactor concepts are used in practice. However, the problem of an overload is common to all these concepts, except for minor variations in the waste load. Hence support of qualified personal is necessary, which makes such plants uneconomical for smaller companies. Only in recent years attempts were made to avoid this problem by the use of more control engineering. But the main problem is detection of the state of the process. By the use of common measured quantities, like pH value, methane concentration in the biogas, rate of gas production, and not so common, chemical oxygen demand (COD) or total organic carbon (TOC), hardly any satisfying prediction of the state can be made or can be made with big temporal delays only (Kaiser, 1993). Moreover, the online measurement of COD or TOC is relatively expensive and also needs much maintenance. In recent years, measurement of the hydrogen concentration has been considered by many authors (Archer et al, 1986; Pauss et al, 1993; Tartakovsky and Guiot, 1997; Guwy et al, 1997) to be expressive and without long delays in relation to the process state. However, although there is strong evidence that the hydrogen concentration is an excellent parameter, it is hardly measured and used in practice. There are only few applications with control systems using hydrogen values (Archer et al, 1986; Müller et al, 1997) and no big scale applications are known. In real world applications mostly the pH and the temperature are controlled, whereby the command variable is usually kept constant. Austermann-Haun et al (1993) suggests controlling the circulation rate depending on the pH value for fixed bed reactors. However, such local control strategies are not apt for an efficient optimisation and control (Steyer et al, 1997). Supervisory strategies, which combine the individual local values, are needed. Hence, control systems have been developed recently, which mostly use the fuzzy logic, sometimes in connection with artificial neural nets (ANN) (Steyer et al, 1997;

Pöppinghaus et al, 1994). Through the use of such systems, the state of the process can be predicted more or less reliable and sufficient. Steyer et al (1997) features fault diagnosis, whereby an attribute vector which is then classified as dangerous or harmless using an ANN is calculated using fuzzy logic.

Estaben et al (1997) controlled a fluidised bed reactor by using only the pH value and the gas flow rate, together with their derivatives in time, in order to keep the gas production rate constant.

Müller et al (1997) calculated the fermentation state from the hydrogen concentration in the biogas and the production rate of the biogas, both from a pretaster, using fuzzy clustering (Fuzzy C-means). The feed rate into the digester is controlled with fuzzy logic rulebase according to the state. As the two latter systems depend mainly on the gas flow rate, problems will arise, if no feed at all occurs for a certain period of time, as it would be the case for a stand-alone biogas reactor for batch production effluents. Furthermore, verifications were made with small overloads only.

1.3 The Scope of the Thesis

In order to utilize the whole capacity of anaerobic wastewater-treatment plants and to avoid overloads which could lead to a break-down, the efficient fixed bed process should be combined with a control system based on fuzzy logic.

In concrete, the engineering should be developed and tested on a lab scale plant using wastewater from the potato processing industry, whereby the upscale to the practice should be possible and relatively simple. As no existing plant which met the requirements, was available, particularly in consideration of the automation, the plant had to be developed and constructed. The wastewater loading profile and composition are considered as difficult, as there was no wastewater stream at the weekend and the organic load was expected to be between almost zero and more than 5 kg m^{-3} COD. Moreover, the investment should be kept small through the construction of a relatively small plant in relation to the wastewater stream. For the same reason, i.e. the capital expenditure, no expensive and maintenance-intensive analysis systems should be used. An extensive automation was necessary in order to reduce maintenance by human beings and to economize the system for smaller companies

The following tasks were necessary in order to meet the requirements:

- Establishing of the process-engineering concept
- Planning and construction of the lab scale pilot plant
- Automation of the plant

- Development of the fuzzy logic expert system
- Creation of the HMI interface
- Online-test of the control system
- Development of a computer simulation model
- Offline-test by means of the computer simulation

1.4 Reference to Other Theses

The scope of this thesis was the development of the control system, starting with the development of the reactor concept and ending up with an experimental and theoretical validation.

In the doctor thesis “Experimentelle Untersuchungen an einer zweistufigen fuzzy-geregelten Abwasserreinigungsanlage mit neuartigem Festbettmaterial” (Experimental investigations using a two-stage fuzzy-controlled wastewater treatment plant with novel fixed bed material) of Martin Grepmeier (2002), this control system is applied by means of a real time dependent course of the wastewater inflow. He also investigates the performance of the fixed bed material (mat of coconut fibre), which was used in this work.

2 Relevant Aspects with Regard to the Thesis

In order to be able to develop a capable reactor configuration with a sophisticated control system and also for the development of a simulation model, some aspects have to be regarded more in detail. Thus, microbiology and reactor concepts are discussed in this chapter in detail. Also, different control algorithms are discussed, and a short introduction into fuzzy logic is given. At the end of this chapter, the experimental setup chosen is introduced.

2.1 Microbial Considerations

In contrast to the aerobic wastewater treatment, where the particular families of bacteria degrade the pollutants in parallel, in the anaerobic process the different bacteria degrade them successively. The anaerobic processes are usually divided into four steps: hydrolysis, acidogenesis, acetogenesis, and methanogenesis (Figure 1). As the end product of one species serves as substrate for the other species, accumulation of metabolic products can lead to inhibitions or even to a breakdown of the process. Therefore, a basic understanding for the particular processes is necessary in order to achieve an efficient wastewater treatment in respect to both the process engineering and the control engineering. Such knowledge is also necessary in order to create or adapt a simulation model of the process, which in turn helps to better understand and control the process.

Not only the sequential flow of the metabolic steps, but also the lesser yield of energy identifies the anaerobic process. From there less biomass can be obtained from the same amount of substrate or more substrate has to be degraded in order to keep the same biomass alive, respectively.

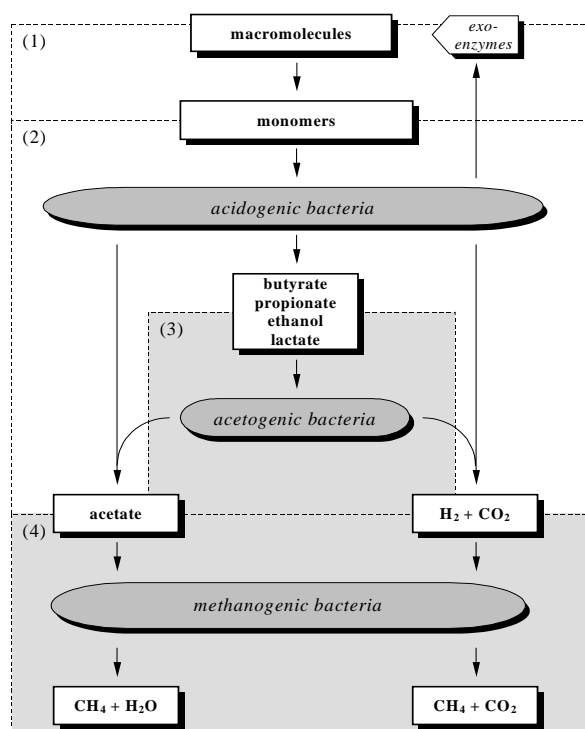


Figure 1. Scheme of the anaerobic digestion - (1) hydrolysis, (2) acidogenesis, (3) acetogenesis, (4) methanogenesis. (1) and (2) usually occur in the acidification reactor, (3) and (4) in the methane reactor.

As well for the aerobic as for the anaerobic process, polymers have to be degraded first since bacteria cannot absorb them directly because they are too large in order to be able to pass the cell membrane. Many bacterial species, which, in case of the anaerobic process, belong mostly to the *Clostridia* family (Schlegel, 1992), are able to excrete enzymes, which degrade the polymers into monomers. This step is called hydrolysis (step 1).

Monomers can then be consumed by most of the bacterial consortium. In this process reduced compounds (NADH_2 ¹, FdH) are generated, which in turn need to be regenerated.

In presence of inorganic electron donors (like oxygen and nitrate) they could be regenerated via the oxidative carboxylation chain (Mitchel, 1966; Schlegel, 1992), whereby much ATP (36 to 38 molecules ATP per molecule of glucose), which is used by many energy consuming reactions inside the cells, can be generated and finally, carbon dioxide and water is produced as metabolic end products.

However, in anaerobic systems, where those electron donors are not present, the reduced metabolic intermediates (NADH, FdH) cannot be used for transfer to oxygen with production of energy and need to be regenerated in another way. While many anaerobic bacteria can release elemental hydrogen from FdH, all the NADH, and the FdH in bacteria not capable of hydrogen release, have to be transferred to an acceptor molecule (mostly pyruvate). Figure 2 shows one possible way of anaerobic degradation of glucose (Schlegel, 1992).

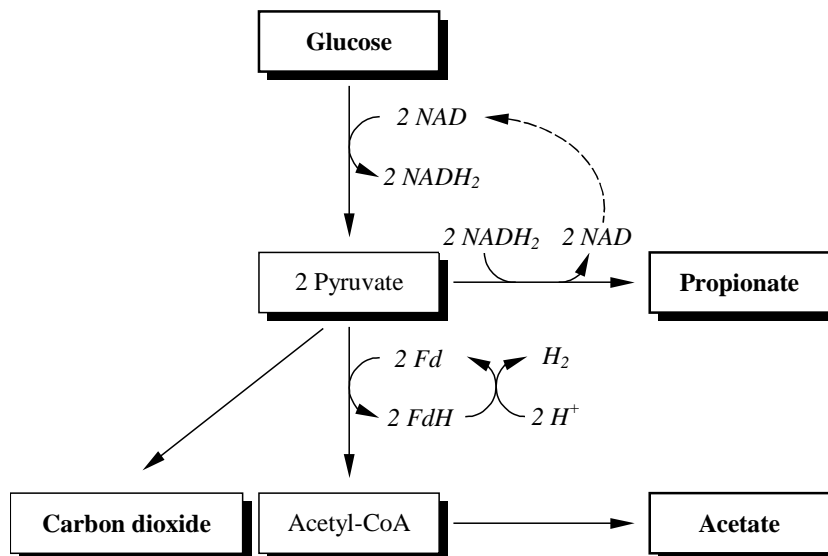


Figure 2. Conversion of glucose into propionate, acetate, carbon dioxide and hydrogen by some *Clostridia* species. Fd: Ferredoxin.

¹ NAD^+ and $\text{NADH}+\text{H}^+$ are represented electroneutrally (NAD , NADH_2)

First, glucose is degraded to pyruvate (glycolysis), whereby two molecules of NAD are reduced. As the NADH_2 need to be regenerated, propionate is formed from half of the pyruvate. The remaining pyruvate is decarboxylated whereby acetate and carbon dioxide is formed. In this step Ferredoxin, which can be regenerated by releasing of hydrogen, becomes reduced. Here, hydrogen release is possible, because of the low redox potential (= high energy content) of Ferredoxin.

The degradation of monomers (mainly glucose) is called acidification as the products of this step (2) are mainly acids or their salts, like acetate, propionate, butyrate, lactate, formate, valerate and thus the pH drops. Other products formed are the gases carbon dioxide and hydrogen and alcohols like ethanol and propanol.

No bacteria is known degrading monomers, like glucose, amino acids and higher fatty acids directly to the most reduced and oxidised product possible, which are methane and carbon dioxide, respectively. Even not most of the end products of step 2 (acidification) can be directly degraded to methane. Therefore a third step (acetogenesis), where the acidification products are converted to acetate, carbon dioxide, hydrogen and methanol is necessary, as only these four substances can be consumed by methanogenic bacteria.

Finally, acetate, hydrogen and carbon dioxide (methanol is hardly present) are converted into methane and carbon dioxide by Methanobacter, Methanococcus and Methanosarcina (step 4). Regarding the whole system, the production of carbon dioxide and methane is favourable, as these products leave the system as gas and thus cannot inhibit the reactions.

Some aspects of these 4 steps, which are relevant for the engineering, control and modelling, are discussed more in detail.

2.1.1 Hydrolysis and Acidogenesis

The three relevant substance groups, which play an important role in the nutrition of leaving organisms, are carbohydrates, proteins and lipids. As these substances are too large to pass the cell membranes, they are degraded by enzymes into smaller units, the monomers. In order to break down the polymers, some acidogenic bacteria excrete hydrolytic enzymes, which degrade the polymers into monomers. But not only these excreting bacteria profit from the monomers, they are also utilised by the other acidogens.

Fat (lipids) contains a glycerol molecule, which is esterified with up to three long chain fatty acids. Lipases convert lipids to long-chain fatty acids. *Clostridia* and the *micrococci* are responsible for most of the extracellular lipase produced. The long-chain fatty acids produced are further degraded by β -oxidation to produce acetyl-CoA.

Proteins are synthesised from the 21 essential amino acids. Proteins are hydrolysed to amino acids by proteases, secreted by *Bacteroides*, *Butyrivibrio*, *Clostridium*, *Fusobacterium*, *Selenomonas*, and *Streptococcus*. The amino acids produced are then degraded to fatty acids such as acetate, propionate, and butyrate, and to ammonia as found in *Clostridium*, *Peptococcus*, *Selenomonas*, *Campylobacter*, and *Bacteroides*.

Carbohydrates (polysaccharides) consist of sugar molecules, mostly glucose. Polysaccharides such as cellulose, starch and pectin are hydrolysed by cellulases, amylases, and pectinases.

As glucose is the main monomer, its metabolism will be discussed more in detail. The introductory step in the glucose metabolism of the acidogenic (fermentative) bacteria follows mostly the Embden-Meyerhof-Parnas pathway, called glycolysis (Schlegel, 1992). In its course, hydrogen is splitted off and transferred to the coenzyme Nicotinamide-Adenin-Dinucleotide (*NAD*), creating pyruvate.



As much *NAD* is needed in this reaction, it is necessary to regenerate the *NADH*₂ in order to keep the metabolism alive. Further fermentative steps thus have to be considered under the viewpoint that a regeneration of *NADH*₂ is possible. Often, the hydrogen is transferred to pyruvate or the acetyl-CoA, which is formed successively from pyruvate.

Acetyl-CoA is formed in two common pathways.

Aerobic and facultative anaerobic bacteria use the pyruvate dehydrogenase multienzyme complex whereby *NADH*₂, from which the hydrogen needs to be transferred to another molecule for regeneration, is generated.

Strictly anaerobic bacteria like Clostridia use the pyruvate:ferredoxin-oxidoreductase whereby *FdH* is generated. As the redox potential of *FdH* is –420 mV (biological frame of reference, pH 7) gaseous hydrogen can be formed.

Many of these anaerobic bacteria (e.g. *Ruminococcus albus*) can even release hydrogen from the *NADH*₂, as they have the enzyme *NADH*₂:ferredoxin-oxidoreductase. Here, the hydrogen is transferred to four *Fd* and subsequently released from the four *FdH* (Figure 3). As the ORP of *NADH*₂ is –320 mV and the equilibrium is unfavourable for the formation of gaseous hydrogen, this reaction can only work if the **hydrogen partial pressure is low**. Therefore, these bacteria live in symbiosis with methanogenic bacteria which consume the hydrogen and, therefore, the concentration can be kept low (interspecies hydrogen transfer).

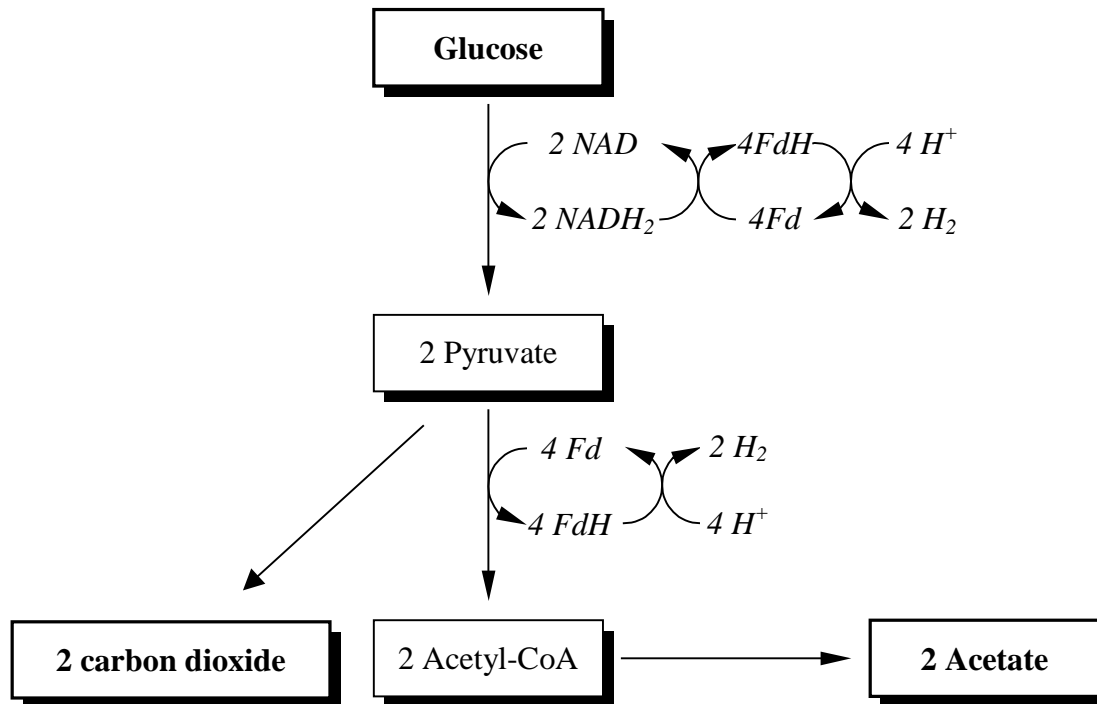
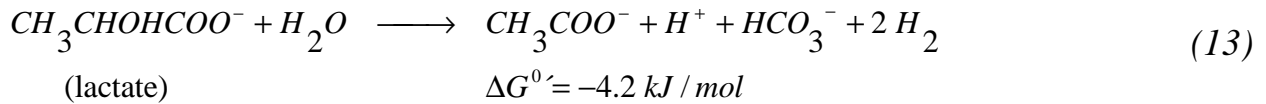


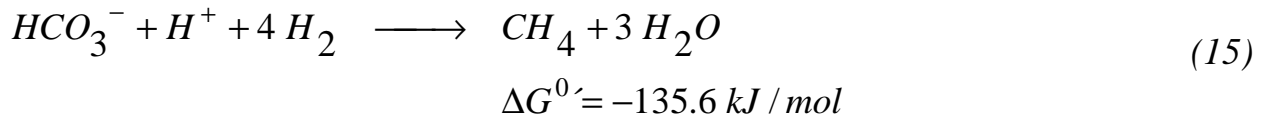
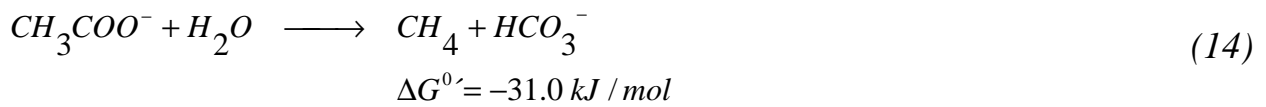
Figure 3. Homofermentative acetate formation from glucose by *Ruminococcus albus*.

It depends on the composition of the substrate and on the microbial consortium, which fermentation products are formed. Different species often produce different fermentation products from the same substrate. To give an example, *Propionibacter* produces propionic acid from glucose, while *Escherichia coli* produces a mixture of ethanol, succinate, lactate, acetate, formate, hydrogen, and carbon dioxide. It is not well known under which conditions particular bacteria are favoured. Some authors suggest the pH value as important selective parameter (Hwang and Hanson, 1997). It is well known that at pH values of 4 and lower, only yeasts and lactic bacteria can grow. Therefore ethanol and lactic acid will be formed at low pH. Some authors suppose that hydrogen plays an important role in the selection of the microorganisms. At low hydrogen partial pressure mainly acetate, at higher hydrogen pressure more ethanol, butyrate and finally propionate is produced (in this sequence) (Wolin, 1976; Schlegel, 1992; Jian et al, 1997). Other authors state, that the ratio of the fermentation products does not vary much (v. Münch et al (1999), Kalyutshni et al (1997)).

The influence of the particular parameters on the acidification is difficult to investigate, as many more different acidogenic reactions are possible and as the produced fermentation products of one species can work as a substrate for another. As an example, ethanol can not only be formed by acidification but also by the reduction of acetate. The most common acidogenic reactions are given in eqs. 2 – 9. The acids are given in the protonised form as these reactions often occur at low pH values (in the acidification reactor).



The reaction enthalpies show that these reactions are endergonic or only slight exergonic. Therefore, growth of acetogenic bacteria depends on the removal of the fermentation products. This is achieved by symbiosis of the acetogenic and the methanogenic bacteria (*Methanobacterium*, *Methanobrevibacter*, *Methanococcus*, *Methanomicrobium*, *Methanogenum*, *Methanospirillum*, *Methanosarcina* etc.), whereby the latter consume the hydrogen which is produced by the former ones. Methanogenesis occurs in two paths (eqs. 14 and 15).



Hereby, $\Delta G^{0'}$ denotes the reaction enthalpy at pH 7, 25 °C and molar concentrations.

Most methanogenic bacteria can utilise both paths. As can be concluded from the enthalpies, the consumption of hydrogen and hydrogen carbonate is favoured to the utilisation of acetate. Thus, hydrogen can be removed until smallest concentrations are achieved, as long as the methanogens are not affected by unfavourable conditions like an inhibition by propionate or a pH value less than 6. Beneath pH 6 usually no methanogenesis occurs as only one methanogenic species can grow at a lower pH value (*Methanosarcina*).

As acetogenesis only occurs at low hydrogen partial pressures and as methanogenesis becomes endergonic at too low hydrogen partial pressure, this reaction system is only possible in a small thermodynamic gap. Concerning the anaerobic degradation of propionate this is particularly small. Figure 4 shows the enthalpies of degradation of propionate (eq. 11) and methanogenesis (eq. 15) according to the law of mass conservation (eq. 16; Kiupel, 1997).

$$\Delta G' = \Delta G^{0'} + R \cdot T \cdot \ln \frac{[C]^c \cdot [D]^d}{[A]^a \cdot [B]^b}, (16)$$

while A and B are the educts and C and D are the products of the reactions, a to d are the stoichiometric coefficients.

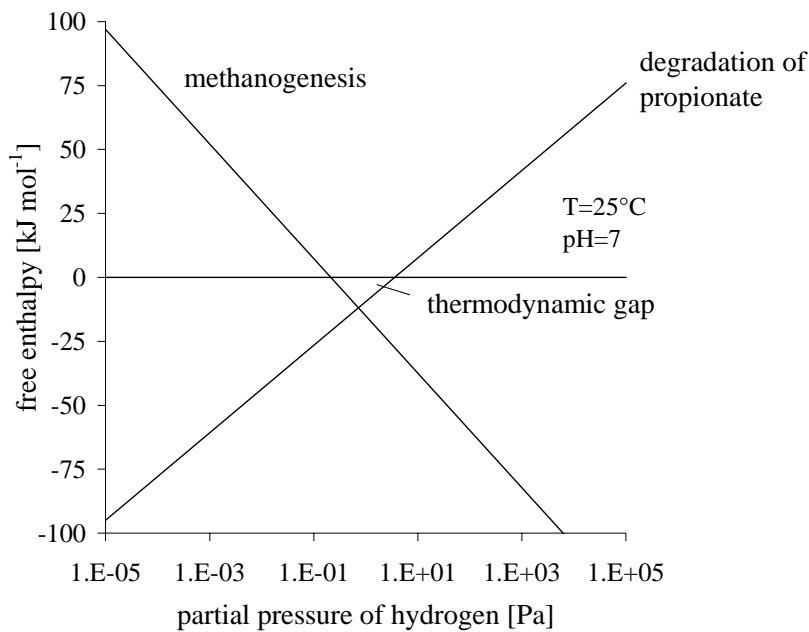


Figure 4 Enthalpy of the methanogenesis and the propionate degradation in relation to the hydrogen partial pressure according to the law of mass conservation. Concentration of the other educts and products is 1000 mol m^{-3} .

In practice, the degradation of propionate is therefore often the limiting step in the anaerobic wastewater treatment. Furthermore, propionic acid inhibits methanogenic bacteria and thus even more hydrogen is accumulated which in turn inhibits degradation of propionate.

In practice, a degradation of propionate also occurs at relatively high partial pressure ($> 100 \text{ ppm}$) which is certainly due to a concentration gradient within the biofilm. Acetogens and Methanogens grow more interiorly while acidogens grow externally or in the bulk liquid, mostly in a separate reactor. Therefore, a high hydrogen concentration does not stop acetogenesis in any case.

2.1.3 Sulphate Reducing Bacteria

Methanogenic bacteria are not the only species which are able to consume hydrogen, but also the obligate anaerobic sulphate reducing bacteria (= desulphuricants or sulphidogenic bacteria) can grow using hydrogen. *Desulfovibrio* and *Archaeoglobus* belong to this group amongst many others.

As these bacteria play an important role only if the wastewater contains much sulphate, they are not discussed in detail.

2.1.4 Temperature and pH value

Temperature and pH value are important parameters, which easily can be influenced in a bioreactor. All the bacteria groups discussed before have species

which grow at different **temperatures**. The whole methanogenic process (from hydrolysis to methanogenesis) is known to work from 5 to more than 65 °C (Ndon and Dague, 1997; Kettunen and Rintala, 1997).

In the case of increased temperature, chemical reactions can proceed faster. Thus, cells should grow faster as temperature is raised. However, there is a limit beyond which temperature-sensitive macromolecules such as proteins, nucleic acids, or lipids will become denatured, and therefore non-functional. There is also a minimum temperature for growth, below which the lipid membrane is not fluid enough in order to function properly. In general, organisms can grow at a temperature range of 30 to 40 °C. However, species differ in range, and four categories have been delineated on this basis. **Mesophiles** have optimal growth temperatures within the range of 20-50 °C; that is the most common temperature on the earth's surface or in animals. **Psychrophiles** have optimal temperatures below 15 °C. These organisms are killed by exposure to room temperature. They function at low temperature by having high contents of unsaturated fatty acids in their membranes. These molecules remain fluid at temperatures where membranes containing saturated fatty acids are non-functional. **Psychrotrophs** grow fastest at temperatures beyond 20°C but are capable of slow growth at refrigerator temperatures. Organisms that grow best beyond 50°C are **thermophiles**. Some bacteria can grow up to temperatures where water boils; those with optimal growth temperatures beyond 75 °C are called **extreme thermophiles**. Most of these are Archaea. Thermophiles contain proteins and lipids that are not denatured at the those high temperatures where they grow. Most anaerobic wastewater treatment plants are operated within the mesophile temperature range. Sometimes however no heating is applied (psychotrophic) or a temperature of around 55 °C is adjusted (thermophilic).

Temperature dependency of non-adapted microbial community of the methane reactor can be described with an Arrhenius-derived model (Kettunen and Rintala, 1997), where the activity becomes about half per 10 degrees of decrease.

Most microbes grow somewhere within the **pH** range of 5 to 9 as most natural environments fall into this range. The influence of the pH value on the activity of microorganisms cannot be easily identified as the pH influences also the dissociation of inhibitory substances like weak acids (e.g. propionic acid) and bases (e.g. ammonia). Therefore, organic acids and hydrogen sulphide become more toxic at decreasing pH while ammonia becomes toxic at increasing pH.

The acidogenic group includes many different species, thus the temperature range where hydrolysis and acidification takes place is also wide. Lactic acid producing bacteria can grow even at pH values below 4. However, acidification is expected to be best at pH > 4.5 and acetogenesis and methanogenesis at approximately 6.5 to 8 (Braun, 1982; Ghaly, 1996; Kalyuzhuyi and Davlyatshina, 1997). Although there exists one methanogenic species (*Methanosarcina*) which grows at pH 4.5, mostly no methane formation occurs at pH values below 6.

2.2 Process engineering aspects

One task of this work was the development of the reactor system. Hence this chapter

- shows the difference between one and two stage process and
- introduces the most important reactor types.

2.2.1 One or Two Stage Process

Hydrolysis and acidogenesis are carried out by fermentative bacteria (acidogens), which show relatively high growth rates and which do not need such a small pH range as the methanogens. The successive steps, acetogenesis and methanogenesis, occur in symbiosis, only show small growth rates and cannot be separated from each other.

Due to the different demands and characteristics of the participating bacteria groups, anaerobic wastewater treatment plants often consist of two stages, whereby in the first, the acidification reactor, the degradation occurs down to the acids. In the following methane reactor the conversion into acetic acid and production of methane occurs. Hence a spatial separation is made in the two stage process in order to adjust the environmental conditions to the different groups of bacteria.

Compared to the one-stage process, different fermentation products are formed. Hence, using only one reactor for all the processes, due to the interactions between the bacteria, only acetate is produced as intermediate product as far as no overload or inhibition occurs. However, in overloaded situations the hydrogen partial pressure can increase and thus the production of propionate is forced or its degradation inhibited, whereby primarily propionate and butyrate are accumulated. Finally the process breaks down due to inhibitory effects of propionate or due to a decrease of the pH value.

Much propionate, butyrate, ethanol or lactate is produced or not consumed in the first stage of the two stage process (acidification), which is due to the higher hydrogen partial pressure or lower pH value. Degradation of these products can be achieved optimally in the second stage (methane reactor) if not more of this substrate is fed than can be consumed. Thus the pH value of the second stage can be kept at approximately 7 as the first stage works as buffer tank for the acids. Therefore, the methanogens are subjected to optimal conditions and from there, the hydrogen partial pressure is kept low, too. However, the production of propionate should not to be too high in the acidogenic stage, because its degradation is rate limiting. On the other hand, some production of propionate is desired, because only then propionate degraders can grow in the methane reactor.

Different generation times of the different microorganisms in the two stages cause different hydraulic retention times. Due to the higher growth rates of the acidogens compared to the acetogens and methanogens, a much higher hydraulic throughput of the acidogenic reactor is possible. Inversely, the methanogenesis takes place in a reactor with bigger volume or better retention of biomass.

2.2.2 Reactor types

As anaerobic bacteria can produce only between a tenth or a twentieth of the energy from the same amount of substrate, compared to the aerobic, an enormous turnover of substrate occurs with comparable little growth. The small biomass yield is an important advantage of the anaerobic process compared to the aerobic one as only small amounts of sludge have to be disposed. However, only small dilution rates are allowed in order to avoid a wash out of the biomass.

The reactors, which are introduced in the following, are designed to retain biomass in order to intensify the turnover and thus, to reduce the volume of the reactor, as it for biochemical and thermodynamical reasons is not possible to accelerate the anaerobic degradation process substantially.

The continuously stirred tank reactor (CSTR) does not have any biomass retention, but often a settler is placed subsequently in the wastewater stream where sludge is fed back into the CSTR.

The anaerobic sequencing batch reactor (ASBR) also depends on the ability of bacteria to form flocs with the ability to sediment. Bacteria are retained due to the sequence of filling, reaction, sedimentation and withdrawal, where mixing is done only in the reaction phase. During such a sequence the substrate concentration steadily decreases. As at the end the substrate concentration becomes low, bacteria form flocs, whereby the ability of settling is increased. While these reactors are sufficient for the acidification and often even no biomass retention is made, because of the relatively fast growth rates of some hours of acidogenic bacteria, the requirements for retention of biomass are much higher for the acetogenic and methanogenic bacteria because of their small growth rates in the order of some days.

The following reactors are mainly used as methane reactors. In fixed bed reactors, which are also called anaerobic filters (AF), bacteria grow on fixed surfaces. Rings made of plastics or mats of fibre are often used as filter material. Substrate is fed into the reactor at the bottom and flows upwards through the filter, which is attached with a film of bacteria. On the one hand, the filter should densely be packed in order to achieve a big surface area, on the other hand, it should not become blocked because of the growing film. Usually, only the outer part of the film (some millimeters) contains active bacteria, as diffusion limitations occur and exterior bacteria only are exposed to relevant substrate concentrations. Therefore, thick biofilms do not have a

significantly higher performance in the degradation of substrate, because active biomass concentration is similar (Tartakovsky and Guiot, 1997).

An improved variant is the fixed-bed loop-reactor, where the liquid phase is circulated by means of a pump in order to minimise the gradient of substrate concentrations. A general disadvantage of fixed bed reactors is the possibility of clogging.

In fluidised-bed biofilm-reactors (FBBR) the biofilm grows on sand particles with a diameter of approximately one millimeter. Here, the liquid is circulated relatively fast in order to keep the particles suspended. Because of the movement of the particles, no clogging occurs. This reactor has the best performance of all reactors, but much energy is needed for the circulation.

In the upflow anaerobic sludge blanket reactor (UASB), microorganisms form pellets, which settle. Fresh wastewater is introduced into the reactor at the bottom and removed at the top, while the letting off is constructed in order to retain the particles. The gas is removed below the liquid level in order not to disturb settling of the pellets. This reactor does not need energy for circulation, but pellets are not formed with every type of wastewater.

The internal-circuit reactor (IC) is an improvement of the UASB. It consists of one or more loop reactors where one is placed upon the other. On top of these reactors a UASB unit is placed. Due to its construction concept only a small installation area is needed. Furthermore, no energy for circulation is needed because auto circulation occurs due to gas production.

2.3 Control Aspects

For non-linear, time-dependent systems, as it is the case for the anaerobic wastewater treatment, it is difficult to realise an automatic control of the whole system by means of classical control methods only, like PID controller etc. Moreover, the amount of influence of relevant parameters on such complex systems often cannot be determined exactly enough for the classical methods. Therefore, in recent years alternative control methods have been developed. For this thesis, classical controllers (PID) were chosen as subsidiary controllers but the fuzzy rulebase (fuzzy expert system) was chosen for the superordinated controller (representing the expert), as much qualitative expert knowledge is available in literature.

Even the control of the pH value is not trivial. Therefore a survey is given in section 2.3.1.

The use of data based methods, like Fuzzy C-means or artificial neural networks (ANN) is expected to be more difficult for the overall control, as due to the slowness of the controlled system there would be needed much time in order to obtain proper

training data. These and other knowledge and data based methods are shortly introduced in subchapter 2.3.2 (Alternative Control Methods). The fuzzy logic, which has been used in this thesis, is explained in detail in subchapter 2.3.3.

2.3.1 pH Control

There are several possibilities for the control of the pH value in wastewater treatment plants. The simplest one is to use a buffer tank, which is sometimes sufficient without the need of using any controller. This method is useful if the pH value of the influent is subjected to large fluctuations around the desired pH. When the inflowing wastewater is mixed with a larger volume, an average pH value is achieved in the mixture. However, this simple method is often not sufficient, because vessels need to be very big, the average pH value is generally too low or too high or other problems occur, like the formation of bad odour. Anyway, the construction of high performance biogas plants, without the possibility of changing the pH in case of emergency, is certainly risky. Moreover, most waste waters from the food processing industry have a big potential for rapid acidification, which suggests also the adjustment of the pH.

pH controllers which add lye (and/or sometimes acid) thus have to be applied,. The main difficulty arises because of the fluctuating composition of the influent, which is particularly true for industrial wastes and which causes a non-linear and non-repeatable answer (curve of titration) after the addition of lye or acid due to their buffer capacity, especially, weak acids and bases as well as their salts, whose amounts and types are rarely known in detail, influence the titration curve and thus, the step response.

In the wastewater treatment, most often two (bang-bang) and three point controllers (bang-bang with hysteresis) are used (Ghaly and Pyke, 1991), which dose lye or acid until the desired pH value is achieved. Although this method is suitable for many cases, especially for municipal wastewater, it is critical for the acidification buffer tank and not at all applicable for the methane reactor, because the characteristic times of the controlled systems are quite high. PID controllers, which are sometimes used, show the benefit of faster reaching the desired pH. They could be used as inline controllers without the use of a buffer tank. A PID controller has to be parameterised at a working point whereby a linear characteristic line is assumed. However, pH curves are not at all linear. However, if the titration curve was known, a linearisation would be possible. In practice, however, composition varies and therefore also the response to the addition of lye or acid, by what the parametering does not meet the real conditions anymore. In this case, the set point is not reached or an overflow occurs. In the worst case, the control loop would then be instable. While in most industrial applications PID controllers are parameterised as PI controllers only, here the use of the differential part (D) is useful as the response of slow processes is accelerated (Pfeiffer, 1995).

Sometimes fuzzy controllers are also applied to pH control, but they are subjected to the same difficulties as classical controllers. Good results are only achieved with additional installations and input variables, like additional sensors or additional dosage points (Parekh et al, 1994). Artificial neural nets would eventually succeed because of their learning ability. However, learning algorithms are slow (Zell, 1994), and no practical applications in pH control were found in literature.

2.3.2 Alternative Control Methods

Appart from from the fuzzy logic rulebase, there are other cognitive algorithms, which are widely used. These methods are introduced in the following.

2.3.2.1 Rule Based Interpolation Controller (RIP Control)

A rule based interpolation controller is also a knowledge based controller, such as a fuzzy rulebase controller (2.3.3). Compared to the fuzzy controller, the RIP controller is more robust against lacking rules because it gains data by interpolation. A further advantage is the possibility of combination of knowledge based methods and classical methods (there is also a further development of the classical fuzzy logic, the Sugeno type controller). Principally speaking, a RIP controller represents a fuzzy logic controller where the set of characteristic curves is calculated once and subsequently, the output values are calculated by extrapolation between the grid points of the curves. Hence, using only linguistic output variables and a fully defined rule base, both systems (Mamdani type fuzzy logic controller, see section 2.3.3, and RIP) show similar results.

2.3.2.2 Classification Control

Concerning the classification control, the input values– all together – are associated with a certain process situation. Instead of the evaluation of rules the input values are compared with training data. Afterwards a control action which suits to the process situation is set. For this method, experimental data but no a-priori knowledge about the relations are needed. A disadvantage of this method is the discontinuity of a change from one situation to another.

2.3.2.3 Fuzzy C-means

Fuzzy C-means is a fuzzy cluster method. Like the classification method, it determines the class prototypes for an existing data set and a specified number of classes. In contrast to the classification control, each data set is a member of all classes but at different membership values (between 0 and 1). Hence the shift from one situation into another is achieved more smoothly.

2.3.2.4 Artificial Neural Nets

Artificial neural nets (ANN) are data based methods. ANN can learn a certain controller behaviour. No a-priori knowledge between input and output data is needed. The objects of the feature space are represented by the weight factors of the particular neurons. During the learning phase, the weights are adjusted in such a way that the total feature space described by the training data is covered as well as possible. Some net architectures allow unsupervised learning (e.g. Kohonen network).

One disadvantage is that relatively much training data, depending on the type and size of the net, is needed. However, many applications allow good results to be achieved with few data records. The behaviour of the controller can only hardly be predicted.

2.3.3 Fuzzy Rulebase

Fuzzy logic is a super set of the conventional logic, which was extended in order to handle the concept of partial truth, values between completely true and completely false. It was introduced by Lotfi Zadeh (1965) and first applied for control by Assilian and Mamdani (1975). Attention to fuzzy systems was given relatively late, in 1985, when S. Yasunobu and S. Miyamoto of Hitachi, demonstrated the superiority of fuzzy control systems for the Sendai railway by simulations. Their ideas were adopted and fuzzy systems were used to control accelerating, braking, and stopping when the line opened in 1987.

Fuzzy rule based systems (=fuzzy logic expert systems) are used, when knowledge on the input/output behaviour of a process is available, but cannot (or should not) be put into a pure mathematical form. This knowledge is stored in the form of “IF ... THEN ...” rules. No training is necessary, as the rules are once generated by a human expert. The rules use linguistic variables like “feed rate”, which consists of sets like “small”, “normal” and “high”. The input values are converted into the fuzzy variables by the use of the so-called “fuzzification”. The rules are applied on these by means of the “inference engine”. The results are the fuzzy output variables. At last, a crisp value is received by “defuzzification” of the output variables. The transfer behaviour is equivalent to a static, non-linear function.

Instead of using fuzzy variables as outputs, as in this classical and most widely used system (Mamadani type controller), also mathematical functions could be applied. Such a system is then called Sugeno type fuzzy controller.

Before the particular aspects of the fuzzy logic are discussed in detail, the function of the fuzzy logic rulebase will be illustrated with an example.

2.3.3.1 Example

The following example illustrates, how the fuzzy logic rulebase works.

Rule 1: IF hydrogen is NOT high AND pH is normal THEN state is normal (17)

Rule 2: IF state is normal THEN feed_setp² is keep (18)

Hydrogen (offgas of methane reactor) is assumed to be 300 ppm and the pH value (methane reactor) should be 6.5.

The fuzzy variable *hydrogen* (Figure 5a) is divided into the three sets *low*, *normal*, and *high*. *Normal* begins at 50 ppm at a truth value of 0, and reaches a truth value of 1 at 100 ppm. From 100 to 200 ppm *hydrogen* is 100 % *normal*, and it is 0 % *normal* at 500 ppm and more.

Having a look at Figure 5a, *hydrogen* is partly *high* (truth value of 0.33) and partly *normal* (truth value of 0.67), but not at all *low* (truth value of 0). Fuzzification of the pH value is assumed to give 25 % *low* and 75 % *normal*.

The standard definitions of the logical operators in fuzzy logic are the following:

$$\text{truth}(\text{not } x) = 1.0 - \text{truth}(x) \quad (19)$$

$$\text{truth}(x \text{ and } y) = \text{minimum}(\text{truth}(x), \text{truth}(y)) \quad (20)$$

$$\text{truth}(x \text{ or } y) = \text{maximum}(\text{truth}(x), \text{truth}(y)) \quad (21)$$

Because of these definitions, for *Rule 1*, the truth value of “hydrogen is NOT high” becomes 0.67 (eq. 19), while the truth value of “pH is normal” was 0.75. Thus, the logical AND yields 0.67 (eq. 20). The set *normal* of the fuzzy variable *state* (conclusion of rule 1) is then activated at a truth value of 0.67, too. If the set was already activated by

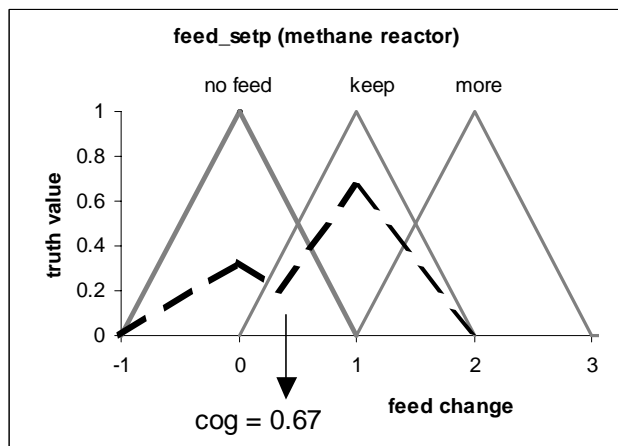
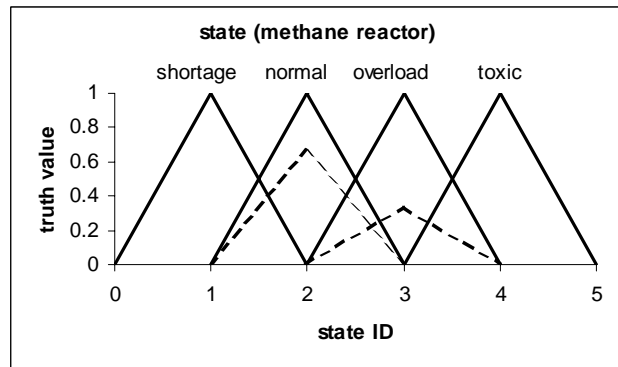
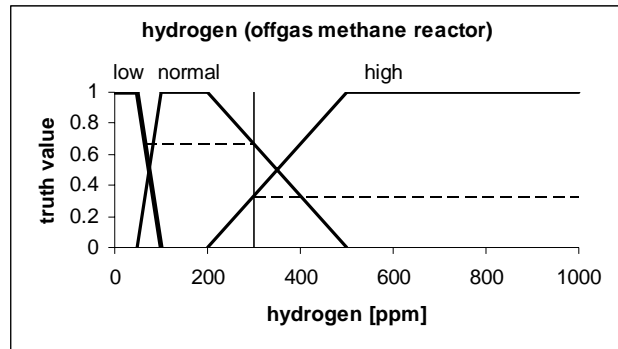


Figure 5. Fuzzy variables (methane reactor): (a): hydrogen(2). (b): state(2). (c): feed_setp(2). Exemplary truth values are shown (see text).

² feed_setp = feed setpoint. See following text.

other rules, usually the maximum is taken. Let us assume the set *overload* of the variable *state* is activated with 0.33. Now, the state of the methane reactor (Figure 5b) can be interpreted as slightly overloaded.

After applying rule 2, also the set *keep* of the variable *feed* is activated at 0.67. Some other rules, which are not shown, have also activated “feed is no_feed” at 0.33, hence, the *feed_setp* should be slightly lowered. As the feed controller needs a crisp value, the fuzzy variable *feed* (Figure 5c) needs to be defuzzified. Defuzzification is done by the center of gravity method (COG), where the gravity of the activated areas of the sets is calculated. As the defuzzified crisp value becomes 0.67, feed is decreased to 67 % of the last feed rate.

2.3.3.2 Fuzzification

Fuzzification calculates the membership value from the crisp input value of the sets of the respective fuzzy variable using the membership function (see example above). The membership function is defined as the curve used in a fuzzy set, triangles or trapezes in this case, which maps a crisp value to a degree of membership value. Sometimes, also other membership functions, like the Gaussian distribution, are applied. A Gaussian curve would be used when probability was handled or if the set of characteristic curves should be very smooth.

If a fuzzy expert system was converted into an artificial neural net (Buckley et al, 1993), also Gaussian membership functions would be needed. However, in control applications usually only triangles and trapezes are used because they are sufficient (Kiendl, 1997).

2.3.3.3 Inference

In the inference process, the truth-value for the premise of each rule is computed, and applied to the conclusion part of each rule. In the end, the sets of the output variables are determined.

The inference can be classified into three sub processes.

- (A) Aggregation: determination of the truth-value of the premise of the rule (IF part)
- (B) Activation: determination of the truth-value of the conclusion part of a rule (THEN part)
- (C) Accumulation: determination of the membership value of each fuzzy set from the results of all rules

(A) If there is only one linguistic term as in rule 2 (eq. 18), the degree of membership of the set is already the truth-value of the premise of the rule (0.66 in the example above). If there are two or more linguistic terms connected with the AND

operator as in rule 1 (eq. 17), the MIN (eq. 20) or the PRODUCT (eq. 22) are most frequently used (Koch et al, 1996).

$$\text{truth}(x \text{ and } y) = \text{truth}(x) * \text{truth}(y) \quad (22)$$

In the example, the truth-value of *0.67 AND 0.75* would hence become 0.50 instead of 0.67 using the PRODUCT instead of the MIN which reminds the probability theory. However, Fuzzy logic is not probability (but it could be used for it, as all probability distributions are fuzzy sets). A minimum requirement of probability is additivity, that is, the truth-values must add to the sum of 1 (Kampé and Fériet, 1982; Kosko, 1990). In Fuzzy control however, it is a good practice to define the membership functions of the sets the way the sum gives 1 (Kiendl, 1997).

Another useful AND operator is the FUZZY-AND, which combines the MIN with the arithmetic average (eq. 23). By the use of this operator, a high membership value of one set can compensate a less value of the other (γ can be selected between 0 and 1; 1 means 100 % MIN inference, 0 means 100 % arithmetic average). Moreover, this operator adheres to strict monotony only as an increase of one of the membership values leads to an increase of the truth-value of the whole term.

$$\text{truth}(x \text{ and } y) = \gamma \min(\text{truth}(x), \text{truth}(y)) + 0.5 * (1 - \gamma) (\text{truth}(x) + \text{truth}(y)) \quad (23)$$

In practice, the MIN is mostly sufficient (Cordón et al, 1997). Another advantage of the MIN operator is, that it fulfils (together with the FUZZY AND) the stability criteria, which requires that

$$\min(\text{truth}(x), \text{truth}(y)) \leq \text{truth}(x \text{ and } y) \leq \max(\text{truth}(x), \text{truth}(y)) \quad (24)$$

and the idempotency, which requires that the aggregation of two or more identical truth-values has the same truth value (Kiendl, 1997, Zimmermann, 1991).

Usually, the OR operator is not taken into account at this place, as each rule with an OR operator can be rewritten into two rules (see (C)).

(B) Having the premise of the rule, the truth-value is transferred to the conclusion part.

Usually, only MIN or PRODUCT is used as activation methods. With PRODUCT (eq. 22), the output membership function is scaled by the rule premise's computed degree of truth (Figure 5c). With MIN (eq. 20), the output membership function is clipped off at a height corresponding to the rule premise's computed degree of truth (Figure 6). As the shapes of the areas, which are activated, are different, there is also a small difference in the output when the fuzzy variable is defuzzified using the centre of gravity method.

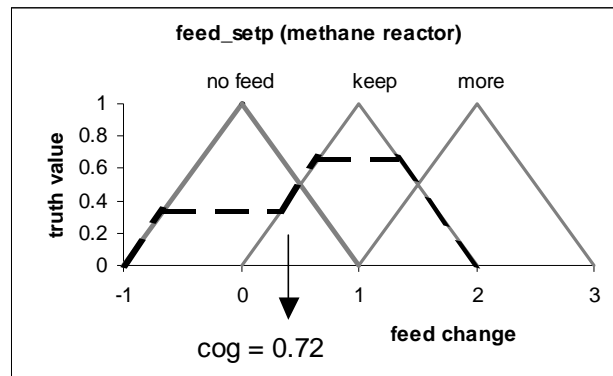


Figure 6. Degree of membership of output variable calculated with MIN activation, defuzzification by means of the centre of gravity method.

(C) As a fuzzy set could have received more shots (i.e. the truth value of a rule was more times greater than 0 and thus the membership value is set more than once) the values have to be combined with the fuzzy OR operator. Usually only MAX (eq. 21) or SUM (25) is used (calculated pointwise over the whole set).

$$\text{truth}(x \text{ or } y) = \text{truth}(x) + \text{truth}(y) \quad (25)$$

Using the SUM instead of the MAX, the membership of the set increases the more often it is hit. Once more, the SUM can be related to the theory of probability. Like the PROD (see (A)) this operator does not fulfil the idempotency and stability.

Again, there are compensatory operators, whereby the FUZZY-OR is most popular (eq. 26).

$$\text{truth}(x \text{ or } y) = \gamma \max(\text{truth}(x), \text{truth}(y)) + 0.5 * (1 - \gamma) (\text{truth}(x) + \text{truth}(y)) \quad (26)$$

2.3.3.4 Defuzzification

In the end, there is the (optional) defuzzification, which is used whenever it is useful to convert the fuzzy output set to a crisp number. There are more than 30 defuzzification methods. Two of the more common techniques are the CENTROID and MAX methods. In the CENTROID method, the crisp value of the output variable is computed by finding the variable value of the centre of gravity (COG) of the membership function for the fuzzy value (Figure 5c). In the MAX method, one of the variable values at which the fuzzy subset has its maximum truth-value is chosen as the crisp value for the output variable. By using the MAX instead of the COG, the output (feed change) were 1.0 instead of 0.67. With the MAX, the output is restricted to the centroid values of each set (0 or 1 or 2 in the example used).

2.4 Experimental Setup

In this section an overview over the experimental setup, which was used in this work, is given.

A reactor configuration, which is shown in Figure 7, was chosen from theoretical considerations presented in previous sections.

In order to achieve high efficiency and fail-safeness in respect to the composition of the wastewater, a fully automated **two-stage** plant was constructed (Figure 7), whereby hydrolysis and acidogenesis should mainly occur in the first (acidification buffer tank, C1), acetogenesis and methanogenesis in the second reactor (methane reactor, C2).

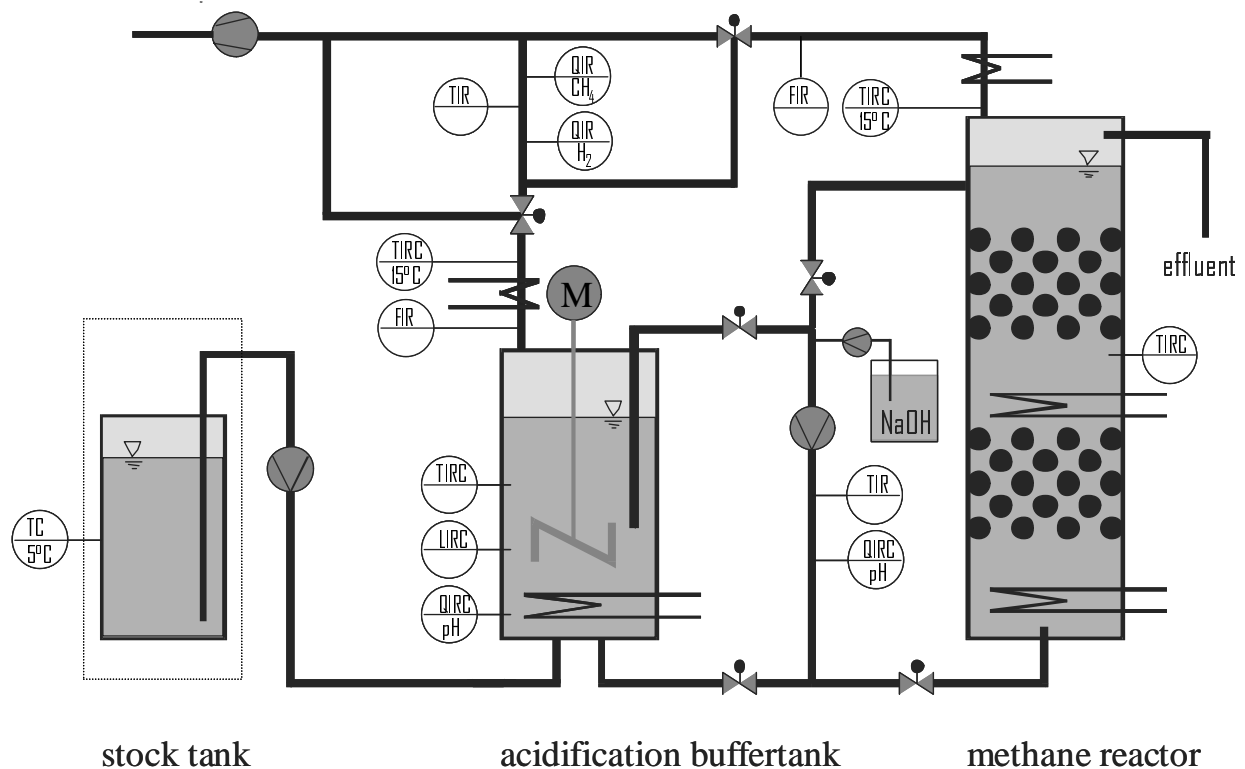


Figure 7 Piping and installation diagram (P&ID) of the laboratory scale plant. T = temperature, I = indication, R = record, C = control, L = level, F = flow, Q = quality measurand

The first reactor, the **acidification buffer tank**, is constructed as a **periodically stirred reactor**, where mixing occurs only for short periods, and settling is applied before removal of liquid in order to retain solids and thus microorganisms. The removal of liquid is done 10 % above the bottom, hence, it is never completely emptied.

The second reactor (**methane reactor, C2**) is constructed as a **fixed bed loop reactor**. Biomass is retained in the biofilm and circulation is applied in order to minimize concentration gradients.

Automatic controlled dosage of lye into both reactors in order increase the pH value is possible. Both reactors are also temperature controlled. Feed from the acidification into the methane reactor and also back feed from the methane reactor into the acidification is done semicontinuously.

Measured quantities should be economic but nevertheless appropriate for the determination of the microbial state and hence should allow to set the proper output values in order to separate the degradation steps in space and to achieve at last a good reactor performance. After intensive literature study, the measured values, as given in Table 1, were chosen.

Table 1. Measured quantities for the reactors. Place: C1 = acidification buffer tank, C2 = methane reactor, QG = gas test point, QF = liquid test point. Gas and liquid can be switched to QG and QF respectively.

measured quantity	place
rate of gas production	QG
concentration of methane	QG
concentration of hydrogen	QG
concentration of hydrogen sulphide	QG
temperature of the gas	C1, C2 and QG
pH	C1 and QF
conductivity	QF
ORP	QF
temperature of the liquid	C1, C2 and QF
additional measurement device of the liquid	QF

The reactor system was constructed in the way that the measured quantities could be acquired by using only one set of sensors for both reactors. This was achieved by placing the measurement test points (QF, QG) outside the reactors (C1, C2) and using valves in order to switch the gas or the liquid, respectively, alternating to the test points.

The pH value of the acidification and the temperatures of both reactors were measured not only at the test points but also inside the reactors as these measurands

- could change relatively fast due to feeding into the acidification (pH, temperature of acidification) or
- their tolerances are required to be small (temperature of methane reactor).

An additional measurement device, a sensor for density, UV absorbance or the COD should be tested during the project's course.

The manipulated variables, their place and the actuators, which are used to manipulate the system, are given in Table 2.

Table 2. Relevant manipulated variables and actuators for the reactors. Place: C1 = acidification buffer tank, C2 = methane reactor

manipulated variable	place	actuator
pH	C1 and C2	dosage of NaOH by peristaltic pump
temperature	C1 and C2	electric heater
feed	into C1	peristaltic pump
feed	from C1 into C2	peristaltic pump and valves
feed	from C2 into C1	peristaltic pump and valves
circulation	C2	peristaltic pump
stirring	C1	stirrer

The temperature at the outflows of the gas was not shown in Table 2, as it is not relevant for the process. It was only controlled in order to avoid condensation in the gas sensors.

the dosage of acids is not necessary in anaerobic wastewater treatment plants, as well as cooling is not necessary, because temperature is not increased relevantly by anaerobic microorganism activity and therefore, it was not provided.

As there is only one gas test point, only one liquid test point, and only one circulation pump in order to save costs, operational states of the reactor have to be coordinated in the course of the time. This concept is presented in chapter 3.1 (Overall Concept).

The gas test point, which has been developed in this work, is described in chapter 3.2. For details of the hardware used, see chapter 5 (Materials and Methods).

3 Presentation and Discussion of the Results

In this chapter, the results of the particular parts of the thesis are presented and discussed. In paragraph 3.1 the overall concept of the control system is presented. Emphasis is put on the particular operations (sequential control) of the system, which interact, by a system of request/release/activation. The integration of the sub controllers is shown there, too. In order to validate the control parameters chosen and the fuzzy logic system, a simulation model was developed, which is presented and validated in paragraph 3.6. Paragraph 3.2 describes the gas test system, which was developed in order to be able to measure the concentrations of hydrogen and methane online. These values are necessary input values for the fuzzy logic control system. In paragraph 3.3, the adaptive on/off controller for the acidification buffer tank and the modified PID controller for the methane reactor are described. In paragraph 3.4, the fuzzy logic expert system, which acts as supervisory control system, is presented. Finally, the whole system is validated by experiments (paragraph 3.5) and simulation (paragraph 3.6).

3.1 Overall Concept

Aim of this work was the control of an anaerobic wastewater treatment plant, whereby a comprehensive process control system (PCS) should be constructed. Due to theoretical considerations (chapter 2.3) fuzzy logic rulebase was chosen as an adequate control system for the anaerobic wastewater treatment process with biogas production. However, the fuzzy logic is only one important part of the whole system, also the reactor configuration, sequential controls and subcontrollers had to be designed in order to achieve a comprehensive process control system.

According to Olsson and Piani (1993), a PCS should fulfil the following tasks:

- acquisition and handling of data of the technical process and process supervision
- control of some quantities of the system
- logical combination of the input and output variables of the technical process and automatic sequential and loop back control

Consequently, the tasks of the software were classified into different fields:

<ul style="list-style-type: none"> • measurement and data logging • sequence control of the operational states of the plant • simple loop back control (on-off and PID controller) 	→ PLC
<ul style="list-style-type: none"> • complex loop back control (Fuzzy expert system) • human-machine interface (HMI) 	→ Microcomputer

The simpler tasks of the control system, like A/D conversion and the scaling of the measured quantities, sequence control of the operations and the underlying controllers were carried out on a programmable logic controller (PLC) because of its high reliability and availability (section 3.1.1).

The more complex tasks, like the calculation of the reference values for the underlying (subsidiary) controllers by the fuzzy logic system and post processing of data resided on a personal computer (PC) as does the human-machine interface (HMI) does (section 3.1.2).

The interaction of the subsidiary fuzzy logic controller and the subcontrollers is illustrated in Figure 8. Why the particular control parameters are chosen, is described in section 3.4 (Development of the Fuzzy Logic Expert System)

3.1.1 Sequential Controls and Subcontrollers on the PLC

The subcontrollers are either encapsulated in sequential controls (Figure 8: A, B, C, E) as they interact with other operations (sequential controls), or they are called independently in equal intervals as it is necessary for the PID controllers (D, F, H). The manipulated variables of the latter controllers are only set when the current active operation for it. The circulation speed (G) is directly calculated by the fuzzy logic system and transferred to the pump (and translated into a current signal), whenever the default operation *circulation C2* is active.

See Table 3(on page 31).

Next page: Figure 8.

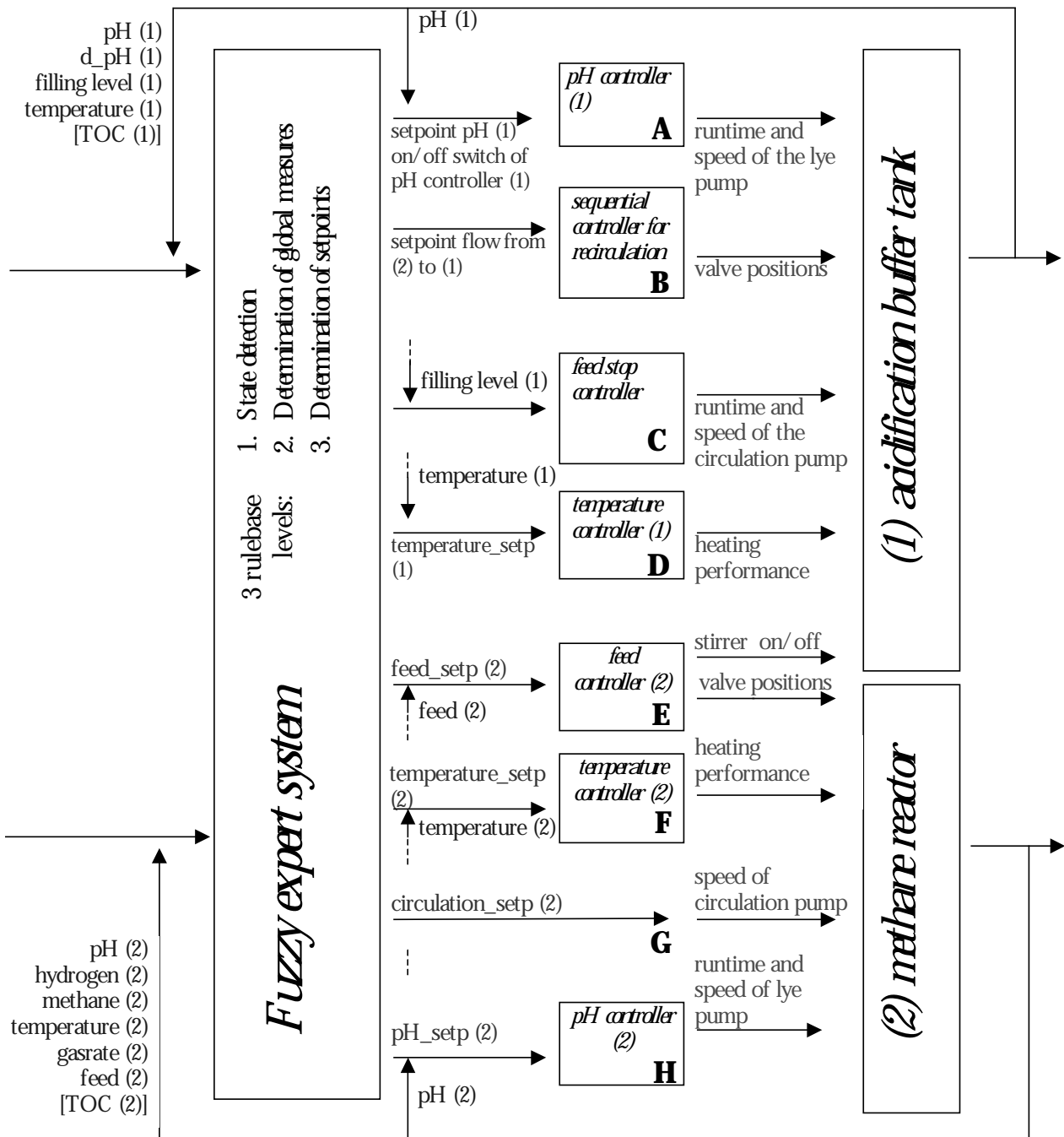


Figure 8. Fuzzy logic expert system and subsidiary controllers. (1): acidification, (2):methane reactor. d_pH: d(pH)/dt, corrected for change due to substrate addition.

Table 3. Possible sequential operations. Several compatible ones can be active at the same time.

operation	description
circulation C2	circulation of the methane reactor, liquid from the methane reactor passes liquid test point (applies circulation rate)
circulation C1	circulation of the acidification buffer tank, liquid from the acidification passes liquid test point (for measurement of C1)
feed from C1 to C2	substrate is pumped from acidification into methane reactor, liquid from acidification passes liquid test point (feed(2) controller)
feed from C2 to C1	substrate is pumped back from methane reactor into the acidification, liquid from acidification passes liquid test point (sequential controller for recirculation)
feed into C1	substrate is pumped from stock into the acidification buffer tank (feed stop controller)
stirring C1	stirrer of the acidification buffer tank is switched on
lye dosage C1	lye is dosed/stirring (alternatively) in order to increase the pH value of acidification (includes pH controller C1)
lye dosage C2	lye is dosed in order to increase the pH value of the methane reactor (as lye dosage is requested by the PID controller)
gas test C1	gas of acidification is measured
gas test C2	gas of the methane reactor is measured
gas test flush	the gas test point is flushed with air

Sequential operations are encapsulated into particular function blocks (FB; Table 3). The on-and-off switching of the automatic operations is done by a system of **request/release/activation**; similarly it is sometimes used in cooperative multitasking computer operating systems (Custer, 1992). There, too, the priorities of some processes are changed from time to time in order to execute all processes. A process can only be ended if it deactivates itself (e.g. *lye dosage C1* deactivates itself only when the lye is flushed from the pipe and reached the reactor).

In case an event occurs, which makes a new operational state necessary (like completion of a timer or reaching of a boundary value), the FB of that particular operation makes a request. A scheduler function releases these requests according to their priority and compatibility (Figure 9).

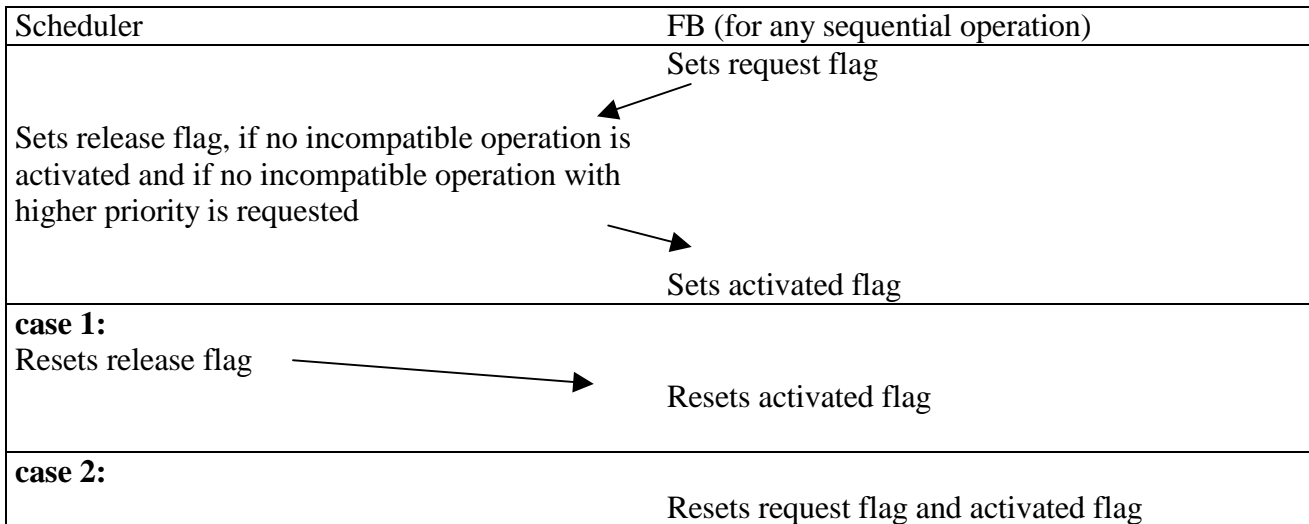


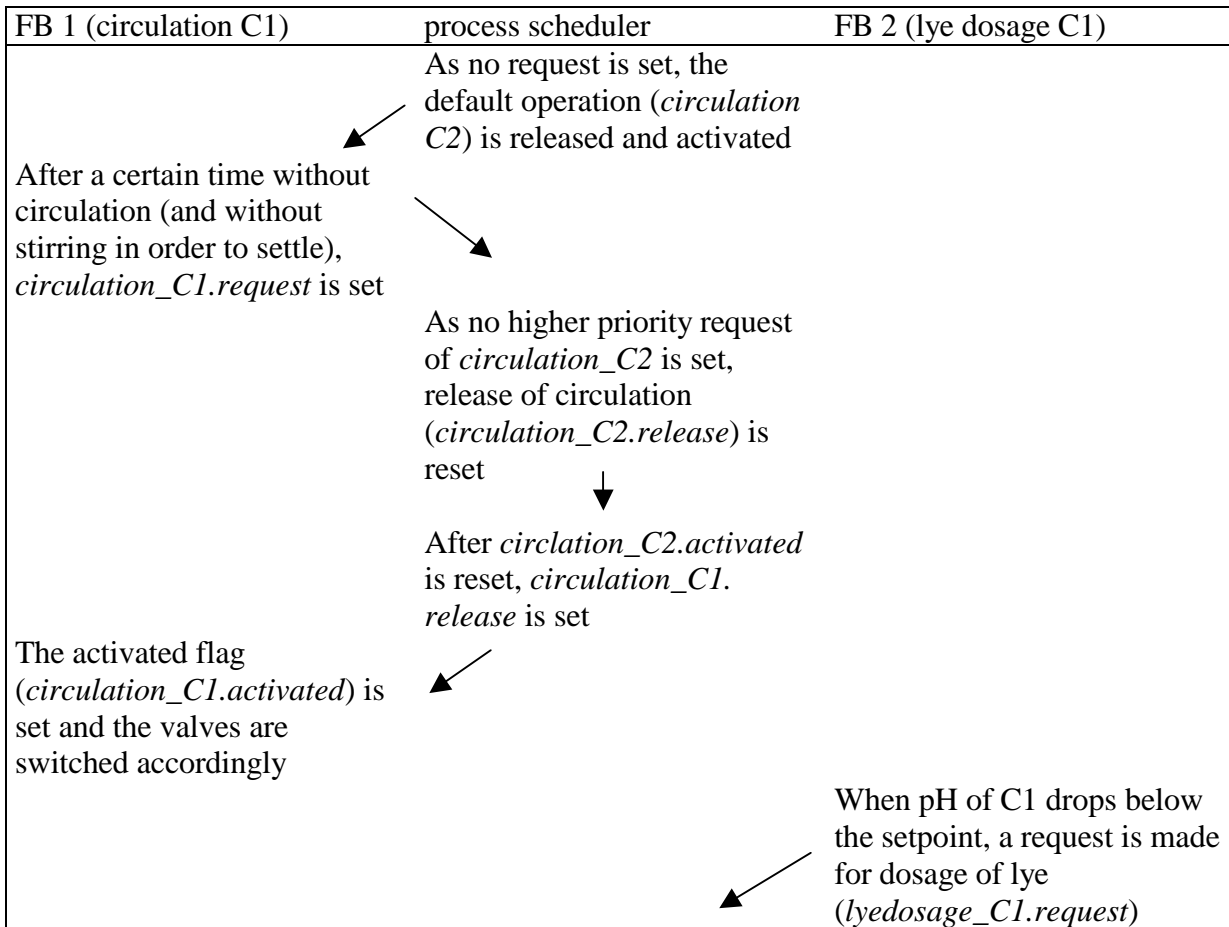
Figure 9. Request, release and activation of sequential operations. FB: function block for the sequential operation. A sequential operation can be finished in 2 ways: Case 1 – release is cancelled; case 2 – request is cancelled.

If a release is set, the function block of the particular operation activates itself and executes the necessary actions. It disables itself (i.e. resets activated flag) by pulling back the request, in case it does not receive further acknowledgement. If no competing operations are requested, circulation of the methane reactor (*circulation C2*) and gas measurement of the methane reactor (*gas test C2*) is active. If more requests are placed, enabling is a result of priority and compatibility according to Table 4.

Table 4. Incompatible operational states, only one operation of each group can be active at the same time. Priorities in descending order. Some states can have two priorities: (+) means high priority and (-) low priority. Switching from low (-) to high (+) priority occurs if the operation was not active for a certain period of time (controlled by particular timers). Incompatible groups: 1 = operations which require control of the circulation pump, 2 = operations which need control of the stirrer, 3 = operations which need control of the gas test point, 4 and 5 = gas measurement is affected by possible vacuum or false gas due to feed.

incompatibility group	operations	incompatibility group	operations
1	circulation C2 (+)	3	gas test C2 (+)
	circulation C1 (+)		gas test C1
	lye dosage C1		gas test flush
	feed from C1 to C2		gas test C2 (-)
	recirculation from C2 to C1	4	feed from C2 to C1
	circulation C1 (-)		gas test C2
	circulation C2 (-)		
2	circulation C1 (+)	5	recirculation from C1 to C2
	lye dosage C1		gas test C1
	recirculation from C1 to C2		
	feed into C1		
	stirring C1		
	circulation C1 (-)		

Usually, the circulations of the reactors have a low priority (denoted as “(-)”) in Table 4) and therefore dosage of lye or feed is preferred. If for any reason circulation did not occur for a certain period of time (i. e. the particular timer, which is restarted during circulation, has finished), it gets a higher priority (+) for a certain time (which is controlled by another timer) in order to be activated. The function of the system is illustrated with the case study shown in Figure 10 (activation of a sequential operation), Figure 11 (case A – no release for interrupting operation), and Figure 12 (case B– interruption by higher priority operation). In this example an operation (*circulation C2*) is activated and then another (*lye dosage C1*) sets an request (case A: interrupting operation has lower priority, B: it has higher priority).



case A: no circulation for more than 2 hours thus high priority. case B: low priority of circulation, see...

Figure 10. Request, release and activation of a sequential operation (circulation of C1). FB: function block for the sequential operation.

case A: no circulation of C1 for more than 2 hours thus the priority of circulation is higher than for dosage of lye

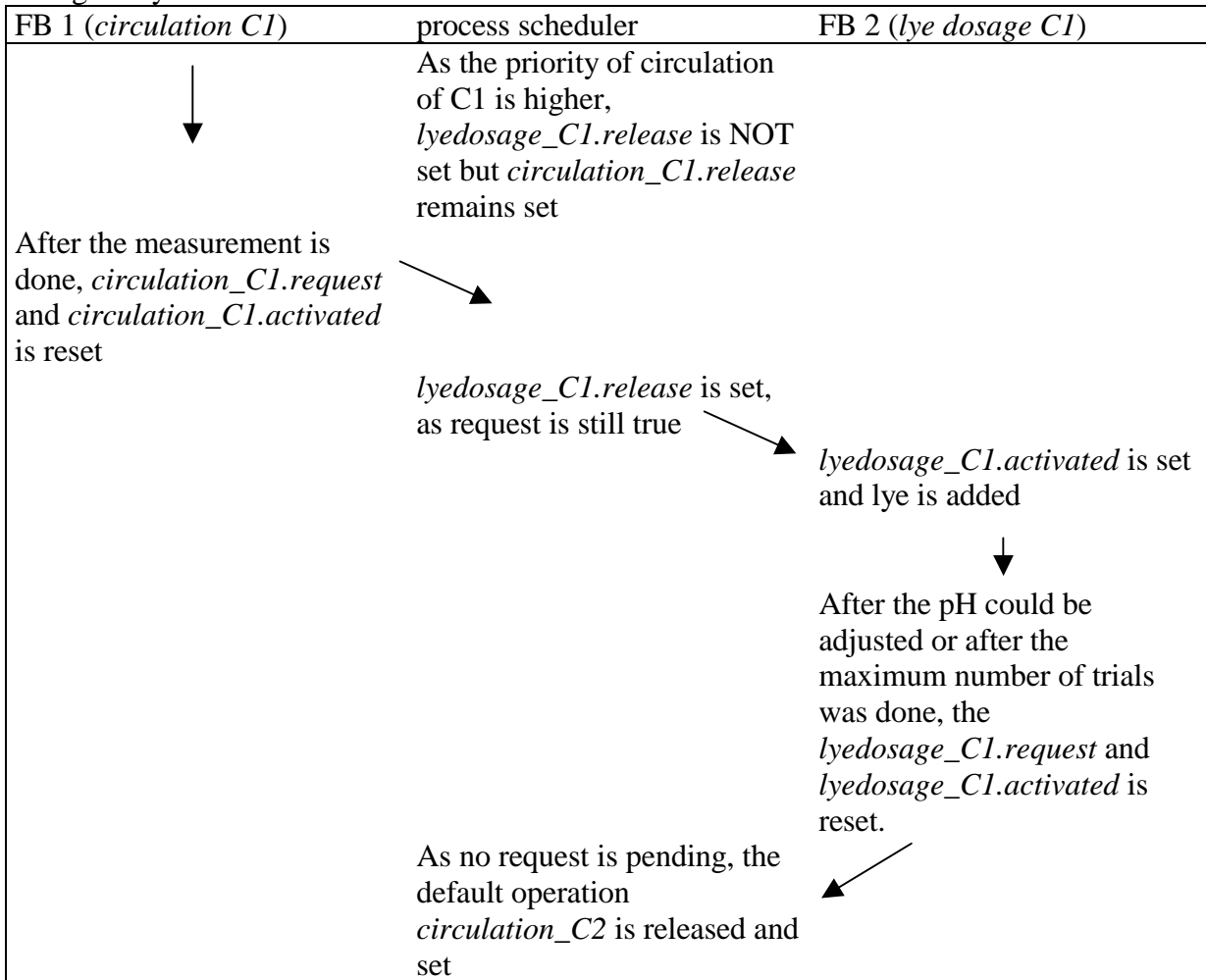


Figure 11. One operation is activated (circulation). Another operation (dosage of lye) cannot interrupt it because its priority is lower at this time. FB: function block for the sequential operation.

case B: circulation of C1 was done less than 2 hours before

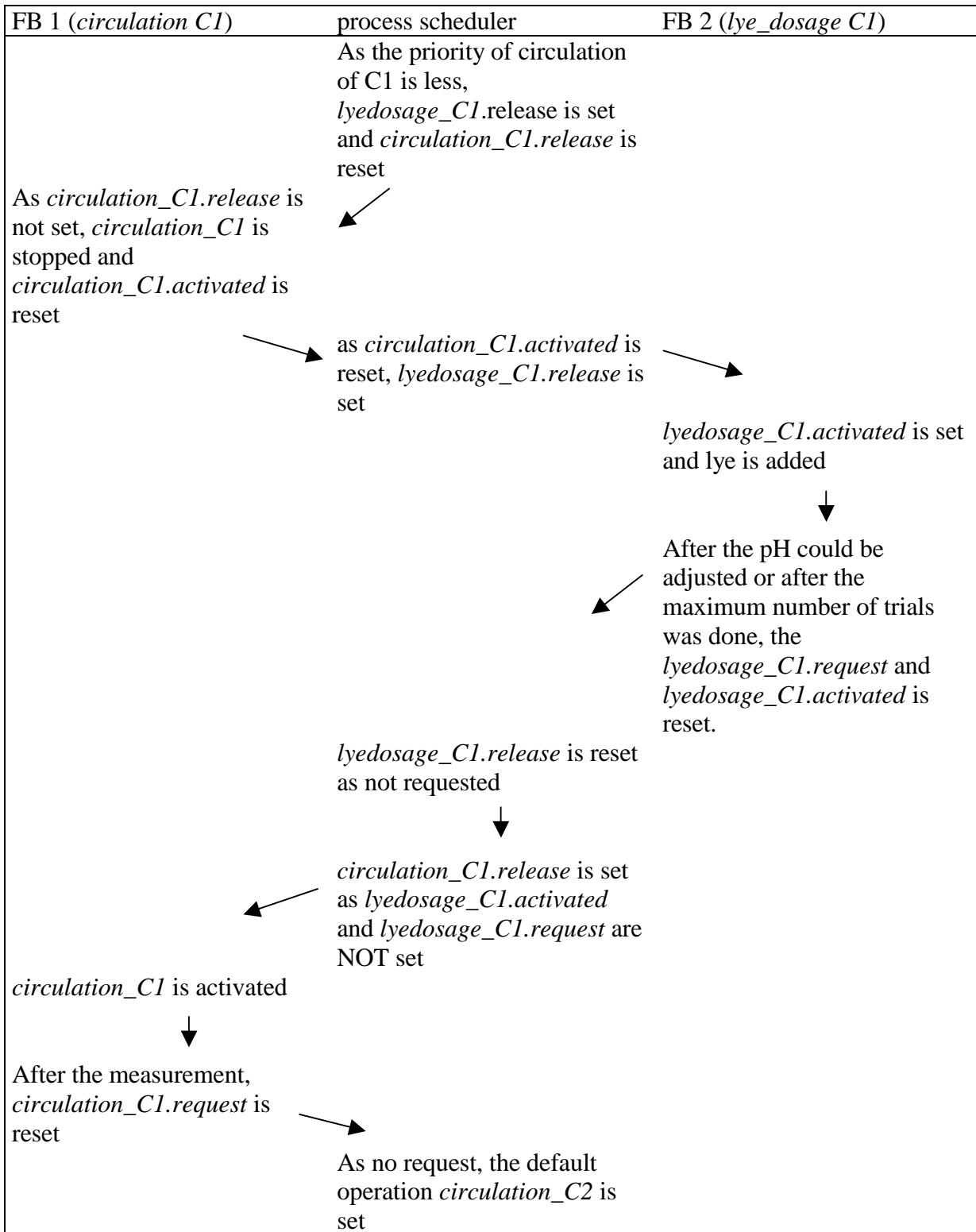


Figure 12. One operation is activated (circulation C1). It is interrupted by another one (dosage of lye). FB: function block for the sequential operation.

The way other possible sequential operations, as given in Table 3, are dispatched and are interacting is described in the following. Usually, the default operations *circulation C2*, *stirring C1*, and *gas test C2* are active. If the reference counter becomes higher than the actual counter for feed, *recirculation from C1 to C2* is requested. After the timer for stirring finishes, and after C1 is settled, enabling is given for *recirculation from C1 to C2*. With both, request and release, feed is activated and substrate is pumped from C1 to C2, until the desired volume is achieved (thus, request is reset) or the pumping interval is elapsed (thus release is withdrawn). When *recirculation from C1 to C2* is active, feed from C2 into C1 (*recirculation C2 to C1*), and *circulation C1* or *circulation C2* is not released and thus not activated, as these states are also in the same group 1 (Table 4) and have lower priority. However, feed could be interrupted by e. g. circulation, if circulation has not occurred for a certain time for any reason and thus its priority is raised (+). As *recirculation from C1 to C2* is also listed in group 2, *feed into C1* and *stirring C1* is not possible that period, as these are also in group 2 and have lower priority. This is done in order to avoid the mixing of the settled tank during the removal of liquid. Furthermore, no gas test (*gas test C1*) is possible (group 5), as during the feed from C1 into C2, the headspace of the reactor could contain a slight vacuum which would result in a reverse gas flow from the gas test point into the reactor. Obviously, ambient air is sucked into the acidification buffer tank during removal of liquid, which is one reason against the measurement of the gas of C1.

Circulation C1 is carried out every hour in order to get an additional pH measurement using the sensor at the liquid test point QF (Figure 7), which can be used to check the pH sensors. Here, also the oxidation-reduction potential (ORP), temperature and optionally the COD are measured.

Lye dosage C1 is requested and released if the pH value drops below the set point, which is usually set by the supervisory fuzzy controller.

Recirculation from C2 to C1 is requested and released like feed from C1 into C2, using a reference and an actual counter. The reference counter is altered accordingly by the fuzzy system.

Feed into C1 is also controlled by means of a counter, which is usually set by the human operator or an external profile, using the spreadsheet software MS Excel in order to simulate the arise of wastewater. In a real size wastewater treatment plant, request/release will have to be altered in order to activate this operational state, whenever a wastewater flow arises.

Stirring C1 is requested periodically in order to suspend the solids and to avoid temperature gradients during the heating period. Therefore, C1 is only heated when stirring is active.

Gas test C2 is carried out in order to obtain measured values. From time to time, *gas test flush* is carried out in order to regenerate the hydrogen sensor with air-

oxygen. *Gas test C1* is implemented but not used. As no pump is installed, a certain volume has to be flushed the test point. If no gas is produced, request is cancelled. If the gas flow is low, the gas measurement could take a rather long time. Therefore a higher priority of *gas test C2 (+)* can interrupt *gas test C1* and also flushing with air.

Lye dosage C2 (PID controller) is only possible, if the active operation of group 1 (Table 4) is *circulation C2* or recirculation from C1 to C2. This is because the PID controller used needs a constant sampling rate of the pH value. Due to the reactor concept, where different operational states influence each other, which substrate flows through the test point at a certain time, a synchronisation of these states is necessary. Therefore a schedule, where the states “feed allowed” and “feed forbidden” are alternated by means of two timers, was developed (Figure 13: 1+2). As feeding from the acidification into the methane reactor only happens when “feed allowed” is true, the pH controller is active when “feed forbidden” is true. In this phase, substrate from the methane reactor is cycled through the test point. The duration of the two states is selected on the one hand in the way that enough substrate can be fed into the methane reactor and that the test point is flushed with substrate (3) of the methane reactor as well as the response time of the sensor (4) is expired one the other hand, respectively. The sum of the two timers plus the period, which is eventually needed to add lye (5) thus specifies the scanning interval of the pH value for the pH controller, which should be kept as small as possible. For other operational states, which have a higher priority, the timer can be ignored as the standard operation of the plant is then interrupted anyway and the pH controller will not be active.

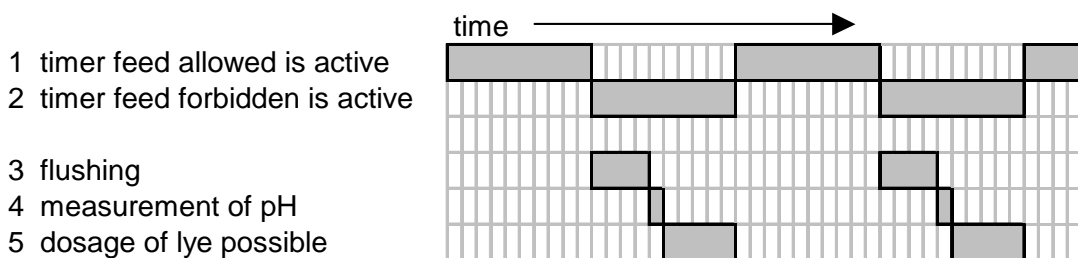


Figure 13. Periods where feed is allowed and for the measurement of the pH value were determined by means of 5 timers.

Timer settings are given in Chapter 5. The pH controller is presented in section 3.3. of this chapter. Together with the concept of sequential operations presented, the operations with highest priority are performed first. After a certain period of time, the priority is lowered for some operations giving other operations the possibility to be released.

Due to its modular design, the basic control system on the PLC is not affected by a breakdown of the PC, which hosts the supervisory information and the control

system. However, a failure of the supervisory system should not last too long because reference values are not altered anymore and therefore are kept constant.

Not only the PLC program, but also the fuzzy logic system, which uses redundant measured quantities (section 3.4), is designed for stability.

3.1.2 Tasks on the PC

Parts of the control system which need more computer resources, a more sophisticated operating system or a graphical interface, are implemented on a personal computer running a multitasking operating system (Windows NT). These components are the following:

- Fuzzy logic software
- HMI software
- Spreadsheet software
- Data processing module

The interaction of these components with the whole system is illustrated in Figure 14.

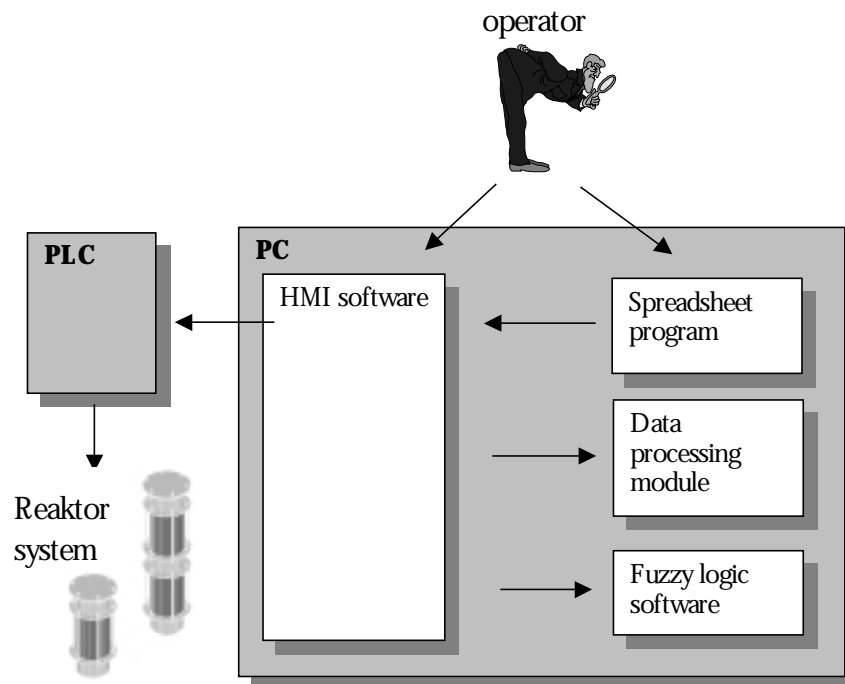


Figure 14. Automation components and their interaction. Arrows indicate direction of initiation.

The control system was designed in the way that the fuzzy logic system can simply be switched on and off. If it is switched off, the human operator can alter the reference values instead. The output of the fuzzy logic system (which is retrieved by

the HMI component) or input of a human operator is transferred to the PLC by the HMI component. The scaling of the physical units into the required signals is done by the PLC. As the Fuzzy logic system does not only need measured values but also some derivatives and mean values, a data processing module was developed for it. Waste water profile could be set by the human operator using a fuzzy logic spreadsheet application, which calculates and transfers the actual counter over and over again to the HMI software which in turn transmits it to the feed sub controller on the PLC.

The HMI was implemented using the standard software package WinCC (chapter 5.6). The Fuzzy logic software “LFP-Fuzzy” was initially developed by Thomas Becker (Becker, 1995; Wollenweber et al, 1997) and extended by myself in the framework of this thesis (implementation of a rule parser, a graphical user interface, and an interface for data exchange - chapter 5.7). The data processing module is described in chapter 5.

3.1.3 Conclusions

The basic process control was implemented on a programmable logic controller. As it receives only reference variables from the PC system, it will not fail if the PC does not work for a certain period of time. In such a case the old reference values will be kept. However, without the supervisory system on the microcomputer no state detection can be carried out and the system cannot react to altered conditions. The particular sequential controls are scheduled by a system of request/release/activation, which resembles to a cooperative multitasking operating system. The software components on the microcomputer were partly developed for the present thesis and partly standard software modules. During all the experiments (which will be introduced later in this chapter), the system performed very well and without any problems.

3.2 Development of the gas measurement system

A gas measurement system, where the concentrations of methane and hydrogen could be measured, was developed (Figure 15).

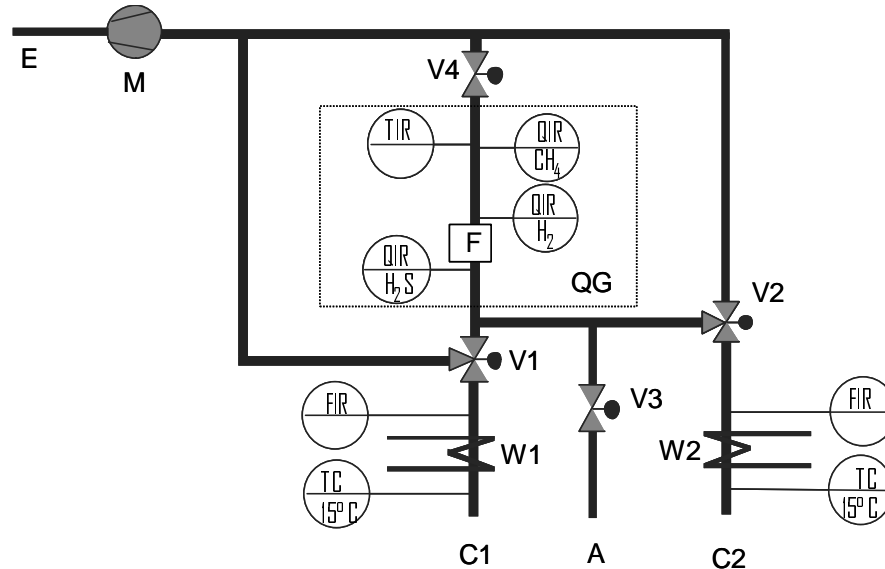


Figure 15. P&ID diagram of the gas test point. FIR = flow indication and registration, TIR = temperature indication and registration, TC = temperature controlled, QIR = quality measurand indication and registration, V1 – V4 = valves, W1 – W2 = heating, M = compressor, E = gas exit, A = ambient air/sampling place, QG = intrinsic gas test point, C1 = reactor 1 (acidification), C2 = reactor 2 (methane reactor), F = Filter

Due to the fact that the gas test point *QG*, gas of both reactors (*C1* and *C2*) can be measured, only the quantities of one reactor can be obtained simultaneously at the same time. The advantage of this concept is that only one set of sensor is needed in order to measure both reactors. The operations *gas test C1*, *gas test C2* and *gas test flush* (cf. section 3.1) are therefore executed cyclically. The flushing with air is necessary in order to regenerate the electrochemical sensor (hydrogen). As the gas which is flowing through the sensors changes (i.e. biogas from the reactors or air), it has to be ensured that the measurement value is only taken over after a certain volume has flushed the gauge. This is achieved by counting the volume of the gas which passed the sensors since switching of the valves. When the volume is reached, gas measurement becomes valid, and the values are taken over (Figure 16).

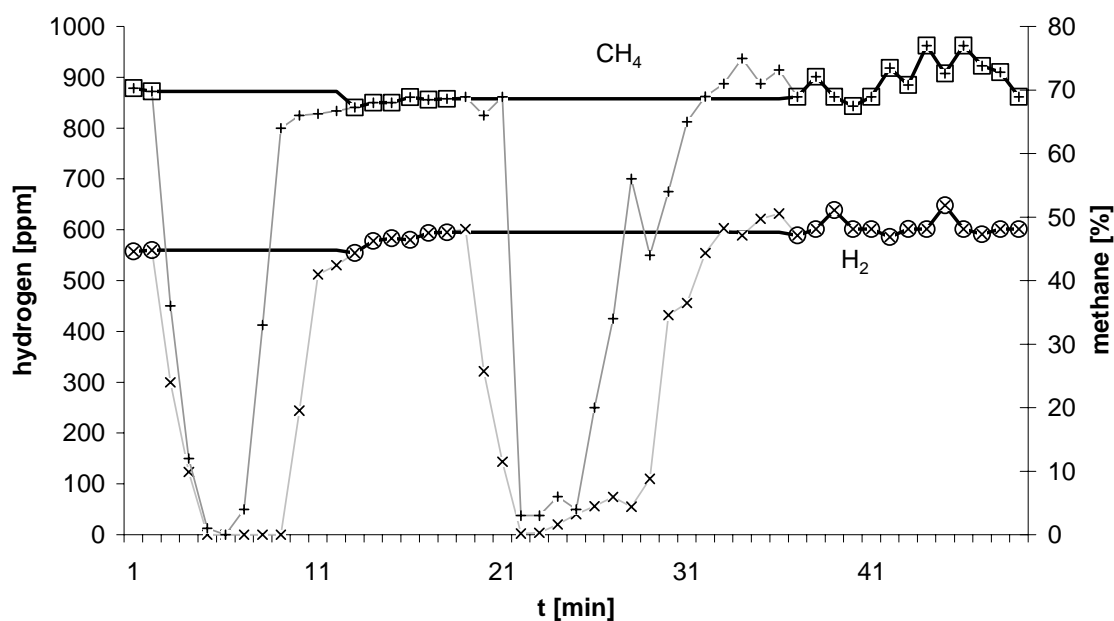


Figure 16. Obtained measurement values from the gas test point taking all values (methane: +, hydrogen: x) and taking only the values after 0.05 l of gas have flushed the sensors after the switching of the relevant valves (□, o).

3.2.1 Choice of Sensors

An overview of gas sensors, which could be used for the measurement of biogas, is presented in Table 5. Theoretically, also the detectors developed for gas spectroscopy could be used for the detection of the gases (mass spectrometry, flare ionisation detector, ... summarised and denoted as *GC detectors* in the table). In order to keep the maintenance effort low, non-invasive sensors should be used, which, in addition, should not be too expensive in order to keep the system economical. For methane, the IR absorbance was selected, because semi-conductor and electrochemical sensors are too inaccurate, as they show inaccuracies of 5 % and drifts of 1 % per month. Sensors with IR are accurate (1 %), reliable and even cheaper than other measurement principles (e.g. mass spectrometer). For the measurement of hydrogen, IR is not applicable, as this gas has no proper selective absorbance in the infrared. A semi conductor sensor is not applicable, as such sensors need oxygen in the gas in order to work correctly. As the requested accuracy of the measurement of hydrogen is lower than for methane, - because hydrogen changes in magnitudes (from 10 ppm to more than 10^4 ppm) while methane in contrast is usually always in the range of 60 ± 20 % - an electrochemical sensor was selected (cf. Materials and Methods). However, this sensor is invasive and has, therefore, a limited lifetime (> 2 years).

Table 5. Overview of gas sensors for methane and hydrogen. Mass spectrometry, flare ionisation detector, ... are summarised and denoted as *GC detectors*

measurement principle	price (EUR)	accuracy/drift per month	gas
semi conductor	100	5 %/?	methane, hydrogen
electrochemical	200	2 %/1 %	methane, hydrogen
IR absorbance	1000	2 %/0 %	methane
GC detectors	> 5000	< 2 %/0 %	methane, hydrogen

3.2.2 Integration of the Sensors

The integration of the sensors into the gas line is illustrated in Figure 15. Gas from the reactors first passes a gas cooler (W1 or W2) where it is cooled to 15 °C. The temperature is controlled and measured by a PT100, sensor which is integrated at the upper part of the cooler. After the cooler the gas passes a flow meter (FIR) and reaches then a valve (V1 or V2), where it can be switched to the gas test point (QG) or to the waste gas (E). Instead of gas from the fermenters, also air (A) is temporarily switched (V3) to the gas test point. The inlet of air can also be used for taking samples of the fermenters by closing valve V4 and opening V3.

A sensor (QIR) for hydrogen sulphide (electrochemical, similar to the hydrogen sensor) was also incorporated into the gas test point, but its values were not needed in this thesis. In front of the other sensors, a filter (F) for removal of hydrogen sulphide is placed, which oxidises the sulphide to elemental sulphur and sulphate, and which is filled with KMnO_4 . The filter was introduced in order to lengthen the life span of the sensors, as hydrogen sulphide would harm them. The Sensors for hydrogen (electrochemical) and methane (IR) are placed behind the filter. In addition, a temperature sensor, which can be used for correction of temperature dependencies of measured values, is built in. However, as the temperature at the gas test point had always been at room temperature, no correction was applied.

The ratio of the diameter of the main air line to the tubing for the biogas, which flows through the test point, was selected in order to generate a slight vacuum before the filter (4 cm water column = 4 mbar). This was necessary for passing through the air, which is necessary for regeneration of the hydrogen sensor.

The gas measurement was programmed in order to have a sufficient volume of gas passed the sensors after changing the measured reactor or after flushing with air and also after short term interruptions in order to reduce outliers. Short term interruptions occurred as because of the feeding from the acidification buffertank into the methane

reactor the liquid level fluctuated somewhat, and therefore, valve V4 (Figure 15) was closed and valve V3 was opened for one minute in order to avoid back-flow from air through the sensors (via valve V4). After one minute, gas from the reactor was again switched to the sensors and was kept, if a gas flow was detectable after another minute. This was also done in order to avoid a building-up of pressure, V3 and V4 are switched every minute. In this case, the gas test point would not be properly flushed and therefore, the measured value is not taken over as long as not 0.05 l of gas have passed. Therefore, it was not necessary to post process the measured values by means of a low-pass filter for example. The volumes of 0.2 and 0.05 l respectively were chosen in accordance with experiments, whereby the gas tube was disconnected from the bioreactor for a certain period of time. In these experiments, 0.1 l (line from C2 or C1 to the outlet of QG) and 0.03 l (line from C2 to a point somewhere between V1 and the inlet of QG) of gas had to be flushed through the sensors in order to receive a constant signal.

For measurement of the gas flow (FIR) a thermal conductivity sensor, which was calibrated (by the manufacturer) for 50 % methane in carbon dioxide, was applied. This measurement principle could be used as the thermal conductivity of methane and carbon did not differ more than 5 % (data sheet of manufacturer). Hydrogen has a tenfold thermal conductivity but is expected to be always less than 1 % in the biogas of the methane reactor.

3.2.3 Validation of the Gas Test System

The precalibrated sensors were flushed with calibration gas (60 % methane, 1000 ppm hydrogen), whereby the gas was introduced into the system directly after the methane reactor (C2, Figure 15), in order to have the same path as in the measurements. Every six months the calibration was checked. There was a decrease in the signal of the hydrogen sensor (Table 6) which was within the expected range of drift (< 2 % per month), and a failure due to temperature dependencies (≈ 5 % per 10°C , taken from the data sheet of the manufacturer). The signal of the methane sensor, which is temperature compensated, remained accurate and constant. As already mentioned, hydrogen values do not need to be accurate; it appears reasonable to recalibrate the sensor every 6 to 12 months.

Table 6. Calibration data at the begin and at the end of the experiments. Percentage of expected signals of the calibration gas using the calibration data at the begin of the experiments. The calibration gas was 60 % methane and 1000 ppm hydrogen. Temperature was 22 ± 5 °C.

sensor	signal in air	signal with calibration gas
hydrogen	0 %	95 %
hydrogen, after 6 months	0 %	88 %
hydrogen, after 13 months	0 %	79 %
methane, after 0, 6 and 13 months	0 %	60 ± 1 %

Although the signals were expected to be linear (data sheets from manufacturer), linearity was checked by adding air to the calibration gas. As the ratio of air to calibration gas was not known, the signals of both sensors were plotted one against the other (Figure 17). This method could be applied, as both sensors use different measurement principles and therefore it is very unlikely that both of them show the same in-linearity. As also linearity of the ratio of the signals of both sensors is nearly equal, both sensors are regarded as linear.

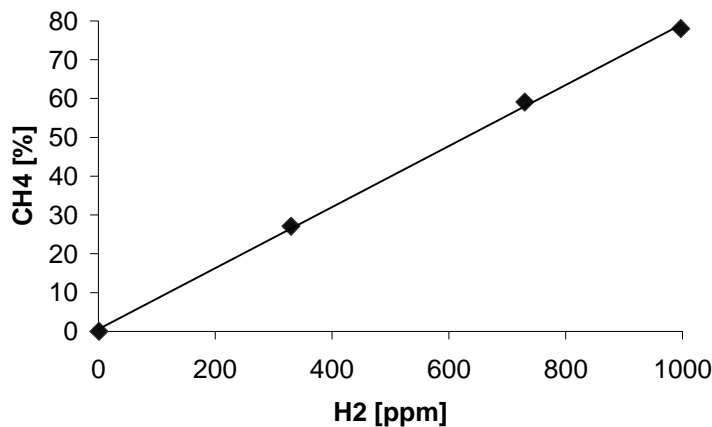


Figure 17. Linearity of the sensors for methane and for hydrogen. The results for calibration gas mixed with air show that both sensors are of equal linearity.

3.2.4 Conclusions

A gas measurement system, which uses economic sensors, was developed and validated. With the concept of switching gases of different fermenters to the sensors, only one set of sensors was needed, whereby the costs of the installation could considerably be reduced. As the hydrogen concentration was expected to vary in magnitudes during the experiments, a less accurate sensor could be chosen. Although, the sensor for hydrogen was less accurate, less stable and has a shorter life-span (2 years), it is expected to be sufficient for the requirement of this thesis.

For the measurement of the flow, the thermal conductivity method could be applied, as the main components in biogas, methane and carbon dioxide, do not differ much in conductivity at the operating temperature of the selected flow meter.

3.3 Development of the pH Controllers

The pH control of both the acidification buffer tank and the methane reactor is not trivial. In order to save costs only one pump for the addition of lye was projected. Thus not only the methane reactor but also for the acidification buffer tank shows long delay periods between the addition of lye and response of the pH sensor.

3.3.1 Requirements for the pH controllers

Both pH controllers, for the acidification buffer tank and the methane reactor, should be able to correct slow (due to microbial metabolism) and fast (due to addition of substrate) decreases of the pH value. As due to the construction of the plant, where only one pump is needed, control actions at the acidification (*C1*) interrupt default operation (*circulation of C2*). Hence they should not be applied too frequent. Therefore a hysteresis of 0.2 (acidification) and 0.1 (methane reactor) around the setpoint was allowed. For the acidification buffer tank, the pH should be kept within the range of 4 to 6 (see chapter 2.1.4) and for the methane reactor of 6 to 8, whereby a dosage of acid is not provided. The setpoints for the pH controller are adjusted quasi-continuously by the fuzzy logic system. Overshooting should not occur for economical reasons, but is not dangerous for the microorganisms, presumed the overflow is not too large. There is no critical time for the microorganisms for reaching the setpoint as they are expected to be only inhibited for the time where the pH is low, but during dosage of lye some other operations are not possible (see 3.1).

Thus, time for adjustment of the pH value in the acidification buffer tank should be not longer than several minutes. Further, lye should be flushed with liquid from the methane reactor instead of using liquid of the acidification, because the latter one is not settled during addition of lye and therefore could contain much solids. On the

other hand also less lye is needed using methane reactor liquid, because its pH value normally is higher, which would save lye.

In the methane reactor, whose microorganisms are more sensitive to pH variations, and which is not subjected to very high fluctuations in both substrate composition and amount due to buffering and feed control respectively, the pH value should never go too far beneath the setpoint. pH values lower than 6 should not occur.

In chapter 2.3.1 some possibilities of pH control are discussed.

As all the introduced methods do not seem to be very suitable either for the pH control of the acidification or for the methane reactor, adaptations have to be applied. One possibility would be to compare the measured value with the prediction made by the use of a mathematical model, whereby in case of a deviation a correction factor is calculated (Mann et al, 1997) or the parameters are changed directly (Olsson and Piani, 1993).

For the acidification buffer tank, a new concept is applied, whereby a small amount of lye is added and depending on the pH change, the amount is altered for the next dosage.

For the methane reactor, a conventional PID controller is applied. Although the delay is very large due to the slow circulation, this concept is used, because composition of the substrate in the methane reactor is not expected to change as much as in the acidification.

3.3.2 Adaptive Controller for the Acidification Buffer Tank

For the adjustment of the pH value of the acidification buffer tank the concept of the two point controller (bang-bang servo) was modified. Lye is not dosed continuously but in intervals, where the lye is added for a certain period of time and afterwards flushed into the acidification with substrate from the methane reactor. Substrate of the methane reactor is taken for flushing because it contains no solid particles which could harm the sensors at the inline test point QF. Afterwards, the circulation pump is switched off and the acidification buffer tank is stirred for a certain time in order to measure the correct pH (data are given in chapter 5.8). Depending on the new pH, the amount of lye is altered and a new lye addition cycle is started in order **to reach the pH set point asymptotically**. The amount of lye added also depends on the pH response of former pH control actions and on the fill level of the tank. However, controller settings are rejected if there is no lye addition for a longer period of time. In this case a relatively small amount of lye is added in the first cycle.

In each pH controller cycle the pH value is increased by a $\Delta\text{pH}_{\text{inc}}$, which is a fraction of the control deviation e (eq. 27). From the desired pH increase, the volume of lye ($V_{\text{lye_abs}}$) is calculated according to eq. 28 from the desired pH increase, the fuel

level of the reactor h (given as fraction of the full volume), the amount of lye which is necessary to increase the pH of the full reactor by one unit (V_{lye_rel}), and from the molar concentration of the strong base. V_{lye_rel} is arbitrarily set at the beginning.

$$\Delta pH_{inc} = e * f \quad (27)$$

$$V_{lye_abs} = \frac{\Delta pH_{inc} \cdot h \cdot V_{lye_rel}}{C_{lye}} \quad (28)$$

From the amount of lye which has to be added, the runtime of the lye pump is calculated by a simple multiplication with a factor. After each step, the actual increase of the pH value (ΔpH_{act}), which occurred due to dosage of the calculated amount of lye V_{lye_abs} , is measured and the new value for V_{lye_rel} is calculated according to eq. 29.

$$V_{lye_rel} = \frac{V_{lye_abs} \cdot C_{lye}}{h \cdot \Delta pH_{act}} \quad (29)$$

V_{lye_rel} is calculated after each step of lye addition, because the buffer depends on the pH value and changes gradually.

If the amount of lye V_{lye_abs} would be zero or negative due to a pH value, which is lower after the lye addition, V_{lye_abs} is set to 1.2 times the old value. Herewith a deadlock is prevented in case that acid is added during the activity of the pH controller.

According to the methods, which are described in chapter 5.8.1, the controller was parameterised and tested. The controller could adjust the pH value in any case with a maximum of 4 cycles of lye addition.

Behaviour of the controller after a change of the set point from pH 4.1 to 4.5 are shown in Figure 18, first graph. After only three cycles of lye addition the set point could be reached. At the beginning, lye is dosed only for 10 seconds as V_{lye_rel} is set arbitrarily to a relatively low value (eq. 28). As the pH increase is not very high, in the next cycle more lye is added (28 seconds). For the third cycle the deviation from the setpoint was small and therefore only a short runtime for the lye pump was necessary (7 seconds). A higher increase of the set point is shown in Figure 18, second graph, where the pH could be adjusted from 4.5 to 5.5 in three cycles, too. In this experiment the V_{lye_rel} was not initialised and therefore the value from the previous control action was used.

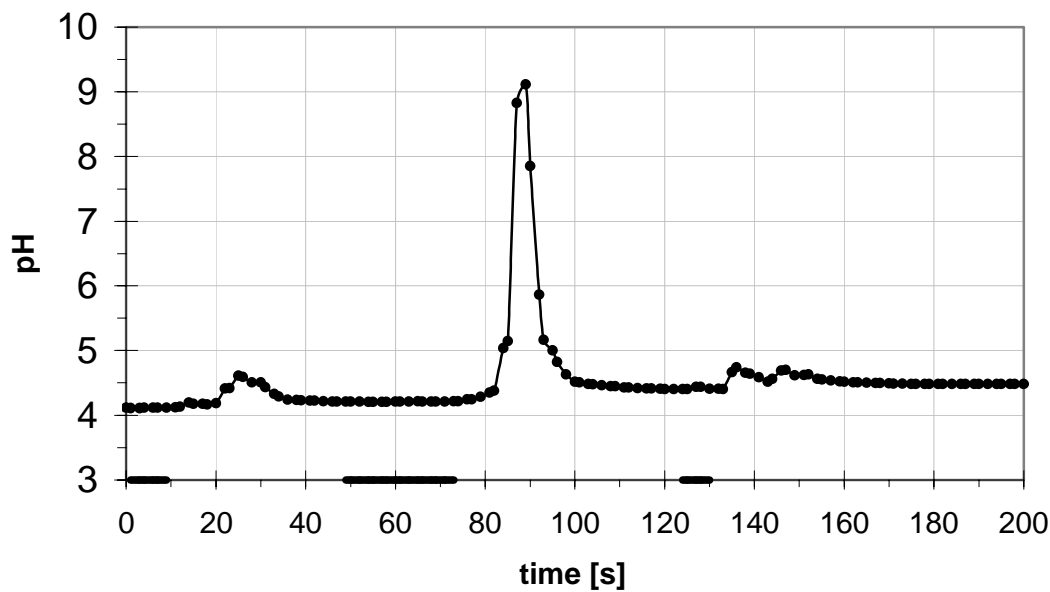


Figure 18 Response of the pH controller of the acidification buffer tank after the change of the set point. Beginning with a stationary state, the set point was changed at time 0 seconds from pH 4.1 to pH 4.5 and from pH 4.5 to pH 5.5. The operation of the lye pump is indicated on the X-Axis

The behaviour of the controller after a change of the actual value by adding strong acid and switching on the controller is shown in Figure 19, where the set point could also be reached after three cycles of lye addition. The experiment shown in Figure 20 illustrates the importance of the prevention of negative amounts of lye ($V_{\text{lye_abs}}$). As acetic acid was added during the activity of the controller, the pH reached a value lower than the tolerated deviation. Immediately the pH control began to react, but during that time the pH decreased further, which resulted in an even lower pH value after the first cycle of lye addition. Nevertheless, the controller could adjust the pH value within 4 cycles of lye addition.

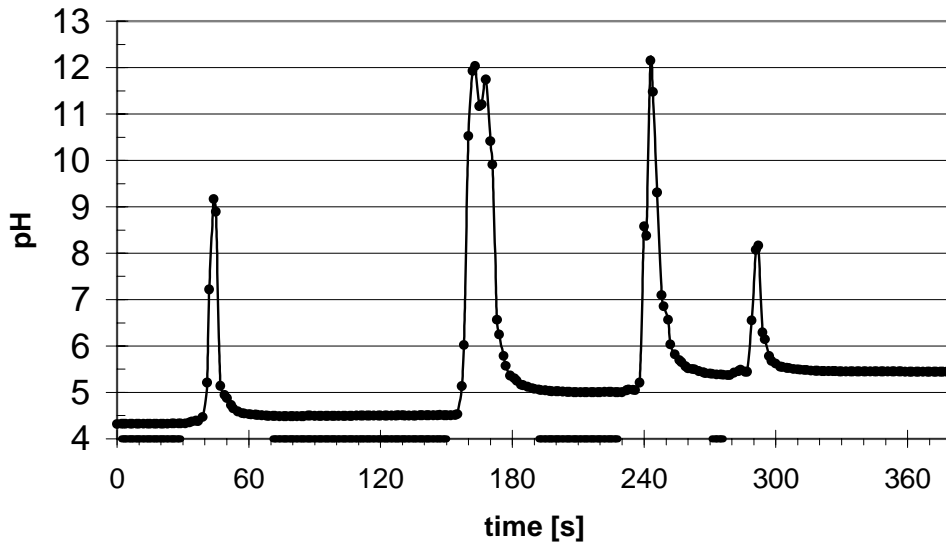


Figure 19 Response of the pH controller of the acidification buffer tank after the change of the actual value from pH 5.5 to 4.3. The controller was switched on at time 0 seconds. The operation of the lye pump is indicated on the X-Axis

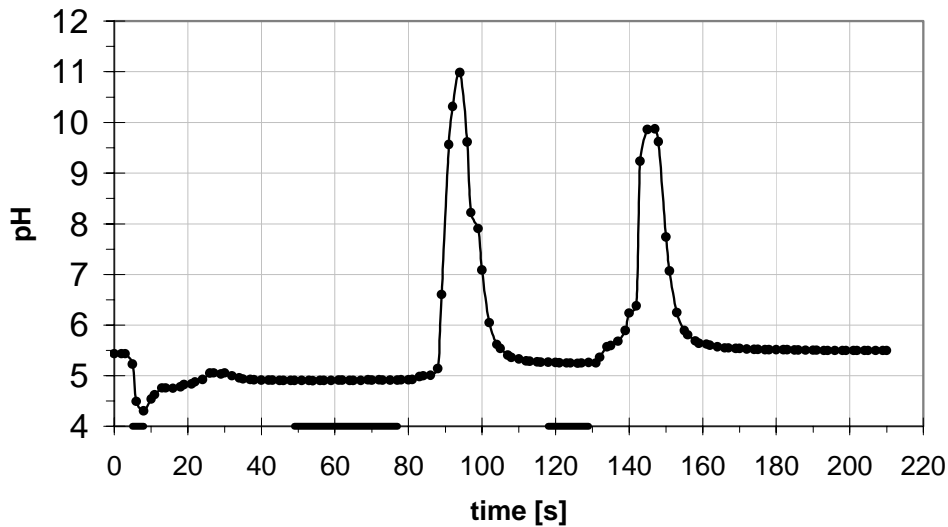


Figure 20 Response of the pH controller of the acidification buffer tank after a disturbance. At time 0 seconds 0.5 ml of conc. acetic acid were added. The operation of the lye pump is indicated on the abscissa.

The high peaks of the pH value, which can be seen on the figures, are due to the position of the pH sensor which is very close to the inlet of the lye/substrate mixture.

3.3.3 PID Controller for the Methane Reactor

A classical PID controller is used for adjustment of the pH value of the methane reactor. Due to the design of the reactor, the pH value can only be measured at the test point in the circulation pipe, therefore substrate from the methanogenic stage has to be circulated. However, this is the default operational state of the system (3.1). As the inlet of the lye is arranged directly in front of the pH sensor, the measurement of the pH value and dosage of lye have to be carried out in sequence. In between, the timespan in which the test point is filled and flushed with substrate as well as the response time of the pH sensor has to be waited for. Therefore, a scanning frequency of the pH value of about two minutes occurs (detailed settings are given in chapter 5.8.2). However, this is sufficient as is shown in the following. The schedule and the synchronisation of the states is described in paragraph 3.1.

The conventional PID controller algorithm

$$y = K_p \left(e + \frac{1}{T_n} \cdot \int e \cdot dt + T_v \cdot \dot{e} \right) \quad (30)$$

was extended in order to be able to use different circulation rates (\dot{V}), any concentrations of lye (C_{lye}) and a changed buffer capacity (f_{puffer}):

$$y = K'_p \left(e + \frac{1}{T_n} \cdot \int e \cdot dt + T_v \cdot \dot{e} \right) \cdot \frac{f_{puffer} \cdot \dot{V}}{C_{lye}} \quad (31)$$

The derivation of eq. 31 is given in the appendix. With the methods given in chapter 5.8.2, the PID controller was tuned; the obtained parameters are presented in Table 7.

Table 7. Parameters for the PID controller for the pH value of the methane reactor.

Parameter	Symbol	Value	Unit
proportional action coefficient, normalized for both, flow and concentration	K'_p	5509	$\frac{\text{mol}}{\text{m}^2} \cdot \text{h}$
integral action time	T_n	22.4	h
derivative action time	T_v	5.6	h

The controller was tested for 22 hours, in which several disturbances were raised (Figure 21). The quality of the control was not very good, as pH deviated up to one unit from the set point.

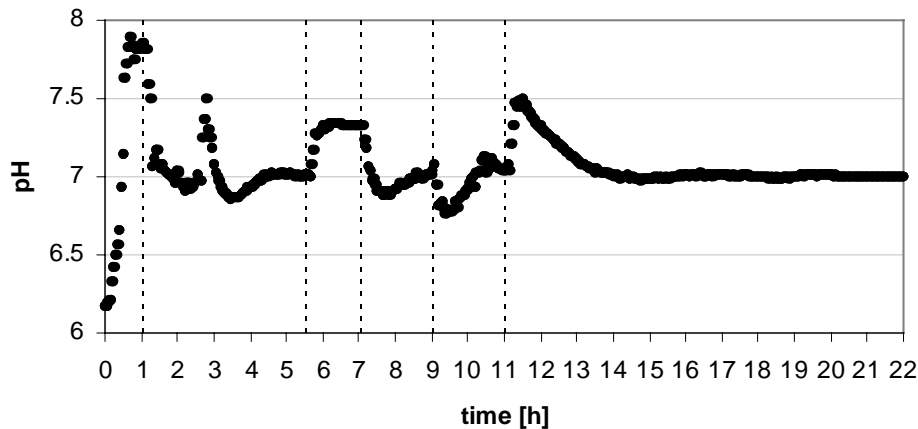


Figure 21 Course of the pH value in the methane reactor at the test of the controller for 22 hours. At the times which are indicated with dotted lines, disturbances were raised.

After the controller was switched on, the pH value increased up to a value of 7.9 and did not decrease, because no microorganisms, which could decrease it by metabolic products were in the reactor, nor was substrate from the acidification fed. At time 1 hour, substrate with pH 4 was fed into the methane reactor, whereupon the pH value decreased. The controller was able to maintain a pH of 7 ± 0.1 , except for the peak of 0.5 units after nearly 3 hours. At time 5.5 hours, feed was stopped and the pH increased until 7.3. After restart of the feed, pH decreased but was adjusted to 7.0. At 9 hours, when the feed was doubled, pH decreased down to 0.2 below the setpoint but could then be adjusted to 7 ± 0.1 .

As the pH value exceeded the set point every time the feed was stopped, the internal variables of the PID controller were examined. It could be observed that only the integral part of the controller caused the overrun, as the proportional and differential parts were near to zero, because the setpoint was reached before the stoppage.

Therefore, the program was modified in a way that the integral part of the controller was reset every time the feed was stopped. Hence the exceed could be avoided (Figure 22).

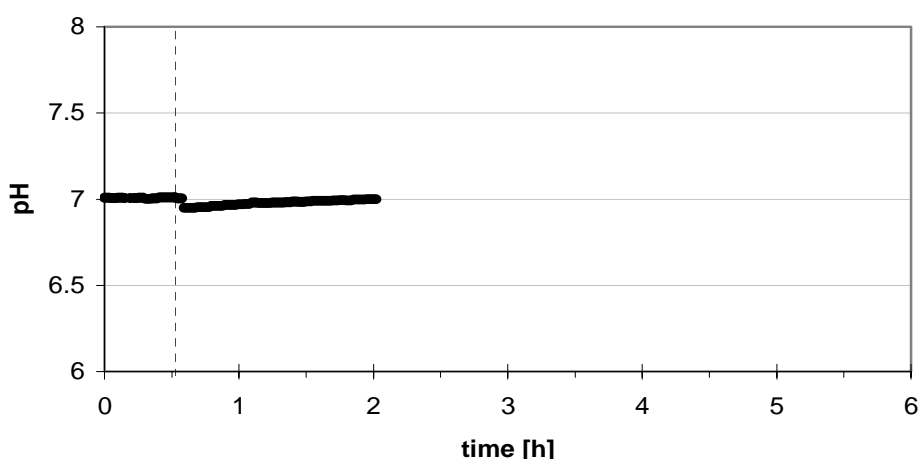


Figure 22. The pH value of the methane reactor after a modification of the controller. At the beginning substrate (pH 4) was fed into the methane reactor. When feed was stopped (dotted line), the integral part of the controller was reset.

The controller could not always adjust the pH value within 0.2 units. However, the substrate used in the testing (acetic acid and sodium hydroxide) shows no buffer capacity around the setpoint used (pH 7.0). Thus, it is quite difficult to obtain better results. For real substrate, there is always some buffer capacity around pH 7 (hydrogencarbonate), which might result in a better control quality.

3.3.4 Conclusions

The adaptive pH controller for the acidification buffer tank performed very well. The pH value could always be adjusted within a few cycles of lye addition. It adapted itself to new wastewater compositions. After a certain time without use, it resets the data learned automatically in order to achieve save settings.

The pH controller of the methane reactor sometimes exceeded the reference variable using acetic acid as controlled substrate. However, in all the experiments (sections 3.6.5.1 and 3.5) made with real substrate, which had a buffer capacity (hydrogen carbonate) within the desired pH range (pH 7), no critical exceeding occurred. Thus, the controller was sufficient for the present reactor. However, for larger reactors, where dead time increases, the concept might be modified.

3.4 Development of the Fuzzy Logic Expert System

A classical Fuzzy logic expert system (Mamdani) was applied, where the rules are generated from human expert knowledge. A detailed description of the Fuzzy logic methods and terms mentioned in this thesis is given by Zimmermann (1991); an introduction, including an example, in chapter 2.3.3. The general structure of the fuzzy logic rulebase, which was used in this thesis is described in section 3.4.1 of this subchapter. Details of the input variables are given in 3.4.2. The two levels of intermediate variables are described in sections 3.4.3 and 3.4.4. The output variables, which work as setpoint values for the subsidiary controllers, are described in section 3.4.5. Validation by experiments and by simulation is shown in the subsequent subchapters 3.5 and 3.6.

3.4.1 Structure of the Fuzzy System

Prior to setting up the fuzzy logic system, a knowledge base was created by an extensive literature review and by the use of data from own experiments. In order to obtain more insight and to separate the rules, which are used for the state detection, from the rules which determine the output, intermediate variables were introduced (Figure 23).

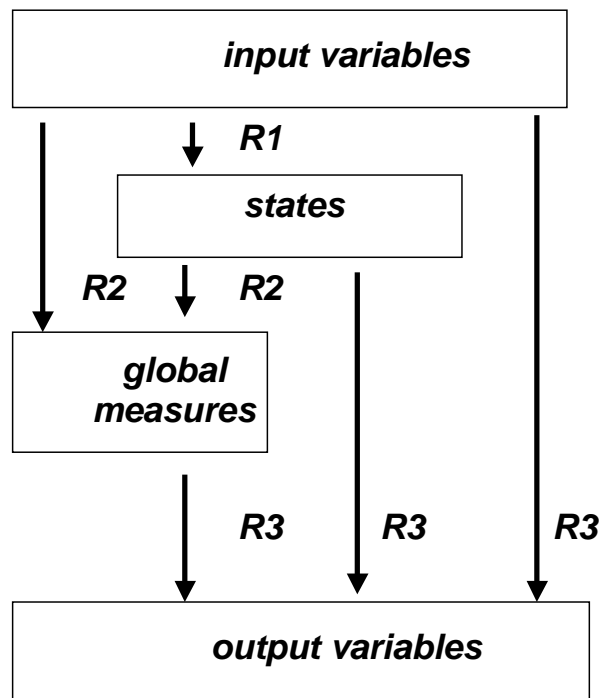


Figure 23. Structure of the multilevel fuzzy-logic rulebase. rule-levels *R1*, *R2*, *R3* are calculated consecutively. *R1*: rules which calculate states; *R2*: rules which calculate global measures; *R3*: rules which calculate the output variables.

Hence, a multi-level rulebase is applied, where the intermediate variables are calculated from input variables (Table 8: var. 1 .. 11). The first level of them describes the state of the system (var. 12, 13), the second the global measures, like the change of the conditions (var.14, 15) or of the feed_setp (var. 16). Finally, the output variables (var. 17 .. 22) are calculated, which act after defuzzification as set values for the subsidiary controls.

Next page:

Table 8. Variables for the fuzzy logic system. Sets can be left open (L), right open (R), triangles (D) or trapezes (T). Volumetric rates (var. 8, 10, 11, 21, 22) are scaled with the methane reactor volume. Places: 1 = acidification buffer tank, 2 = methane reactor.

Var.	Name	Place	Unit	Sets
1	hydrogen	2	ppm	low (T 0 1 50 100), medium (T 50 100 200 500), high (R 200 500)
2	methane	2	%	low (T 0 1 40 50), not_low (R 40 50), high (R 60 70)
3	pH	2		very low (L 6 6.2), low (D 6 6.2 6.6), optimal (T 6.2 6.6 7.8 8.2), high (R 7.8 8.2)
4	pH	1		low (L 4 5), optimal (T 4 5 5.5 6.5), high (R 5.5 6.5)
5	d_pH	1	h-1	decreasing (L -0.3 0), unchanged (T -0.3 -0.1 0.1 0.3), increasing (R 0.1 0.3)
6	temperature	1	°C	low (L 20 30), normal (D 20 30 35), optimal (D 30 35 42), high (R 35 42)
7	temperature	2	°C	low (L 30 35), optimal (D 30 35 42), high (R 35 42)
8	gasrate	2	h-1	no (T 0 0.00001 0.001 0.007), low (T 0.001 0.007 0.035 0.07), high (R 0.035 0.07)
9	filling level	1	%	empty (L 10 50), half (D 10 50 90), full (R 50 90)
10	feed	1	h-1	no_feed (L 0 0.04) , medium (D 0 0.04 0.08), high (R 0.04 0.08)
11	feed	2	h-1	no_feed (L 0 0.04) , medium (D 0 0.04 0.08), high (R 0.04 0.08)
12	state	1		stagnant, [shortage], [toxic], acidifying, premethanisation
13	state	2		shortage, normal, overload, toxic
14	conditions	1		worse, keep, better
15	conditions	2		worse, keep, better
16	feed_setp	2		no_feed (D -1 0 1), keep (D 0 1 2), more (D 1 2 3)
17	pH_setp	1		low (D 2.8 3.8 4.8), optimal (D 4 5 6)
18	pH_setp	2		low (D 5 6 7), optimal (T 5.8 6.8 7.8)
19	temperature_setp	1	°C	low (D 15 20 25), normal (D 25 30 35), optimal (D 30 35 40)
20	temperature_setp	2	°C	low (D 27 32 37), optimal (D 32 37 42)
21	recirculation_setp		h-1	no (D -0.01 0 0.01), normal (D 0 0.01 0.02), high (D 0.01 0.02 0.03)
22	circulation_setp	2	h-1	slow (D 1 2 3), fast (D 3 4 5)

As one variable-level acts as input for the following, the rulebase-levels R1 to R3 have to be calculated consecutively. The rules, which determine the states, the global measures and the output variables are given in Table 9, Table 10 and Table 11.

Table 9. Fuzzy rulebase - level R1: state detection. (1): methane reactor. (2): acidification buffer tank. R1-9 is weighted with 0.5, R1-10 and R1-11 with 0.1, R1-13 with 0.2.

Rule no.	IF	THEN
R1-1	d_pH(1) = increasing	state(1) = premethanisation
R1-2	d_pH(1) = unchanged	state(1) = stagnant
R1-3	d_pH(1) = decreasing	state(1) = acidifying
R1-4	methane(2) = high AND hydrogen(2) = low	state(2) = shortage
R1-5	TOC(2) = low	state(2) = shortage
R1-6	hydrogen(2) = high	state(2) = overload
R1-7	methane(2) = not_low AND NOT (hydrogen(2) = high)	state(2) = normal
R1-8	pH(2) = very_low	state(2) = toxic
R1-9	pH(2) = low	state(2) = overload
R1-10	pH(2) = optimal	state(2) = normal
R1-11	pH(2) = high	state(2) = shortage
R1-12	TOC(1) = low	state(1) = shortage
R1-13	gasrate(2) = no AND NOT (TOC(2) = high)	state(2) = shortage
R1-14	gasrate(2) = no AND TOC(2) = high	state(2) = toxic

Table 10. Fuzzy rulebase - R2: global measures. (1): methane reactor. (2): acidification buffer tank. , R2-6 is weighted with 0.5.

Rule no.	IF	THEN
R2-1	state(1) = stagnant AND filling_level(1) = empty	conditions(1) = worse
R2-2	state(1) = stagnant AND filling_level(1) = half	conditions(1) = keep
R2-3	state(1) = stagnant AND filling_level(1) = full	conditions(1) = better
R2-4	state(1) = acidifying	conditions(1) = better
R2-5	state(1) = shortage OR state(1) = premethanisation	conditions(1) = worse
R2-6	state(1) = acidifying AND NOT filling_level(1) = full	feed_setp(2) = no_feed
R2-7	state(2) = normal AND filling_level(1) = full	feed_setp(2) = more AND conditions(2) = better
R2-8	state(2) = normal AND filling_level(1) = half	feed_setp(2) = keep AND conditions(2) = keep
R2-9	state(2) = normal AND filling_level(1) = empty	conditions(2) = worse AND feed_setp(2) = no_feed
R2-10	state(2) = toxic	feed_setp (2) = no_feed AND conditions(2) = better
R2-11	state(2) = overload	feed_setp (2) = no_feed
R2-12	state(2) = overload AND (feed_rate(2) = no_feed OR filling_level(1) = full)	conditions(2) = better
R2-13	state(2) = shortage AND NOT filling_level(1) = empty	feed_setp(2) = more AND conditions(2) = keep
R2-14	state(2) = shortage AND filling_level(1) = empty	conditions(2) = worse AND feed_setp (2) = keep

Table 11. Fuzzy rulebase – R3: output variables. (1): methane reactor. (2): acidification buffer tank.

Rule no.	IF	THEN
R3-1	conditions(1) = keep AND (pH(1) = optimal OR pH(1) = high)	pH_setp(1) = optimal
R3-2	conditions(1) = keep AND pH(1) = low	pH_setp(1) = low
R3-3	conditions(1) = better	pH_setp(1) = optimal
R3-4	conditions(1) = worse	pH_setp(1) = low
R3-5	conditions(2) = keep AND (pH(2) = optimal OR pH(2) = high)	pH_setp(2) = optimal
R3-6	conditions(2) = keep AND pH(2) = low	pH_setp(2) = low
R3-7	conditions(2) = better AND pH(2) = low	pH_setp(2) = optimal
R3-8	conditions(2) = better AND pH(2) = very_low	pH_setp(2) = low
R3-9	conditions(2) = worse AND (pH(2) = optimal OR pH(2) = high)	pH_setp(2) = low
R3-10	conditions(1) = keep AND temperature(1) = low	temperature_setp(1) = low
R3-11	conditions(1) = keep AND temperature(1) = normal	temperature_setp(1) = normal
R3-12	conditions(1) = keep AND (temperature(1) = optimal OR temperature(1) = high)	temperature_setp(1) = optimal
R3-13	conditions(2) = keep AND temperature(2) = low	temperature_setp(2) = low
R3-14	conditions(2) = keep AND (temperature(2) = optimal OR temperature(2) = high)	temperature_setp(2) = optimal
R3-15	gasrate(2) = high OR feed_rate(2) = high	circulation_setp (2) = fast
R3-16	NOT (gasrate(2) = high OR feed_rate(2) = high)	circulation_setp (2) = slow
R3-17	state(1) = premethanisation	recirculation_setp = no
R3-18	pH(1) = high	recirculation_setp = no
R3-19	pH(1) = low	recirculation_setp = high
R3-20	pH(1) = optimal AND NOT feed_rate(1) = no_feed	recirculation_setp = normal
R3-21	pH(2) = high AND pH(1) = low	recirculation_setp = high

For the Fuzzy operators, the standard functions MIN (truth (A and B) = minimum (truth(x), truth(y))), MAX (truth (x or y) = maximum (truth(x), truth(y))), and INV (truth (not x) = 1.0 - truth (x)) are most time sufficient (Cordón et al, 1997) and therefore also here used. As a rule, the sets of the Fuzzy variables are defined that way the sum gives a truth value of 1.0 (compare Figure 5 in chapter 2). The shapes of the sets can be triangles (denoted as D in Table 8), trapezes (T), left open (L), and right open (R). All the output variables are defuzzified with the centre of gravity method (COG).

3.4.2 Input values

The most interesting input variable is the hydrogen concentration in the off-gas of the methane reactor (Table 8: var.1; Figure 5a). In own experiments it was seen that the hydrogen concentration was around 100 to 200 ppm at normal operation (defined as pH 7 ± 0.5 , COD in the outflow $< 500 \text{ mg l}^{-1}$ for at least 24 hours, data not shown) of the reactor with all types of investigated waste water. In case of low loading the hydrogen decreased to a minimum of 10 ppm, vice versa after a pulse of substrate from the acidification buffer tank into the methane reactor the hydrogen rose to more than 500 ppm. Similar observations were made by other authors (Harper and Pohland, 1986; Guwy et al, 1997). Due to reliability aspects of the control system the set “low” is defined ≥ 0 in order to avoid erroneous activity of rules in case of measurement failure.

While high hydrogen concentrations inhibit degradation of propionate and therefore can indicate a situation of a beginning overload, low values of methane concentration ($< 50 \%$) and pH (< 6.0) show an already existing overload (Braun, 1982; Ghaly, 1996; Kalyuzhuyi and Davlyatshina, 1997) and are therefore integrated, already for redundancy.

At pH (var.18, Figure 24) less than 6.2 to 6.0 methane production usually does not occur thus it is considered to be “very low”. Inversely, at low loading rates proteins and volatile fatty acids are better digested which is indicated by a higher pH (Guwy et al, 1997) and optimal methane yields. However, “high” pH values of 8 and more amplify toxicity of ammonia.

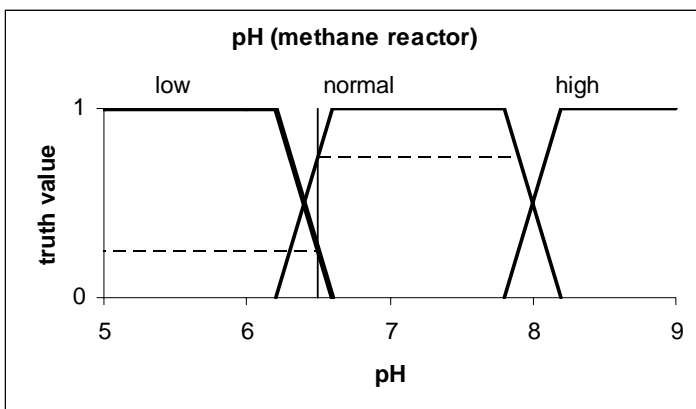


Figure 24. Fuzzy Sets of the input variable “pH” of the methane reactor. Truth values for a pH value of 6.5 are indicated with broken lines.

Methane content of the biogas depends not only on the substrate (Bushwell equation) and the degree of degradation but also on the solubility of the carbon dioxide, which depends much on the pH. However, methane yields of less than 40 to 50 % are considered to be low, more than 60 to 70 % are high (var. 2).

While a very low gas production rate of the methane reactor (var. 8) indicates lack of substrate or toxicity, the rate and composition of the gas from the acidification was not taken into account, because in many applications there will not be a gas flow at all as carbon dioxide resides in the liquid up to several grams per litre. Another reason was that the high content of hydrogen sulphide reduces life time of the sensors. Thus the pH (var. 4) of the acidification buffer tank, which should be kept in the range 4,5 to 6 (Braun, 1982), and its derivative (var.5, averaged over 1 hour and corrected for external pH changes due to feed and lye addition) were used for computation of the state and for the measures.

The input values of the temperature of both reactors (var. 6 and 7) are only used for calculation of their new set points. The filling level of the buffer tank (var. 9) is needed for the determination of the measures, as it is the case for the feed (var. 10, 11).

There are some other parameters which could be of importance for specific types of wastewater, like the sulphur content, the ammonia concentration or the alkalinity. These were not taken into account for the current system, as they were relative constant and in reasonable ranges during the experiments. The observed concentrations (< 5000 ppm hydrogen sulphide, 200 mg l⁻¹ ammonia) were not expected to affect the sensitive acetogenic and methanogenic population much as the pH range was always between 6 and 7.5. Also other parameters which would be of interest (e.g. the volatile fatty acid concentrations) were not considered as input variables as they cannot be easily measured online.

The conductivity, which can easily be measured on-line, could only be used for the calculation of the volatile fatty acid concentrations at a certain pH range and if the concentration of other ions as well as the pH value was known. Considerations about the conductivity in relation to the volatile fatty acids are given in the Appendix.

3.4.3 Fermentation states

Regarding the acidification buffer tank, an increasing pH is a consequence of destruction of proteins (Guwy et al, 1997) and indicates that the retention time of the liquid in the acidification buffer tank is too high. We call this state (var.12) “premethanisation” (Table 9: R1-1). A drop in pH is due to production of volatile fatty acids and is named “acidifying” (R1-3). A constant pH is represented by “stagnant” (R1-2), which can have more reasons, e.g. high buffer capacity, inhibition, complete degradation, or shortage. A more specific characterisation would be possible, but additional sensors like for the TOC (total organic carbon) and volatile

fatty acids were needed. If the TOC was measured, R-12 could be applied. Further, detection of a toxic situation in this tank is not possible without measurement of the concentration of the substances, which can be still acidified, or without using a toxicity-sensor. However, toxic effects seldom appear in the acidification due to its versatile microbial population. The values of the gas composition of this tank were not used, because of the varying filling level and the high volume which was needed in relation to the gas production rate. Additionally, for lower concentrated waste waters there is nearly no gas production, because carbon dioxide remains solved in the liquid up to several grams per litre. However, the state of the acidification buffer tank is not as important as it is of the methane reactor and so it seems not to be necessary to add more measurement devices.

For the methane reactor the prediction of the state is much more important than of the acidification, as its microbial population is much more sensitive than in the latter. For this reactor we defined the states “shortage”, “normal”, “overload” and “toxic” (var. 13). The situation “shortage” is characterised by low hydrogen concentrations together with high methane concentrations (R1-4) while “overload” is indicated by high hydrogen concentrations (R1-6). “toxic” is termed by very low pH levels (R1-8) or no gas production. When gas production goes down, it could be due to a shortage of substrate or toxic inhibition. Therefore the TOC (or a similar parameter, like BOD or COD) could be used as an optional parameter for distinguishing the states shortage (of substrate) from toxicity. However, we didn't use such a measurement because it was not necessary for avoiding an overload, which is the most common problem. If online TOC measurement were available, we suggest to apply the additional rules R1-13 and R1-14 for being able to distinguish between toxicity and shortage, as a decrease in the gas production could be due to toxic effects or depletion of substrate. These rules were only tested with offline COD values and it is not known yet if the toxic state can be detected early enough in order to avoid a halt of the system.

Another measurement which is not as expensive – the absorbance around 254 nm (SAK₂₅₄)- which is often measured in aerobic systems as a correlation with the COD, TOC or BOD cannot be used for the anaerobic treatment as own experiments show, because sulphides have an absorbance of about four magnitudes higher than most other common components. Further, the density could not be used as a replacement for the TOC as the substrate was too much diluted. A kind of COD measurement, the oxidation with hydroxyl ions, was also not applicable as acetic acid, a key component in anaerobic digestion, could only hardly be measured. These investigations about the usability of the SAK, the density or the oxidation method as a parameter for the substrate concentration are shown in the Appendix.

For redundancy reasons there exist additional rules which use only the pH value (R1-8 .. R1-11). pH values less than 6 inhibit formation of methane, therefore we classify this state as “toxic” (R1-8). Less low pH values indicate probably (if not due to acid addition) an overload (R1-9, weighted by 50 %). If the pH is around 7 or more,

it is likely that the state is normal or even shortage. However, higher pH values can also result from dosage of lye, therefore these rules (R1-10, R1-11) are weighted by 10 % only - thus they have significant influence solely if gas measurement fails.

3.4.4 Global strategies

From the input variables and the states the measures are generated. Two global measures can be realised– change of the feed (var. 16) and change of the conditions (var. 14 and 15). Which measures are realised, depends on the determined state and on input values, like the filling level of the acidification buffer tank, which in turn depends on the feed rates.

If the filling level is high or if acidification is still going on, the conditions of the acidification buffer tank are set better in order to increase the pre-digestion rate which finally supports the methane reactor performance, too. If it is empty or if there is no non-acidified substrate left, conditions are made worse in order to prevent production of methane at this stage (R2-1 .. R2-5). If the buffer tank is not full and its state is “acidification”, feed into the methane reactor is lowered somewhat (rule is weighted by 0.5) in order to get a more complete pre-digestion (R2-6).

Generally, feed into the methane reactor is lowered, if it is overloaded or the buffer tank becomes empty. Vice versa feed is increased and the conditions are improved if the buffer is full or if a shortage is detected (R2-7.. R2-14). In case of an overload, the conditions are only improved if the feed rate (averaged over one hour) is already zero or if the buffer tank is full (R2-11, R2-12).

3.4.5 Output values

Using the feed change instead of an absolute feed set value makes it possible to handle very big changes in wastewater concentration. As the center of gravity of the set “more” is 2.0 and the current value of the feed is averaged over one hour, thus feed can be doubled per hour, independent of the current feed rate. On the other hand, as the set “no_feed” is defined as zero, feed can be stopped immediately in case of an overload. The suggested change rate of the feed was calculated outside the fuzzy system by multiplying the old feed rate (averaged over one hour) with the suggested change. At this place a restriction was made, so that the feed rate cannot become infinite large.

For changing of the conditions not the rate for the change is calculated but the manipulated variables pH (var. 17 and 18) and temperature (var. 19 and 20) are set directly by the fuzzy system with an additional set of rules (R3-1..R3-14), but without the need of external processing. This approach was selected because, contrary to the feed, these values are not allowed to change in a wide range. Though temperature dependency of non-adapted microbial community of the methane reactor can be described with an Arrhenius-derived model (Kettunen and Rintala, 1997),

where the activity becomes about half per 10 degrees of decrease, methanogens are often regarded to be sensitive to fast temperature changes, therefore the temperature of the methane reactor was kept in a much smaller range than for the acidification buffer tank.

Recirculation from the methane reactor back into the acidification (var. 21) depends on the pH of the acidification (R3-17.. R3-21) and is made in order to increase a low pH in the acidification. However, recirculation is only possible if the liquid level in the methane reactor is beyond the outlet into the recirculation pipe (Figure 7) and therefore still dosage of lye will be needed sometimes.

Circulation of the methane reactor (var. 22) is set fast if much gas is produced or if much substrate was fed (R3-15). Otherwise, intensive circulation is not necessary and therefore it is set to slow (R3-16).

3.4.6 Conclusions

A multi-level fuzzy logic rulebase was developed, which uses measured values, which can be relatively economically obtained. The first level of the intermediate variables represents the state of the reactors, which give a good insight into the system. However, for the acidification buffer tank, state detection is only very limited, which was a compromise between cost and importance.

Although measurement of TOC or COD was not foreseen in order to keep costs and maintenance low, considering industrial applications, rules are given, which use the TOC. With the use of TOC measurement, toxicity might be distinguished from shortage of substrate. However, main objective was to avoid overloads.

From the detected states and depending on other input variables, global measures are set instead of directly setting the reference values of the underlying subcontrollers (which are the manipulated variables of the fuzzy logic system). This has the advantage, that in case of different reactor configurations adaptations would be easier, as only the last-level rules had to be adapted.

An experimental validation with the use of the fuzzy logic control system is introduced in the next subchapter. Also, a validation using the simulation model, as described in subchapter 3.6, is applied in subchapter 3.7.

3.5 Experimental Validation of the Whole System

Three overload experiments from the testing of the system will be shown, whereas in experiment (E1) only the state detection of the fuzzy system was used and not the suggested control actions. In experiment (E2) the controller had to handle wastewater with strong variations in both, volume and concentration. In experiment (E3) very high COD (120 g l^{-1}) was fed. Influent and effluent concentrations during the experiments are shown in Table 12.

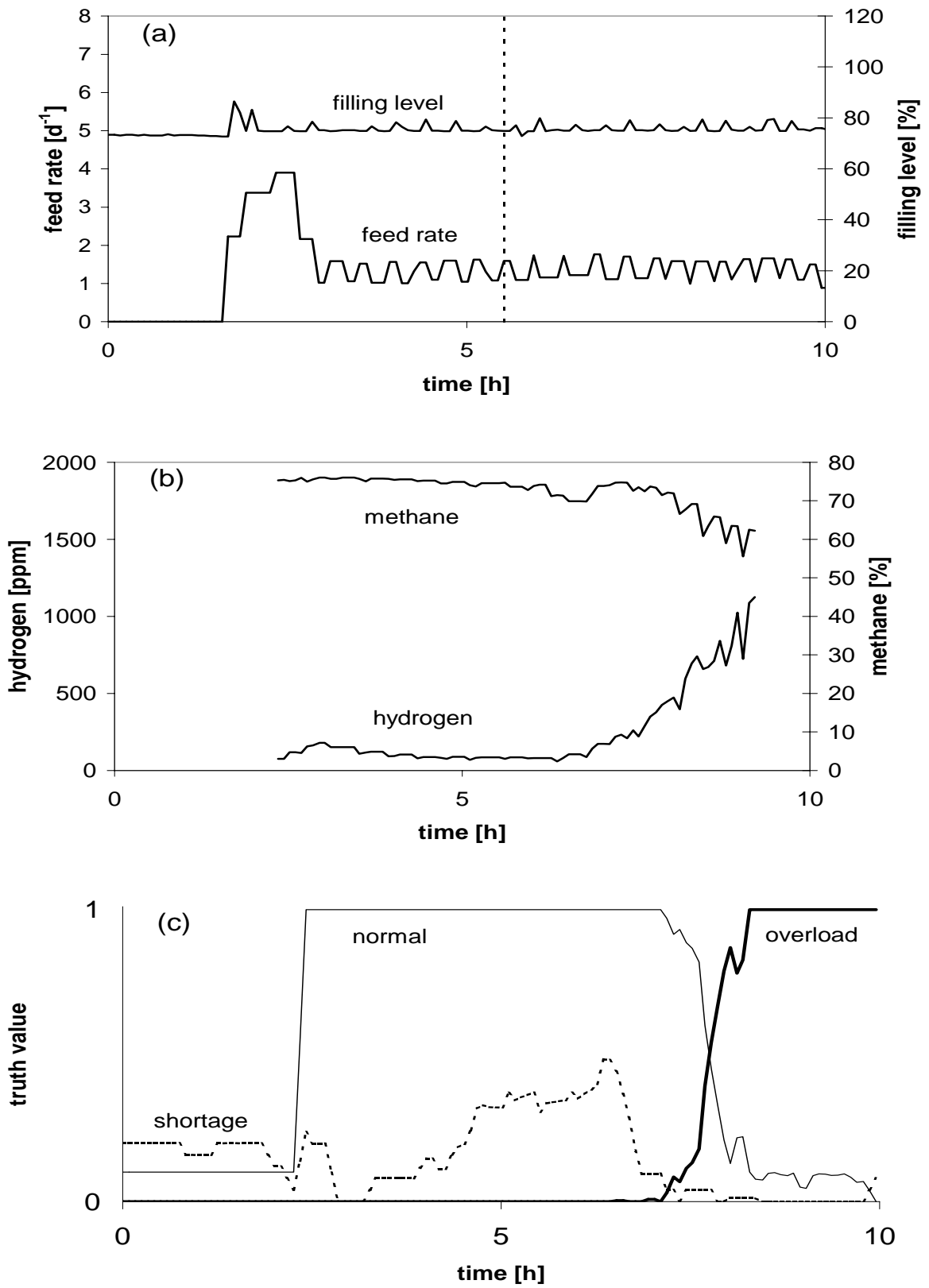
Table 12. Feed rate (d^{-1}), influent and effluent concentrations (g COD l^{-1}) of the experiments (1)-(3) at different times (h). The feed rate is expressed as the volumetric flow into the acidification buffer tank per unit of volume of the methane reactor – see also Figure 25(a) to Figure 27(a). Type: P: wastewater from potato processing, M: mash from pectine production, B: beer. Influent concentration: Into acidification. Effluent concentration: From methane reactor; time when sample was taken in brackets (h). ^x No effluent, sample was taken from methane reactor.

Exp.	Time	Feed rate	Type	Influent conc.	Effluent conc. (time)
(E1)	0 – 2	0			
	2 – 3	0 - 4	P	3.3	
	3 – 5.5	1-1.5	P	3.3	0.61(5.5)
	5.5 – 10	1-1.5	C	28	7.4 (10)
(E2)	0 – 13	≤ 3.5	P	3.3	0.24 (13)
	13 – 22	~ 1	M	28	3.4^x (22)
	22 – 25	~ 1	P	3.3	
	25 – 35	0			
	35 – 67	0 – 2.5	P	3.3	0.74 (45), 1.0 (67)
	67 – 72	~ 1	M	28	
	72 – 83	~ 1	P	3.3	
	83 – 85	0.5 – 1	M	28	
	85- 95	~ 1	P	3.3	0.85 (90)
	95 - 115	0	0		0.44 (110)
(E3)	0 - 1	0			0.65 (1)
	1 - 2	1 - 3	B	120	
	2 - 7	1 – 1.5	B	120	3.2 (7)
	7 - 65	0			1.1 (35), 0.58 (60)

(E1) Filling level (75 %), temperature (30 °C in acidification and 35 °C in methane reactor), pH (≥ 4.0 and ≥ 7.0 respectively) and circulation rate of the methane reactor (4 h^{-1}) were kept constant in this experiment. As the filling level of the acidification buffer tank was not changed, the feed into the methane reactor was equal to the feed into the buffer tank. Before the start of the experiment, there was no feed for several days and therefore no gas production, too. Thus the state (c) was estimated from pH values and gas production only. As these rules (Table 9: R1-10, R1-11, and R1-13) are weighted by 0.1 and 0.2 respectively, the truth value of “shortage” was max. 0.2. Shortly before hour 2, substrate from potato processing with a COD of 3.3 g l^{-1} was added at a high rate for one hour and decreased afterwards (Figure 25a). When gas production started and the values became valid (flushing of the gas measurement installation is necessary) after a relatively short period of about one hour, methane was more than 70 % and hydrogen around 100 ppm (Figure 25b) – the state indicated was “normal”. At hour 5.5 feed rate was kept constant but the wastewater was changed (28 g COD l^{-1} from pectin production). One and a half hour later, hydrogen raised and at hour 8 “overload” was detected with a truth value of 1.0. As the output values of the fuzzy controller were not used, the feed rate was still kept for the next hours. Ultimately hydrogen raised up to 1000 ppm and foam cloaked the gas pipe totally. In the end, before the experiment was stopped the COD of the methane reactor was already more than 7 g l^{-1} .

Next page:

Figure 25. Experiment (E1) without control. (a) shows the feed (volumetric flow into the acidification buffer tank per unit of volume of the methane reactor (d-1)) and the filling level of the acidification buffer tank (%). Switching of wastewater (from 3.3 to 28 g COD l-1) is indicated with a dotted line. (b) concentrations of hydrogen (ppm) and methane (%) in the off-gas of the methane reactor. (c) truth values (degree of membership) of the fuzzy sets of the state variable for the methane reactor. Overload is indicated with a thick line, normal with a smaller line and shortage with a dotted line.

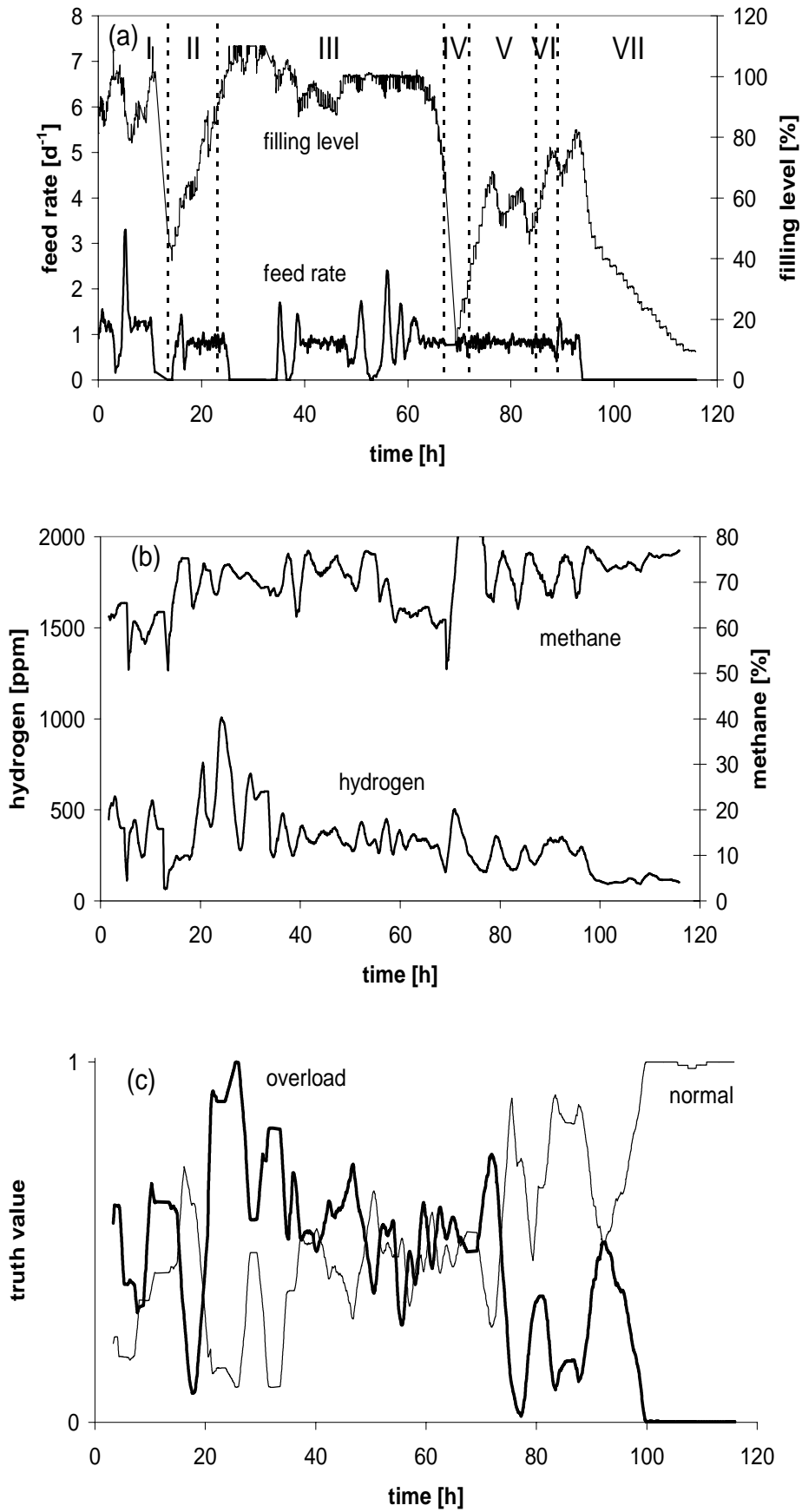


Though methane concentration decreased during the overload, it happened one hour later than the increase of the hydrogen. In addition, methane was always more than 50 % - even at the end of the experiment. Finally, it took more than two weeks for the recovery of the system and a decrease of the COD to less than $0,5 \text{ g l}^{-1}$.

(E2) For the second experiment the plant ran fully automated and was controlled by the fuzzy system. Starting already slightly overloaded (normal and overload was detected at the same time), in the first ten hours approximately as much wastewater (3.3 g COD l^{-1} from potato processing) was added to the acidification buffer tank as could be fed to the methane reactor in order to keep the state constant (Figure 26a, I). As expected, the average of the obtained state was between overload and normal as long as the filling level was more than half, which was due to the rules R2-7ff, whereby generally more substrate is fed the more full the acidification buffer tank is. After the feed was lowered, the state turned to normal and the buffer was emptied relatively fast to 40 % until the wastewater with a COD of 28 g l^{-1} was fed (II). As the state turned to overload the level of the buffer increased until the buffer became full after 25 hours. The fluctuations in the filling level were due to back feed from the methane reactor into the acidification in order to keep the pH of the latter tank in a reasonable range (rules R3-17ff). Until about 60 hours as much wastewater with 3.3 g l^{-1} (III) was added as possible.

Next page:

Figure 26. Experiment (E2) with Fuzzy controller switched on. (a) shows the feed (volumetric flow into the acidification buffer tank per unit of volume of the methane reactor (d-1)) and the filling level of the acidification buffer tank (%). COD of the inflow: 3.3 g l^{-1} (I, III, V, VII) and 28 g l^{-1} (II, IV, VI). (b) concentrations of hydrogen (ppm) and methane (%) in the off-gas of the methane reactor. (c) truth values (degree of membership) of the fuzzy sets of the state variable of the methane reactor. Overload is indicated with a thick line and normal with a smaller one. Shortage was always less or equal to 0.2 and is not shown.

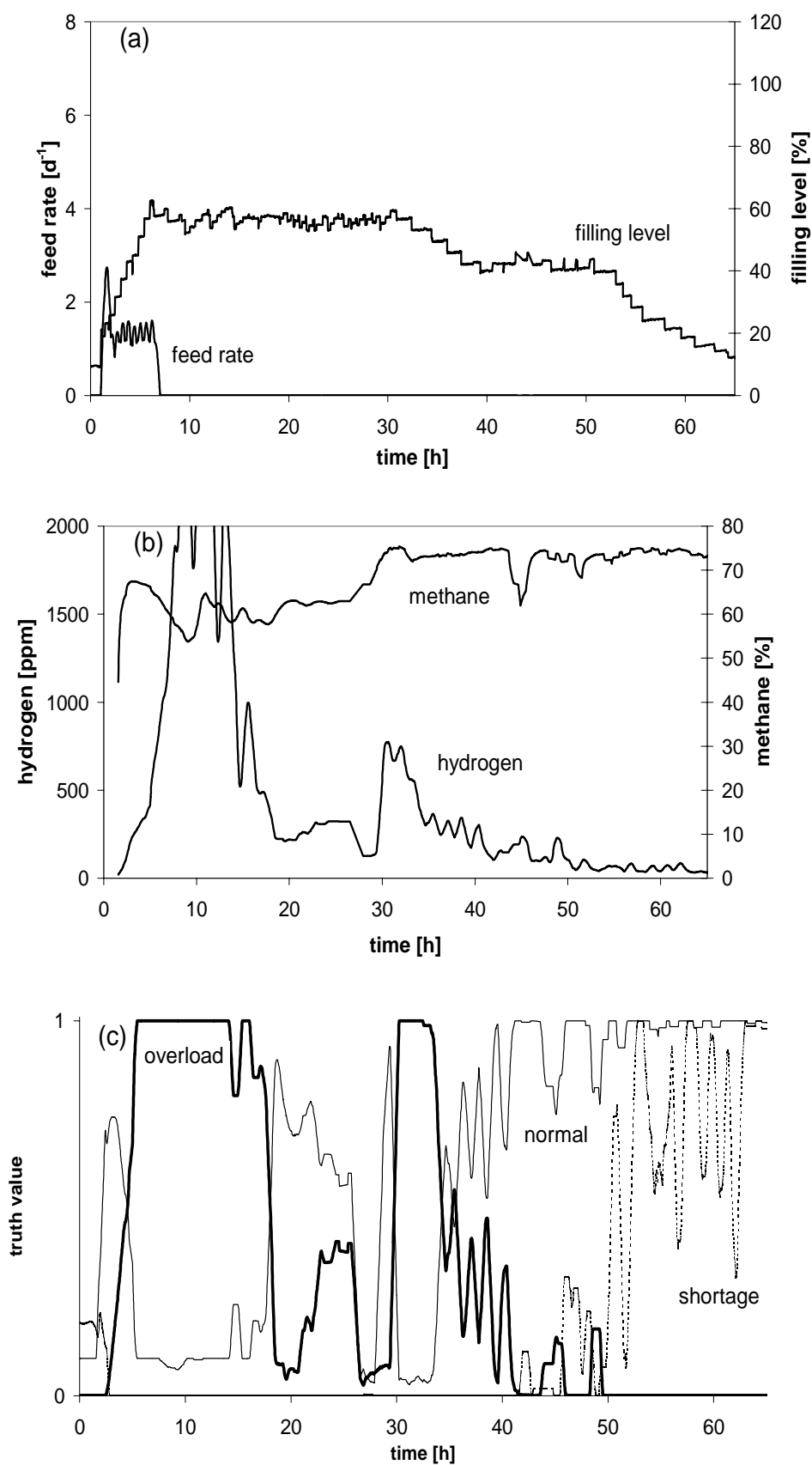


Again, the state was both, overloaded and normal to nearly the same extent. When the overload began to disappear it was switched to the concentrated wastewater two times for 4 to 5 hours (IV, VI), which resulted in an increase of the buffer level each time. After a complete stop of the feed, the overload disappeared and the buffer tank was emptied within one day (VII). From the half filling level on, feed into the methane reactor became slower than before. This is a feature of the rules in order to delay the emptying of the acidification buffer tank. During the experiment the effluent COD concentration was always between 0.4 and 1,0 g l⁻¹.

(E3) In the third experiment, during the first six hours beer (COD 120 g l⁻¹) was added continuously into the acidification buffer tank, though the reactor was not designed for such high COD loading, as not less than 2 % of the methane reactor volume can be added at once. Thus an relevant amount of substrate was fed into the methane reactor (Figure 27a). Consequently the state changed from shortage to normal and further to a substantial overload (Figure 27c). When overload began to disappear, feed into the methane reactor was forced between hours 20 and 30. Yet the filling level of the acidification buffer tank did not decline because feed back from the methane reactor into the acidification buffer tank was done automatically in order to raise the pH in the acidification buffer tank. There was also relevant back feed between hours 40 and 50.

Next page:

Figure 27. Experiment (E3) (beer, 120 g COD l⁻¹) with Fuzzy controller switched on. (a) shows the feed (volumetric flow into the acidification buffer tank per unit of volume of the methane reactor (d-1)) and the filling level of the acidification buffer tank (%). (b) concentrations of hydrogen (ppm) and methane (%) in the off-gas of the methane reactor. (c) truth values (degree of membership) of the fuzzy sets of the state variable for the methane reactor. *Overload* is indicated with a thick line, *normal* with a smaller line and *shortage* with a dotted line.



At other times, when no back feed was necessary or it was not possible due to not enough volume in the methane reactor, the filling level of the acidification buffer tank could be lowered. After about 66 hours the minimum filling level of about 10 % was reached. Comparing the pH (Figure 28) with the methane concentration (Figure 27b) it can be seen, that methane is higher when pH increases and vice versa (hours 10, 30 and 45). During the whole experiment, the effluent COD was less than 3 g l^{-1} , which is a very good value for pre-treatment in respect of the very high feed concentration.

The adjustment of optimal conditions in respect to exclude an overload leads evidently to a good treatment efficiency. Therefore it is very likely, that an COD measurement is not necessary at all for achievement of low effluent concentrations. The set points and actual values of the pH (methane reactor) and the temperature (both reactors) are shown in Figure 28. The set point of the temperature of the methane reactor was varied between 30 and 35 °C while the set point of the acidification buffer tank was varied between 20 and 35 °C. At about hour 5 the set point of pH of the methane reactor became higher than the actual value. Therefore NaOH was dosed in this period. The more the overload disappeared and shortage appeared, the more the set point was lowered while the actual value increased. From hour 43 on no dosage of lye was necessary anymore.

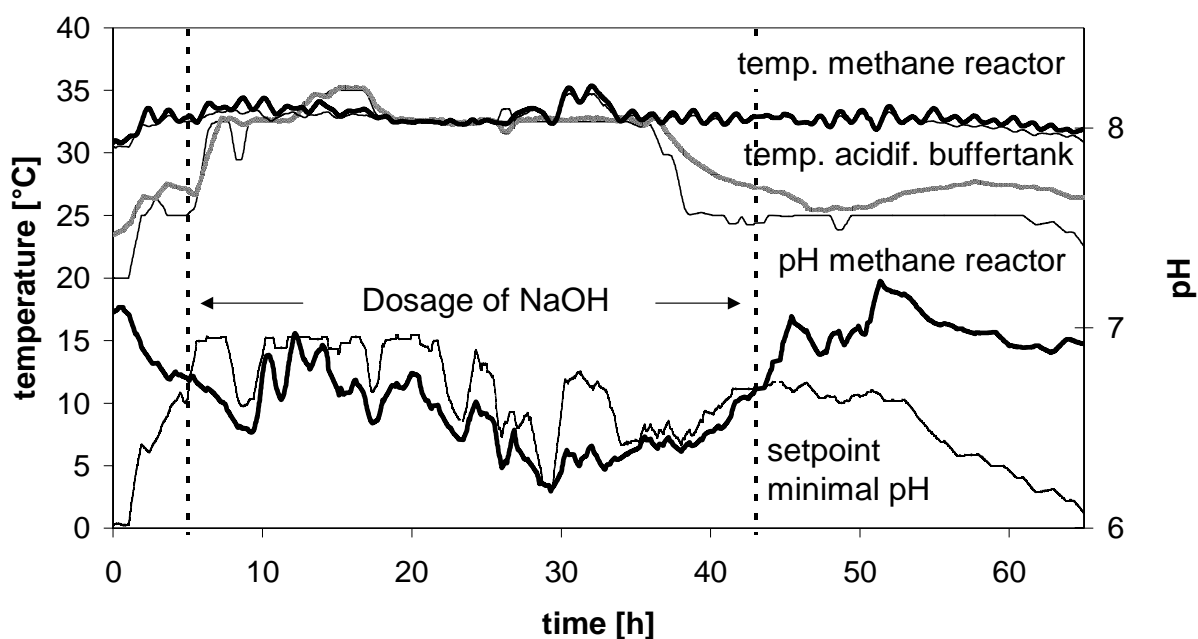


Figure 28 Experiment (E3): pH (methane reactor) and temperature (both reactors). The start and the end of the period of dosage of NaOH (methane reactor) is indicated with a broken line. Measured values are shown with thick lines, set point values with thinner ones.

3.5.1 Conclusions

With the fuzzy-logic system presented in the previous subchapter, the two stage laboratory scale anaerobic wastewater treatment plant was controlled that its overload state could be recognised and an heavy overload could always be avoided. Very strong fluctuations in the loading are handled automatically, even a restart of the feeding with a very high COD concentration ($> 100 \text{ g l}^{-1}$) after several days of stand-by was possible. Moreover, measurement of the wastewater concentration (COD, TOC etc.) was not necessary in order to obtain relative low effluent concentrations. The adjustment of optimal conditions in respect to avoid an overload leads evidently to a good treatment efficiency.

In the next subchapter, the system is further studied using a dynamic simulation model. There, an improvement will be shown, where effluent quality could be enhanced in simulations.

3.6 Modelling and Simulation

A simulation model of the laboratory scale wastewater treatment plant was developed in order to

- validate the control system
- gain more insight into the whole process
- perform sensitivity analysis for identification of the important parameters and conditions
- be able to simulate new reactor configurations in future

3.6.1 Requirements for the Simulation Model

The simulation model should be able to describe the underlying reactor configuration, i. e. a wastewater treatment plant including a tank reactor with partial biomass retention and an anaerobic filter reactor. It should be used for validation of the fuzzy logic controller, which uses the concentrations of hydrogen and methane in the biogas, the gas production rate and the pH as input values. Although, the manipulated variables of the fuzzy logic system should be used as setpoint values in the simulation. Thus it is necessary that the simulation model is able to calculate all these values. In particular the hydrogen peaks, which are observed after substrate additions, should also be shown in the model. As the fuzzy logic controller calculates the set points of the feed into both reactors, circulation rate, back flow from the methane reactor into the acidification buffer tank, temperature and the pH value, it should be possible to change these values in the model. Further, it should be possible to simulate common substrates, including complex carbohydrates, fats and proteins.

3.6.2 Existing Models

In recent years, many models for anaerobic digestion were developed. Some of the most recent papers, which are relevant for the objective of this paper, are introduced.

Angelidaki et al (1999) modelled the whole process from hydrolysis to methane formation including all the important intermediate substances, but did not use hydrogen kinetics as it lead to unrealistic fast dynamic behaviour. They modelled a thermophilic CSTR (40..64°C). Hydrogenotrophic methanogens were not taken into account. Temperature and pH effects were modelled, whereas the temperature dependence of microbial growth was modelled using two linear functions with a slower rise up to the optimum and a sharp decrease for temperatures higher than the optimum. The influence of the pH value was modelled using a normalised Michaelis pH function, which shows a bell-shaped curve. Acetic acid and long chain fatty acids inhibit most reactions in the model, but propionate and butyrate were not taken into account for inhibition of the acetogenic or methanogenic reactions.

v. Münch et al (1999) primarily modelled the production of volatile fatty acids from complex substrates in a CSTR. But they did distinguish between the different acids. Only acidogenic bacteria and acetoclastic methanogens were taken into account, but acetogenic bacteria and hydrogenotrophic methanogens were not considered. A pH dependency was not taken into account either.

Kus (1993) and Kiupel (1997) modelled the anaerobic digestion of glucose in a CSTR taking into account all the relevant bacterial groups, as well as the substrates acetate, propionate, butyrate and hydrogen. Different from other models, the hydrogen inhibition was only placed at the acidification stage and not on the acetogenesis. They took also into account the pH value.

Kalyuzhnyi (1996) modelled the degradation of glucose, ethanol and butyrate. Propionate was treated like butyrate, as its behaviour was similar. Also hydrogen and pH was modelled but not a temperature dependency. Acidogenic products are produced at a fixed ratio. Hydrogen, propionate and ethanol are used as inhibitors for the acetogenic and/or methanogenic steps. Based on this work, a UASB reactor was modelled by Kalyuzhni and Fedorovich (1997) where transport, distribution and mass transfer were taken into account.

Wu and Hickey (1997) modelled an UASB reactor with acetate degradation with special attention to hydraulics and diffusion. They found that none of the three factors, kinetics, mass transfer/diffusion, and hydraulics, can be ignored in modelling UASB reactors, which should also apply to other biofilm reactors. The particle radius showed most influence on the simulation of an acetate pulse experiment, as the biofilm surface area increases exponentially with decreasing radius. Although very important was, which basic reactor types (CSTR, PFR) or a combination of them respectively, was used in the simulation in order to achieve the correct retention time distribution. A combination of a CSTR and a PFR gave good results for the UASB

reactor. For the specific maximum substrate uptake rate ($q_{s,max}$) and the diffusion coefficient (D), a sensitivity of about one was found, but for the latter one only when the value was decreased. Obviously, D was nearly limiting, therefore an increase did not affect sensitivity as much as a decrease. This is a good example that sensitivity analysis has always to be interpreted with care. The Monod type half saturation constant (K_s) did not have much effect on the shape of the acetate degradation peak, as the substrate concentration was much higher than K_s . Not important at all was a mass transfer coefficient (K_L) through a fictive liquid boundary layer.

Huang and Jih (1997) modelled an anaerobic filter for acetate degradation with attention to the flow regime and mass transfer within the biofilm. However, microbiology was only considered little.

Batstone et al (2000) present an extensive model with complex carbohydrates, proteins and fat as substrate, where hydrogen plays an inhibitory role in the acidification as well as in the acetogenesis. This model is a further development of the model of Costello et al (1991), Romli (1993), Ramsay (1997) and is based on the model of Mosey (1983), who had first introduced hydrogen behaviour. Here, propionate is not produced directly but from lactate, which depends, like the production of acetate and butyrate, on the hydrogen partial pressure. pH dependency was modelled for values below the optimum, whereas higher pH values were not regarded. Hydrogen inhibition was modelled for the acidogenic and acetogenic bacteria. For these groups also a product inhibition was introduced, i. e. a competitive one for the first, a non-competitive one for the latter. However, propionate and the other volatile fatty acids were not used as inhibitory substances for methanogenic bacteria, though propionate is often mentioned in literature as an important inhibitor for methanogenic bacteria.

There was no metabolic model available for the biogas process. A metabolic model would reduce the number of parameters needed, because maximal use could be made of both biochemical knowledge of the system and conservation principles of elements and compounds (Murnleitner et al, 1997). Apart from a low number of model parameters, the value of the majority of parameters would be more or less fixed since they are based on biochemical knowledge of the process, which would be an important advantage when calibrating the model. However, development of a metabolic model requires detailed knowledge of the metabolism of the organism, while the concentrations of the converted compounds are sufficient for calibration of the classical models.

3.6.3 General Strategy and Choice of Base Models

None of the existing models fully fulfils the requirements. Either they do not take into account all the relevant bacterial groups and substrates, or they do not consider transport processes, like mass transfer, diffusion or reactor hydraulics. Certainly, one of the reasons for simplifications in previous models is the high computational

capacity, which would be needed, taking all these into account. However, as the performance of computers increases steadily, models can be formulated more detailed now. With such a detailed model, many assumptions and restrictions, which otherwise would limit its use, can be omitted. However, if such a complex model is developed, a full validation becomes very difficult and expendable. Therefore, already validated models are used as base models in this thesis. However, changes and extensions have to be made carefully. It has to be assured, that new features are not already incorporated invisibly in some way. For an example, if an inhibition term for a substance is newly introduced, all the parameters of the base model can remain unchanged as long as the concentration of the inhibitory substance was not significant when the kinetic parameters were estimated from the experiments. But if the concentration was beyond irrelevant levels, inhibition is obviously included into other parameter somehow.

It was observed by some authors, that the dynamic behaviour of some models was unrealistic fast. Therefore, Angelidaki et al (1997) did not use hydrogen for kinetic equations. Such fast behaviour can probably be explained due to the fact that transport processes were not taken into account in most models. This is particularly true for the hydrogen, as generally no mass transfer resistance is assumed in the observed models. The models (Costello et al, 1991; Romli, 1993; Ramsay, 1997; Kalyuzhnyi, 1997; Batstone et al, 2000), which take the hydrogen into account, use the partial pressure rather than the dissolved concentration in their terms assuming that the equilibrium is formed infinitely fast. But this is often not true, as diffusion barrier can exist (Pauss et al, 1993). This would particularly occur, if a reactor with biofilm (UASB, FBBR, AF) was used for receiving experimental data but in the model only a CSTR reactor would be modelled (Batstone et al, 2000), whereby diffusion inside the biofilm is thus omitted. Kinetic data obtained under those configurations (i.e. not taking into account mass transfer) have to be regarded carefully when diffusion will be introduced.

The model presented in this work is mainly based on the model of Costello et al (1991), which was further developed by Romli (1993), Ramsay (1997), and Batstone et al (2000). Some of the altered kinetic constants and simplifications during evolution of this model were not taken over but the original work was used rather. This especially applies to the half saturation constants, which were altered by Ramsay in order to fit full scale reactors without the need of modelling of mass transfer. All relevant substances including the complex substrates (carbohydrates, proteins, fat) are included in the selected base model, except ethanol, which became important if brewery wastewater would be treated. Thus ethanol degradation was taken from Kalyuzhnyi (1997).

As the pH dependency was only defined for pH below the optimum, an inhibition term for higher pH was introduced in this work, which depends on the ammonia

concentration. As the pH value was not calculated in the basic model, it was calculated similar to Angelidaki (1993).

A temperature dependency was introduced as described by Dochain and Perrier (1996). Ammonia uptake was introduced into the model in order to avoid growth on depletion, because in the basic model from Batstone et al (2000), ammonia is only produced but not consumed. The resulting model was then further extended in order to being able to simulate gas exchange and the gas measurement, the different flows between the two reactors, and diffusion in the biofilm. The methane reactor was modelled of different compartments in order to achieve the observed residence time distribution of the methane reactor. Further, a simple pH controller was introduced into the model as well as a temperature controller.

As the model should be used to test the fuzzy logic control system and hence should resemble real qualitative behaviour rather than displaying a good fit of a single experiment, no extensive fitting was performed but sensitivity analysis were performed in order to classify the importance of parameters.

For simulation the software Aquasim was used, where many differential equations for liquid and mass balances for basic reactor types are already implemented (Reichert, 1994). For being able to test the fuzzy logic controller on the simulation model, the core of the Aquasim program was encapsulated into a shell with COM-Automation for making data exchange with the fuzzy logic software.

3.6.4 Development and Details of the Model

The model equations are classified into several relevant groups, which are described separately. These groups are the following:

- (I) physico chemical reactions,
- (II) microbial and biochemical conversions,
- (III) mass transfer and
- (IV) fluxes between compartments.

In principle, all the conversions can occur in every compartment. However, hydrolysis is only possible in the bulk liquid as complex carbohydrates, proteins and fat cannot penetrate into the biofilm. No conversions take place in the headspace, as only the carbon dioxide, methane and hydrogen can enter the gas phase. For the dissolved chemical compounds the balance reads as eq. 32. For an explanation of the subscripts see also Figure 29.

$$\frac{dC_i}{dt} = \left(\frac{dC_i}{dt}\right)_{in} + \left(\frac{dC_i}{dt}\right)_{out} + \left(\frac{dC_i}{dt}\right)_{gas} + \left(\frac{dC_i}{dt}\right)_{film} + \left(\frac{dC_i}{dt}\right)_{hydroly} + \left(\frac{dC_i}{dt}\right)_{conv} + \left(\frac{dC_i}{dt}\right)_{growth} + \left(\frac{dC_i}{dt}\right)_{decay} \quad (32)$$

whereby i =

a anions from strong acids

aa.....	amino acids
ac.....	acetate, acetic acid
b	cations form strong bases
but	butyrate, butyric acid
ch2o	complex carbohydrates
ch4	methane
co2	carbon dioxide
et	ethanol
fat	fat
gluc	glucose
h	Protons (H ⁺)
h2	hydrogen (H ₂)
h2o	water vapour
lac.....	lactate, lactic acid
lcfa	long chain fatty acids
nh4	total ammonia
po4	phosphate
pro.....	propionate, propionic acid
prot.....	complex proteins
val	valerate, valeric acid

Complex substrates, which do not penetrate into the biofilm, are hydrolysed by extra cellular enzymes ($C_{e,i}$, whereby $i = \text{ch}_2\text{o}, \text{prot}, \text{fat}$; eq. 33).

$$\frac{dC_{e,i}}{dt} = \left(\frac{dC_{e,i}}{dt} \right)_{in} + \left(\frac{dC_{e,i}}{dt} \right)_{out} + \left(\frac{dC_{e,i}}{dt} \right)_{form} \quad (33)$$

For each of the relevant monomer substrates, a separate microorganism group (eq. 34), which consume only one particular substrate, was modelled.

$$\frac{dC_{X,i}}{dt} = \left(\frac{dC_{X,i}}{dt} \right)_{in} + \left(\frac{dC_{X,i}}{dt} \right)_{out} + \left(\frac{dC_{X,i}}{dt} \right)_{film} + \left(\frac{dC_{X,i}}{dt} \right)_{growth} + \left(\frac{dC_{X,i}}{dt} \right)_{decay} \quad (34)$$

whereby i indicates the main substrate which is converted by the particular bacteria. Hence

$X, i =$

- $X, \text{aa} \dots \dots \dots$ amino acid degrading bacteria
- $X, \text{ac} \dots \dots \dots$ acetate degraders (acetoclastic methanogens)
- $X, \text{but} \dots \dots \dots$ butyrate degraders (one of the acetogenic bacteria)
- $X, \text{et} \dots \dots \dots$ ethanol degraders (one of the acetogenic bacteria)
- $X, \text{gluc} \dots \dots \dots$ glucose degraders (adidogenic bacteria)
- $X, \text{h}_2 \dots \dots \dots$ hydrogen and carbon dioxide consumers (hydrogenotrophic methanogens)
- $X, \text{lac} \dots \dots \dots$ lactate degraders (one of the acetogenic bacteria)
- $X, \text{lcfa} \dots \dots \dots$ long chain fatty acid degraders (one of the acetogenic bacteria)
- $X, \text{pro} \dots \dots \dots$ propionate degraders (one of the acetogenic bacteria)
- $X, \text{val} \dots \dots \dots$ valerate, valeric acid (one of the acetogenic bacteria)

The flows into a compartment and the conversion processes are illustrated in Figure 29.

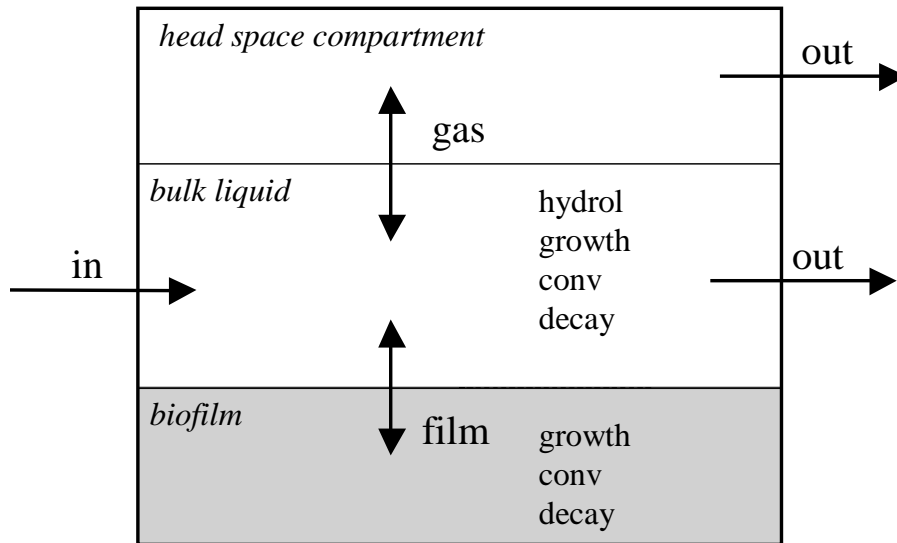


Figure 29. Flows and conversion processes in a compartment.

- in..... liquid flow into the bulk liquid**
- out..... liquid or gas flow out of a compartment**
- film mass transfer between the bulk liquid and the biofilm**
- gas..... mass transfer between the bulk liquid and the headspace**
- hydrol..... hydrolysis of complex substrates**
- growth..... biomass formation**
- conv conversion of substrate for biomass conversion and energy production**
- decay decay of biomass**

Figure 30 shows two possibilities, how the particular compartments could be connected to form the laboratory scale plant as described in chapter 2.4. A pH-step function-response of the real reactor compared with different simulated reactor configurations (including Figure 30 a and b) is shown in the Appendix.

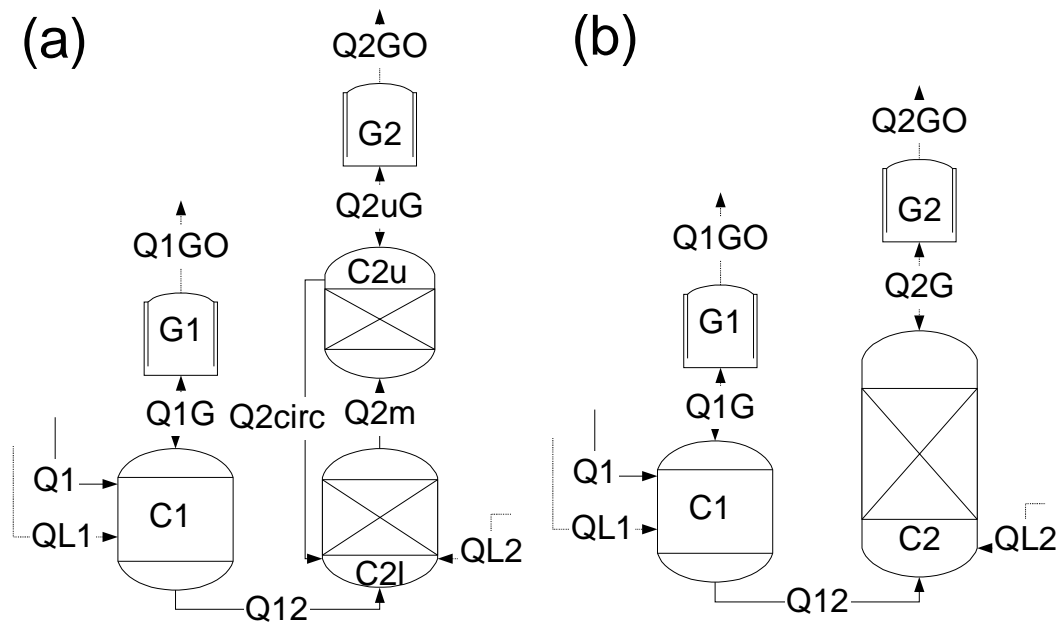


Figure 30. Compartments and fluxes of the simulation model. G1, G2: head space; C1: acidification buffer tank; C2l, C2u: lower and upper compartment of methane reactor; C2: methane reactor; Q1: inflow into acidification, Q12: feed into methane reactor; C2circ: circulation rate; QL1, QL2: lye dosage; Q1G, Q2G: liquid/gas exchange; Q1GO, Q2GO: gas flow

3.6.4.1 Physico Chemical Reactions

The physico chemical reaction system is necessary for calculation of the pH value. As many of the relevant intermediate products in anaerobic digestion are weak acids or bases, they influence and buffer the pH due to incomplete dissociation, which can generally be expressed with the well known equations

$$K_a = \frac{C_h \cdot C_{diss}}{C_{undiss}} \quad (35)$$

$$K_b = \frac{C_{oh} \cdot C_{diss}}{C_{undiss}}, \text{ whereby } C_{oh} = \frac{k_w}{C_h} \quad (36)$$

whereby K_a and K_b is the dissociation constant for the acid and the base, C_h , C_{diss} , C_{undiss} are the (molar) concentrations of protons (H^+), the dissociated and the undissociated anions respectively. Together with the anions and cations from strong acids and bases (as NaOH and HCl), which dissociate fully, the pH can be calculated by solving the charge balance (Angelidaki et al, 1993), which was accordingly used by Batstone (2000).

$$C_h = \sum \frac{K_{a,i} \cdot C_i}{K_{a,i} + C_h} + \sum C_a - \sum C_b + \frac{k_w}{C_h} \quad (37)$$

C_a are the anions from strong acids ($\frac{1}{2} \text{SO}_4^{2-}$, Cl^-) and C_b the cations from strong bases (Na^+). Introducing all relevant substances and taking into account, that the concentrations are given in C-moles, equation 37 can be rewritten, whereby the concentration of protons (C_h) is calculated by solving the charge balance for $b = 0$ (eq.38).

$$b = \frac{K_{a,ac} \cdot \left(\frac{C_{ac}}{2} + \frac{C_{pro}}{3} + \frac{C_{but}}{4} + \frac{C_{val}}{5} \right)}{K_{a,ac} + C_h} + \frac{K_{a,co2} \cdot C_{co2}}{K_{a,co2} + C_h} + \frac{K_{a1,po4} \cdot C_{po4}}{K_{a1,po4} + C_h} \\ + \frac{K_{a2,po4} \cdot \frac{K_{a1,po4} \cdot C_{po4}}{K_{a1,po4} + C_h}}{K_{a2,po4} + C_h} + \frac{K_{a,lac} \cdot C_{lac}}{K_{a,lac} + C_h} + C_a - \frac{K_{b,nh4} \cdot C_{nh4}}{K_{b,nh4} + \frac{k_w}{C_h}} - C_b + \frac{k_w}{C_h} - C_h \quad (38)$$

For acetate, butyrate, propionate and valerate, the same dissociation constant from acetate was used, as the difference is only minor (pK_a is 1.76, 1.88, 1.82, 1.88 resp. (Sillen and Martel, 1964). For calculation of the pK_a [mol m^{-3}] was used, therefore pK_a is 3 Units lower than found in literature. A temperature dependency is not taken into account, because there is only about 0.05 difference in pK_a between 25 °C and 60 °C. Also, for the dissociation of carbon dioxide no temperature dependency is taken into account, but rather the value for 35 °C is applied ($\text{pK}_a = 3.26$), as pK_a is 3.42 to 3.18 in the range of 0 to 55 °C. Dissociation of long chain fatty acids and proteins are not taken into account, as the influence on the pH is not expected to be high. Dissociation constants for phosphate ($\text{pK}_{a1} = -0.851$, $\text{pK}_{a2} = 4.21$, $\text{pK}_{a3} = 9.35$) and lactate ($\text{pK}_a = 0.853$) were chosen from Atkins (1996). However, temperature dependency of K_b for ammonia (eq. 39) is much higher as for all the other substances (pK_a is 3.95 and 3.60 for 25 and 55 °C respectively, Snoeying and Jenkins, 1980) and therefore taken into account.

$$K_{b,nh4} = \frac{k_w(T)}{5.01187 \cdot 10^{-7.00/e^f}}, f = \frac{51965}{8.315} \cdot \left(\frac{1}{273+T} - \frac{1}{298} \right) \quad (39)$$

The temperature dependency for k_w is even higher ($\text{pK}_w = 11,00$ and $10,10$ (k_w in mol/m^3) at 25 and 55°C resp.), and therefore k_w is made temperature dependent (Batstone, 2000):

$$k_w(T) = 10^{-11.00/e^f}, f = \frac{55900}{8.315} \cdot \left(\frac{1}{273+T} - \frac{1}{298} \right) \quad (40)$$

Unlike Angelidaki et al (1993), equation 38 is not solved iteratively, but like a very fast kinetic reaction (eq. 41), which could reduce overall computation time by 2 decades (from several days to some hours) and which was sufficiently accurate and fast.

$$\frac{dC_h}{dt} = b \cdot C_h \cdot 10^6 \quad (41)$$

3.6.4.2 Microbial and Biochemical Conversions

Complex substrates are hydrolysed by extracellular enzymes according to Batstone et al (2000) giving the monomers. They used a bulk-liquid, shrinking-core model. Production rate of the enzymes is connected to growth rates of the glucose degrading (= acidogenic), amino acid degrading and fat degrading bacteria. The microbial equations describe substrate consumption, growth and decay/maintenance. Substrate consumption is used for providing the energy needed for growth and maintenance, whereas the substrate which is incorporated into the biomass is consumed by the growth process. Hence two processes are used for growth, which indeed simplifies the stoichiometric coefficients. All the monomers are degraded according to Costello (1991) except of ethanol (Kalyushnyi, 1997). The difference in the rate equations between Costello and Batstone is, that the latter leaved out substrate inhibition. Maintenance/Decay is modelled as an inverse growth process: biomass is consumed and substrate is produced. Although this process is called decay by Batstone et al (2000), it actually represents the maintenance. Apparently, more substrate must be consumed, whereas for real decay complex carbohydrates and proteins should be formed rather than the monomers. The difference is, that in the latter case substrate cannot immediately be used, because it has to be hydrolysed first. However, both basic approaches are common and do not make much difference, as decay rates are relatively small compared to growth rates.

All these processes, which are described in detail in the following, were made temperature-dependent.

The hydrolysis of complex substrates and the conversion of the monomers can be described (eq. 42) by multiplication of the stoichiometric matrix S_{stoich} (Table 14) with the rate vector R_{rate} (Table 13).

$$M_{conv} = S_{stoich} \cdot R_{rate} \quad (42)$$

M_{conv} describes only hydrolysis and substrate conversion but not growth, decay and formation of enzymes.

Table 13. Rate vector R for hydrolysis and conversions.

Rate	Vector R	Eq.
$\Gamma_{ch2o,hydrol}$	$k_{ch2o} \cdot C_{ch2o}^{4/3} \cdot \left(\frac{C_{e,ch2o}}{\alpha + C_{e,ch2o}} \right) \cdot f_T$	(43)
$\Gamma_{fat,hydrol}$	$k_{fat} \cdot C_{fat}^{4/3} \cdot \left(\frac{C_{e,fat}}{\alpha + C_{e,fat}} \right) \cdot f_T$	(44)
$\Gamma_{prot,hydrol}$	$k_{prot} \cdot C_{prot}^{4/3} \cdot \left(\frac{C_{e,prot}}{\alpha + C_{e,prot}} \right) \cdot f_T$	(45)
$\Gamma_{gluc,conv}$	$k_{gluc} \cdot M_{gluc} \cdot M_{nh4} \cdot I_{nh4,pH} \cdot \frac{1}{1 + \frac{C_{ac} + \frac{C_{lac}}{1.5} + \frac{C_{but}}{2}}{K_{I,gluc,ac_lac_but}}} \cdot f_T \cdot f_{pH,gluc} \cdot C_{X,gluc}$	(46)
$\Gamma_{lcfa,conv}$	$k_{lcfa} \cdot M_{lcfa} \cdot M_{nh4} \cdot I_{nh4,pH} \cdot f_T \cdot f_{pH,lcfa} \cdot f_{h2} \cdot C_{X,lcfa}$	(47)
$\Gamma_{aa,conv}$	$k_{aa} \cdot M_{aa} \cdot M_{nh4} \cdot I_{nh4,pH} \cdot f_T \cdot f_{pH,aa} \cdot C_{X,aa}$	(48)
$\Gamma_{lac,conv}$	$k_{lac} \cdot M_{lac} \cdot M_{nh4} \cdot I_{nh4,pH} \cdot \frac{1}{1 + \frac{C_{ac} + \frac{C_{pro}}{1.5}}{K_{I,lac,ac_pro}}} \cdot f_T \cdot f_{pH,lac} \cdot C_{X,lac}$	(49)
$\Gamma_{ac,conv}$	$k_{ac} \cdot M_{ac} \cdot M_{nh4} \cdot I_{nh4,pH} \cdot f_T \cdot f_{pH,ac} \cdot C_{X,ac}$	(50)
$\Gamma_{pro,conv}$	$k_{pro} \cdot \frac{C_{pro}}{C_{pro} + K_{I,pro,ac} \cdot \left(1 + \frac{C_{ac}}{K_{I,pro,ac}} \right)} \cdot M_{nh4} \cdot I_{nh4,pH} \cdot f_T \cdot f_{pH,pro} \cdot f_{h2} \cdot C_{X,pro}$	(51)
$\Gamma_{but,conv}$	$k_{but} \cdot \frac{C_{but}}{C_{but} + K_{I,but,ac} \cdot \left(1 + \frac{C_{ac}}{K_{I,but,ac}} \right)} \cdot M_{nh4} \cdot I_{nh4,pH} \cdot f_T \cdot f_{pH,but} \cdot f_{h2} \cdot C_{X,but}$	(52)
$\Gamma_{val,conv}$	$k_{val} \cdot M_{val} \cdot M_{nh4} \cdot I_{nh4,pH} \cdot f_T \cdot f_{pH,val} \cdot f_{h2} \cdot C_{X,val}$	(53)
$\Gamma_{et,conv}$	$k_{et} \cdot M_{et} \cdot M_{nh4} \cdot I_{nh4,pH} \cdot f_T \cdot f_{pH,et} \cdot f_{h2} \cdot C_{X,et}$	(54)
$\Gamma_{h2,conv}$	$k_{h2} \cdot M_{h2} \cdot M_{co2} \cdot M_{nh4} \cdot I_{nh4,pH} \cdot f_T \cdot f_{pH,h2} \cdot C_{X,h2}$	(55)

$$M_i = \frac{C_i}{C_i + K_i}, f_{h2} = \text{eq. 67}; M_{nh4} = \text{eq.64}, I_{nh4,pH} = \text{eq. 66}, f_T = \text{eq.63},$$

$$f_{pH,i} = \text{eqs. 65a, b.}$$

For each C-mol substrate converted into fermentation products, $Y_{X,i}$ C-mol biomass is produced (eq. 56), whereby additional substrate and ammonia is consumed (eqs. 57, 58).

$$\left(\frac{dC_{X,i}}{dt}\right)_{growth} = -\left(\frac{dC_i}{dt}\right)_{conv} \cdot Y_{X,i} \quad (56)$$

$$\left(\frac{dC_i}{dt}\right)_{growth} = \left(\frac{dC_{X,i}}{dt}\right)_{growth} \quad (57)$$

$$\left(\frac{dC_{nh4}}{dt}\right)_{growth} = \sum -\left(\frac{dC_{x,i}}{dt}\right)_{growth} \cdot 0.2 \quad (58)$$

Hence, yield is related only to the amount of converted substrate and not to total substrate consumption. There is no big difference as Yield is small (biological parameters are given in Table 15) but S_{stoich} could be kept simpler (Batstone, 2000). The balance remains fulfilled anyway.

Decay is modelled like a simple first order reaction (eq. 59). As degradation products are defined to be substrates (eq. 60), this definition of decay is actually equivalent to maintenance. Biological parameters are given in Table 15.

$$\left(\frac{dC_{X,i}}{dt}\right)_{decay} = -d_{X,i} \cdot C_{X,i} \cdot f_{T,maint} \quad (59)$$

$$\left(\frac{dC_i}{dt}\right)_{decay} = -\left(\frac{dC_{X,i}}{dt}\right)_{decay} \quad (60)$$

Production of hydrolytic enzymes ($C_{e,ch2o}$, $C_{e,prot}$, $C_{e,fat}$) is linked to the growth of bacteria ($C_{X,gluc}$, $C_{X,aa}$, $C_{X,lcfa}$), which excrete them (eqs. 61 and 62).

$$\left(\frac{dC_{e,i}}{dt}\right)_{form} = Y_{e,i} \cdot \left(\frac{K_{I,e,i}}{C_j + K_{I,e,i}}\right) \cdot \left(\frac{dC_{x,j}}{dt}\right)_{growth} \quad (61)$$

$$\left(\frac{dC_i}{dt}\right)_{form} = -\left(\frac{dC_{e,i}}{dt}\right)_{form} \quad (62)$$

Table 14. Stoichiometric matrix for hydrolysis and substrate conversion.

process	rate	C_{ch2o}	C_{fat}	C_{prot}	C_{gluc}	C_{lafa}	C_{aa}	C_{lac}	C_{ac}	C_{pro}	C_{but}	C_{val}	C_{et}	C_{h2}	C_{co2}	C_{nh4}	C_{ch4}
Hydrolysis of carbohydrates	$r_{\text{ch2o,hydr}}$ ol	-1			1												
Hydrolysis of fat	$r_{\text{fat,hydrol}}$		-1			1											
Hydrolysis of proteins	$r_{\text{prot,hydro}}$ 1			-1			1										
Conversion of glucose	$r_{\text{gluc,conv}}$				-1			$\frac{z_{h2}}{1+z_{h2}}$	$\frac{2}{3 \cdot (1+z_{h2})^2}$		$\frac{z_{h2}}{3 \cdot (1+z_{h2})^2}$			$\frac{2+z_{h2}}{3 \cdot (1+z_{h2})^2}$	$\frac{1}{3 \cdot (1+z_{h2})}$		
Conversion of long chain fatty acids	$r_{\text{lafa,conv}}$					-1			1				$(\frac{n_c}{n_c-1} - \omega)$				
Conversion of amino acids	$r_{\text{aa,conv}}$						-1		0.2	0.222	0.2	0.2		0.14	0.1	0.19	
Conversion of lactate	$r_{\text{lac,conv}}$							-1	$\frac{2}{3 \cdot (1+z_{h2})}$	$\frac{z_{h2}}{1+z_{h2}}$				$\frac{2-z_{h2}}{3 \cdot (1+z_{h2})}$	$\frac{1}{3 \cdot (1+z_{h2})}$		
Conversion of acetate	$r_{\text{ac,conv}}$								-1						0.5		0.5
Conversion of propionate	$r_{\text{pro,conv}}$								2/3	-1				1	1/3		
Conversion of butyrate	$r_{\text{but,conv}}$								1		-1			0.5			
Conversion of valerate	$r_{\text{val,conv}}$								0.4	0.6			-1	0.4			
Conversion of ethanol	$r_{\text{et,conv}}$								1				-1	1			
Conversion of hydrogen	$r_{\text{h2,conv}}$													-1	-0.25		0.25

Table 15. Biological Parameters: Growth yields (Y), kinetic constants (k_i, b_i, K_i, K_{I,i}), and pH Inhibitor parameters. Units are combinations of mol, m³, h. The values are taken from Batstone et al (2000), except of those marked with * (Costello et al, 1991) or + (Kalyushnyi, 1997) or ** (Romli, 1991). Values marked with ^x are estimated in this work – see text. K_{I,h2} was calculated from the equation given by Costello et al and Batstone et al for 35°C and pH 7. Hydrogen partial pressure was converted into the concentrations with a Henry constant of 0.74 mol/(m³ * bar) (Atkins, 1996).

i	Y _i	k _i	b _i	K _i	j	K _{I,i,j}	K _{I,h2}	pH _m	pH _i
gluc	$0.768 \cdot \frac{(1+z_n)^2}{4+5 \cdot z_n+2 \cdot z_n^2}$	<u>5</u> <u>9.78*</u>	<u>0.00083</u> <u>0.00125⁺</u>	<u>40</u> <u>0.768*</u>	ac/ but/ lac	<u>5*</u>		<u>5.0</u>	<u>4.0</u>
lac	$0.128 \cdot \frac{1+1/3 \cdot z_n^{**}}{1+z_n}$	<u>3.8</u> <u>1.67*</u>	<u>0.00086</u>	<u>1.14</u> <u>1.14*</u>	ac/pro	<u>5*</u>		<u>6.0</u>	<u>4.0</u>
pro	<u>0.064</u>	<u>0.524</u> <u>0.524*</u>	<u>0.00042</u>	<u>10</u> <u>1.59*</u>	ac	<u>1.5*</u>	<u>0.0037</u> <u>0.0037*</u>	<u>6.0</u>	<u>4.0</u>
but	<u>0.072</u> <u>0.043⁺</u>	<u>4</u> <u>1.14*</u>	<u>0.00125</u> <u>0.00125⁺</u>	<u>7</u> <u>0.332*</u>	ac	<u>15*</u>	<u>0.0037</u> <u>0.0037*</u>	<u>6.0</u>	<u>4.0</u>
ac	<u>0.048</u> <u>0.048⁺</u>	<u>0.35</u> <u>0.39*</u>	<u>0.00083</u> <u>0.00083⁺</u>	<u>3</u> <u>5.14*</u>				<u>7.0</u>	<u>6.0</u>
h2	<u>0.03</u> <u>0.015⁺</u>	<u>3.6</u> <u>1.70*</u>	<u>0.000375</u> <u>0.00125⁺</u>	<u>0.055</u> <u>0.00074*</u> <u>0.008⁺</u>				<u>6.0</u>	<u>4.5</u>
et	<u>0.038⁺</u>	<u>8.2⁺</u>	<u>0.00125⁺</u>	<u>0.12⁺</u>			<u>0.0037⁺</u>	<u>6.0</u>	<u>4.0</u>
val	<u>0.072</u>	<u>1.9</u>	<u>0.00125</u>	<u>5</u>			<u>0.0037</u>	<u>6.0</u>	<u>4.0</u>
lcfa	$0.382 \cdot \frac{n_c}{6} + \frac{2}{3} \omega$	<u>0.081</u>	<u>0.00125</u>	<u>3.1</u>			<u>0.0037</u>	<u>6.0</u>	<u>4.0</u>
aa	<u>0.062</u>	<u>2.05</u>	<u>0.00083</u>	<u>35</u>				<u>7.2</u>	<u>5.2</u>
ch2o	<u>0.01^{**}</u> (Y _{e,ch2o})	<u>535</u>		<u>10 (α)</u>		<u>1000</u> (K _{I,e,ch2o})			
fat	<u>0.01</u> (Y _{e,fat})	<u>363</u>		<u>10 (α)</u>		<u>1000</u> (K _{I,e,ch2o})			
prot	<u>0.01</u> (Y _{e,prot})	<u>1464</u>		<u>10 (α)</u>		<u>1000</u> (K _{I,e,ch2o})			

Table 16 physical coefficients of the relevant substances. Data from Reid et al (1987), ^xAtkins (1996), ^{*} calculated according Tyn and Callus (1975), ⁺ Lide and Frederikse (1995). $D_{i,35^{\circ}\text{C}}$ is used for calculation of the temperature dependent biofilm diffusivity $D_{i,f}$ (eq. 69). $H_{i,25^{\circ}\text{C}}$ is used for calculation of the temperature dependent Henry's low constant for solubility (eq. 60).

i	D_i ⁶ (°C)	[*] 10^{-6} D_i (35 °C)	$D_{i,35^{\circ}\text{C}}$	$H_{i,25^{\circ}\text{C}}$	$\Delta H_{0,i}$
a (Cl ⁻)	0.73 (25) ^x	0.87	<u>0.6</u>		
aa (glycine)	0.38 (25) ^x	0.45	<u>0.6</u>		
ac	0.43 (20)	0.56	<u>0.6</u>		
	0.45 (20) [*]	0.66 [*]			
b (Na ⁺)	0.49 (25) ^x	0.58	<u>0.6</u>		
but		0.51 [*]	<u>0.6</u>		
ch4	0.306 (2)	0.53	<u>0.6</u>	<u>29.7⁺</u>	<u>-14240</u>
	1.136 (60)	0.72			
co2	0.72 (25)	0.86	<u>0.6</u>	<u>1.441⁺</u>	<u>-19410</u>
et	0.36 (15)	0.51	<u>0.6</u>		
	0.41 (25) ^x	0.49			
gluc	0.242 (25) ^x	0.29	<u>0.3</u>		
h	3.35 (25) ^x	3.99			
h2	1.73 (25) ⁺	2.05 [*]	<u>2.0</u>	<u>40.4⁺</u>	<u>-4180</u>
lac		0.53 [*]	<u>0.6</u>		
lcfa (C ₁₆)		0.28 [*]	<u>0.3</u>		
pro		0.58 [*]	<u>0.6</u>		
val		0.47 [*]	<u>0.6</u>		

Hydrolysis and substrate conversion was extended by a temperature dependency according to eq. 63 for all components (Dochain and Perrier, 1996).

$$f_T = a_1 \cdot e^{-b_1/(T+273)} - a_2 \cdot e^{-b_2/(T+273)} - c$$

$$\text{with } a_1 = 3 \cdot 10^{11}, a_2 = 1.25 \cdot 10^{24}, b_1 = 8000, b_2 = 17250, c = 0.04 \quad (63)$$

In the function plot of eq. 63, which is shown in Figure 31, it can be seen that for lower temperatures than the maximum of 37 °C the relative reaction rate decreases slowly, while at higher temperatures a sudden decrease occurs, whereby zero rate is reached at 45 °C. However, inactivation of bacteria and enzymes at even higher temperatures is not modelled.

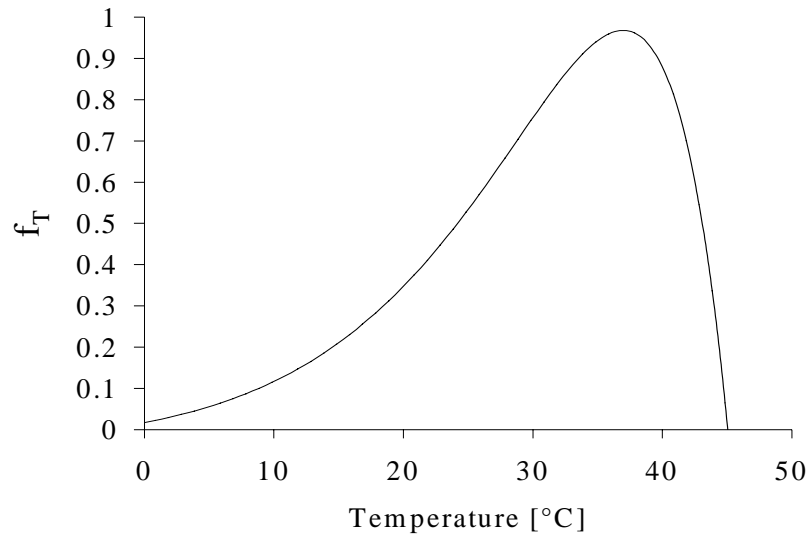


Figure 31. Temperature dependency as used for growth and enzymatic reactions.

In order to avoid growth without a nitrogen source present, eq. 64 was introduced for all microorganisms (and also enzyme catalysed reactions).

$$M_{nh4} = \frac{C_{nh4}}{C_{nh4} + 0.001} \quad (64)$$

As a pH dependency was only modelled for the range less than the optimum (eqs. 65a and 65b) by Batstone et al (2000), eq. 66 was introduced in order to inhibit growth at high pH values and high ammonia concentrations.

$$f_{pH,i} = 10^{-a} \text{ with } a = 0.5 \cdot \left(\frac{pH_{m,i} - pH}{2 \cdot (pH_{m,i} - pH_{l,i})} \right)^2, \quad \text{for } pH < pH_{m,i} \quad (65a)$$

$$f_{pH,i} = 1, \quad \text{for } pH \geq pH_{m,i} \quad (65b)$$

$$I_{nh4,pH} = \frac{1}{\left(1 + \frac{MAX(C_{nh3}, 100)}{K_{I,nh3}}\right)}, \text{ with } C_{nh3} = \frac{C_{nh4} \cdot K_{a,nh4}}{C_h} \quad (66)$$

An ammonia inhibition was introduced, because ammonia is the main inhibitor at $pH > 7$. Kiely et al (1997) show a half inhibition concentration of 7 mol m⁻³ of undissociated ammonia for methanogens, which will be used here for all bacteria. As

hardly any data are available of pH inhibition at higher pH values, and Batstone et al did not model pH above 7, pH inhibition is included into the ammonia inhibition equation (eq. 66). Setting the ammonia concentration $\geq 100 \text{ mol m}^{-3}$, it is guaranteed that growth is slowed down at pH 8.5 and nearly zero at pH 10, which is in accordance to the pH functions for all the relevant bacterial groups given by Kalyushnyi (1997). The dependence of the biological rates from the pH and ammonia (eq. 66) is shown in Figure 32.

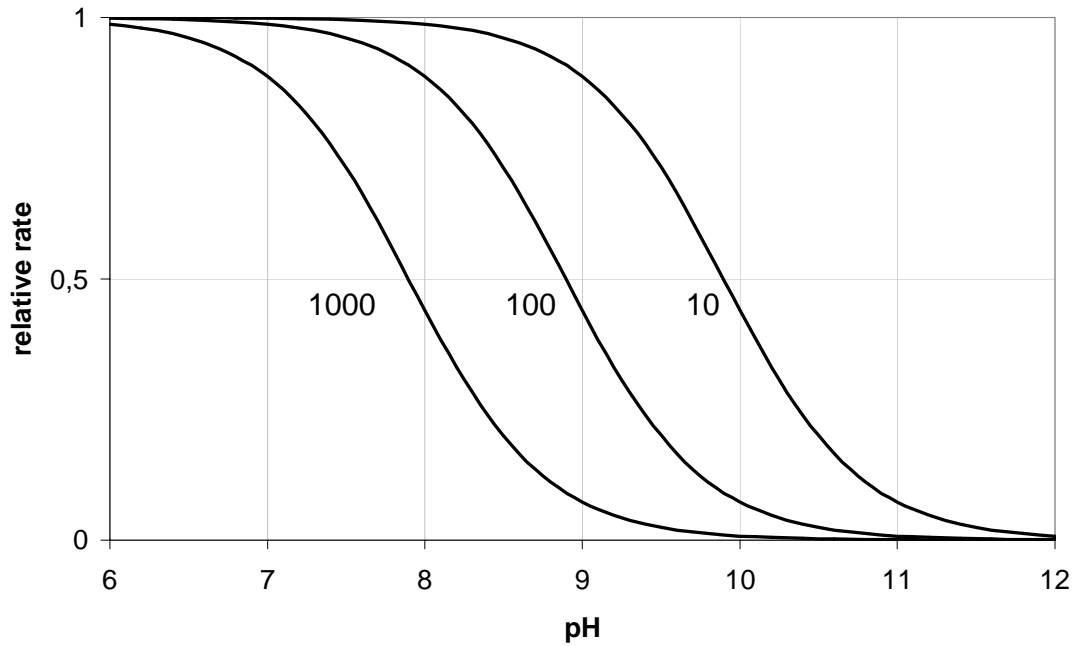


Figure 32 Dependency of the biological rates from total ammonia concentration and pH. $K_{I,nh3} = 7 \text{ mol/m}^3$. Curves correspond to 1000, 100 and 10 mol total ammonia/m³ (from left to right).

Influence of hydrogen (eqs. 67 - 69) was made temperature-dependent as used by Costello et al (1991).

$$f_{h2} = \frac{1}{1 + z_{h2}} \text{ where } z_{h2} = \text{eq.68, 69} \quad (67)$$

$$z_{h2} = z_{h2, factor} \cdot \frac{C_{h2}}{10000 \cdot C_h \cdot 0.74} \quad (68)$$

$$z_{h2, factor} = 10^{7 \cdot \frac{1139}{T+273}} \quad (69)$$

Ethanol degrading bacteria were taken from Kalyushnyi (1997). He used a $K_{I,i,h2}$ of 0.005 bar of hydrogen partial pressure which is exactly the same as used by Costello and Batstone after solving

$$\frac{1}{1 + z_{h2}} = \frac{1}{1 + \frac{C_{h2}}{K_{I,i,h2}}} \text{ with } z_{h2}: \text{ see eqs.68, 69} \quad (70)$$

using a pH of 7 ($C_h = 10^{-4} \text{ mol m}^{-3}$) and 35 °C. Therefore, the same hydrogen inhibition term was used (eq. 67). Kalyushnyi (1997) did not observe product inhibition in the regarded range of 0 .. 50 C-mol m^{-3} acetate. Thus, the rate for substrate uptake is described analogous to the uptake of valerate, long chain fatty acids and amino acids (Table 13). pH inhibition, however, was not taken from Kalyushnyi (1997) but from Batstone (2000), whereby the same values as for the other acetogenic bacteria are used. This was done, because both models used similar pH inhibition parameters for the acetogenic bacteria but the parameters differ between both models. As it can be seen from Figure 33, ethanol degraders are less sensitive to pH now (solid line). However, at pH 7, where the Ethanol experiments were carried out by Kalyushnyi, there is no big difference.

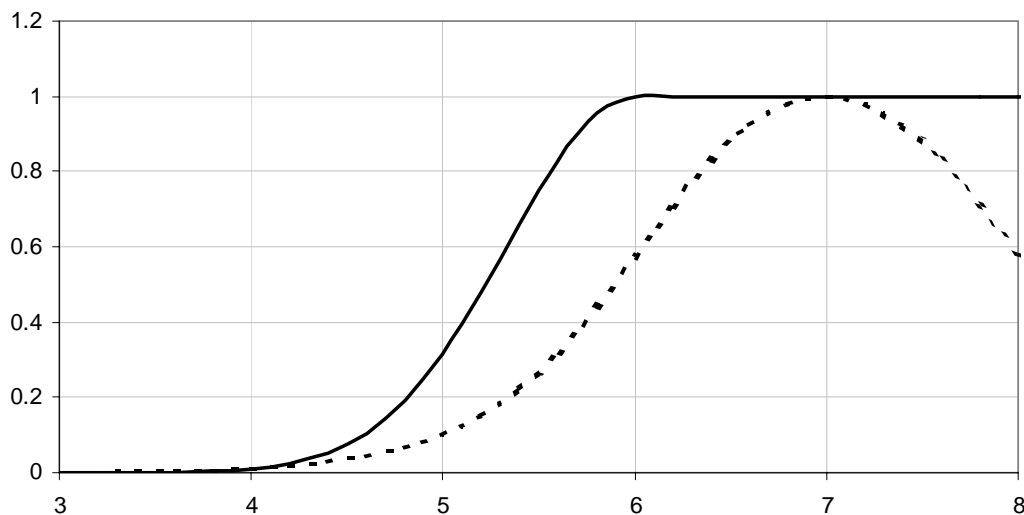


Figure 33. pH inhibition function for acetogens (Batstone, 2000 - solid line) versus ethanol degraders (Kalyuzhnyi, 1997 – dotted line).

For the non-competitive inhibition, the sum of the respective products are used as inhibitor concentration (Costello, 1991). Thus, acetate, lactate and butyrate are taken into account for glucose degraders (see eq. 46 in Table 13). As concentrations are handled on a C-mol basis and because butyrate or lactate has twice or 1.5fold the number of C-mols compared to acetate, these concentrations are divided by 2 or 1.5 (eq. 71).

$$C_{ac} + \frac{C_{lac}}{1.5} + \frac{C_{but}}{2} \quad (71)$$

For lactate degrading bacteria, acetate and propionate are taken as inhibitory substances, as these are the endproducts (term eq. 72 incorporated in Table 13, eq. 49).

$$C_j = C_{ac} + \frac{C_{pro}}{1.5} \quad (72)$$

As already mentioned, decay is modelled like maintenance. As the requirement of maintenance energy is not expected to decrease at temperatures above the optimum, another temperature dependency was introduced for the maintenance term (eq. 73).

$$f_{T,maint} = e^{-8419 \cdot \left(\frac{1}{273+T} - \frac{1}{308} \right)} \quad (73)$$

Eq. 73 represents the relative temperature dependency compared to 35 °C, which was calculated from eq. 74 by setting the maintenance energy at the new temperature and at 35°C into relation. Eq. 74 was taken from Heijnen (1994), who describes the maintenance energy for all chemotrophic microorganisms with the same Arrhenius equation:

$$m_e = 4.5 \cdot e^{\frac{-69000}{8.314} \cdot \left(\frac{1}{T+273} - \frac{1}{298} \right)} \quad (74)$$

He states, that maintenance requirement is comparable for anaerobic and aerobic growth and is independent from the substrate.

3.6.4.3 Mass Transfer

Liquid to gas mass transfer is modelled according to Henry's law and a gas liquid transfer term ($k_{Lgas,i}a$). For methane and hydrogen, eq. 75 was applied, while for carbon dioxide the dissociation ($K_{a,co2}$) had to be taken into account. Hence eq. 76 replaces the total concentration (C_i) by that fraction which is only physically dissolved (non-dissociated) but not chemically bonded.

$$\left(\frac{dC_i}{dt} \right)_{gas} = k_{Lgas,i}a \cdot (C_i - k_{H,i} \cdot C_{gas,i} \cdot p) \quad \text{with } i = ch4, h2 \quad (75)$$

$$\left(\frac{dC_{co2}}{dt} \right)_{gas} = k_{Lgas,co2}a \cdot \left(\frac{C_h}{K_{a,co2} + C_h} \cdot C_{co2} - k_{H,co2} \cdot C_{gas,co2} \cdot p \right) \quad (76)$$

As the mass transfer depends on diffusivity, it is higher for hydrogen (eq. 77).

$$k_{Lgas,h2}a = k_{Lgas,ch4}a \cdot \frac{D_{h2}}{D_{ch4}} \quad (77)$$

Diffusion constants are given in Table 16 on page 87.

As gas solubility is quite temperature dependent (eq. 78), it is corrected by temperature according to Stumm and Morgan (1988, cited in Batstone, 2000).

$$k_{H,i} = k_{H,i,25^{\circ}C} \cdot e^f, \text{ with } f = \frac{\Delta H_{0,i}}{8.315 \cdot \left(\frac{1}{273+T} - \frac{1}{298} \right)} \quad (78)$$

However, the $k_{Lg,a}$ term is only relevant for the transfer from the gas to the liquid. The other way, as it is the case in anaerobic systems, where gas is only produced by bacteria, does not depend on the gas/liquid interface, because bubbles can be formed within the liquid. It is expected, that enough solid particles are present which support nucleation of the bubbles. Bubbles are formed particularly on the surface of the biofilm. However, two cases will be investigated for validation of the model: One with $k_{Lg,i}a$ set to infinite, and one with $k_{Lgas,i}a$ set to the same value as used for liquid/solid mass transfer ($k_{Lg,i}a = k_{Lfilm,i}a$).

Mass transfer from bulk to biofilm surface is described according to eq. 79.

$$\left(\frac{dC_i}{dt} \right)_{film} = k_{Lfilm,i}a \cdot (C_{i,bulk} - C_{i,biofilmsurface}) \quad (79)$$

Transfer within biofilms is generally only due to diffusion and assumed to adhere to Fick's law (Kissl, 1986), where the mass flux depends on the spatial concentration gradient and the diffusion coefficient of the according substance (eq. 80).

$$\left(\frac{dC_i}{dt} \right)_{diffusion} = D_{f,i} \frac{dC_i}{dz} \quad (80)$$

$$D_{f,i} = 0.9 \cdot D_i \quad (81)$$

Diffusion within biofilms is not much slower than in pure water, a ratio of 0.9 (eq. 81) is a good approximation for small molecules like gases, glucose, ammonia (Christensen and Charaklis, 1990).

Diffusion coefficients depend on the viscosity of the solvent, which is temperature dependent, as can be seen from the Stokes-Einstein equation (eq.82), where $D_{i,j}$ is the Diffusion coefficient of a substance i in the solvent j.

$$D_{i,j} = \frac{RT}{6 \cdot \pi \cdot \eta_j \cdot r_i} \quad (82)$$

Tyn (cited in Reid et al, 1987) describes the temperature dependency with

$$D_{i,j}(T_2) = D_{i,j}(T_1) \cdot \left(\frac{374 - T_1}{374 - T_2} \right)^6 \quad (83)$$

whereby the power depends on the vaporization energy and is 6 for water.

Hence, this temperature dependency will be used in the model.

For the substances, where no measured values were available, D was estimated using the equation as proposed by Tyn and Callus (cited in Reid et al, 1987), which has an accuracy of 10 % for most substances. As the estimation of diffusion coefficients is not very accurate, already in respect of the biofilm, and as it can be seen from Table 16, that most of the substances have similar diffusion coefficients, a $D_{i,35^{\circ}\text{C}}$ value of $0.6 \cdot 10^{-6} \text{ m}^2 \text{ h}^{-1}$ will be used for calculation of the temperature dependent biofilm diffusivity for all substances except hydrogen ($2.0 \cdot 10^{-6} \text{ m}^2 \text{ h}^{-1}$), lactate ($0.3 \cdot 10^{-6} \text{ m}^2 \text{ h}^{-1}$) and glucose ($0.3 \cdot 10^{-6} \text{ m}^2/\text{h}$). Temperature correction is applied as already described (eq. 83), therefore for diffusivity,

$$D_{f,i} = 0.9 \cdot D_{i,35^{\circ}\text{C}} \cdot \left(\frac{339}{374 - T} \right)^6 \quad (84)$$

is used.

D is not relevant for protons which concentration is always calculated from the others by solving the charge balance (eqs. 38, 41). Complex substances (proteins, fat and complex carbohydrates) are expected to have no diffusivity inside the biofilm.

The mass transfer coefficient, $k_{L,\text{film},\text{ch4a}}$, is a lumped factor, which depends mainly on the velocity of the liquid around the biofilm surface. For the reactor configuration used, a value of 0.03 h^{-1} was assumed. An estimation will be given in the following. Later, the influence of $k_{L,i}$ will be examined by sensitivity analysis. If it is shown to be necessary, also the mixing effect of the arising gas bubbles could be included into the mass transfer coefficient.

For estimation of the mass transfer coefficient, the hydraulic diameter d_h will be used. The mass transfer coefficient depends also on the diffusion coefficient D_i , as well as on the dimensionless Reynold (Re) and Schmidt (Sc) numbers and will be calculated from eq. 85, which is valid for many geometries (Reid et al, 1987).

$$Sh_i = \frac{k_{Ls,i} \cdot d_h}{D_i} = 0.664 \cdot \sqrt{Re_h} \cdot \sqrt[3]{Sc_i} \quad (85)$$

$$Re_h = \frac{u \cdot d_h}{\nu} \quad (86)$$

$$Sc_i = \frac{\nu}{D_i} \quad (87)$$

$$d_h = \frac{4 \cdot V}{A}, \text{ with } \frac{V_{\text{liquid}}}{V} \approx 1 \quad (88)$$

Using the dimensions and configuration of the laboratory scale reactor, as described in chapter 5.1 ($V = 0.015 \text{ m}^3$, $Q = 0.030 \text{ m}^3/\text{h}$, $H=0.85 \text{ m}$), the Reynolds,

Schmidt and Sherwood number become 20, 1.17, and 3.15 respectively ($v = 0.7 \cdot 10^{-6}$ m²/s at 35°C.). For calculation of the Reynolds number, the hydraulic diameter was used (0.030 m). This is in the same order of magnitude as the grid space (0.015 m) and the space between the webs (0.010 to 0.030 m). An average value of $D = 0.6 \cdot 10^{-6}$ m²/h was used (compare with Table 16). The calculated Sherwood number is not much higher than the minimal Sherwood number without diffusion (2 for a sphere), hence a decrease in the flow rate will not affect the transfer coefficient much. Now then, $k_{Ls,i}$ is $2.1 \cdot 10^{-4}$ m/h and $k_{Ls,i}a$ becomes 0.029 h^{-1} ($a = 2 \text{ m}^2/0.015 \text{ m}^3$).

3.6.4.4 Biofilm

The mathematical model of the biofilm consists of one-dimensional accounting equations, which describe the increasing thickness of the film (the bacteria concentration is expected to be constant with 500 C-mol m^{-3}) and the spatial dispersion of the solved and particular substances in the lapse of time. As there was no restriction made, which bacteria can grow within the biofilm, microbial distribution is a result of local substrate transport, consumption and production.

The rigid biofilm model of Wanner and Reichert (1996), which is already incorporated into the Aquasim software, was used in this work. This model is summarised. The balance of biomass in the film is given by eq. 89.

$$\frac{\partial C_{X,i}}{\partial t} = -u_F \cdot \frac{\partial C_{X,i}}{\partial z} + \left(r_{X,i} - \frac{C_{X,i}}{1 - \varepsilon_l} \cdot \sum_{k=1}^{n_X} \frac{r_{X_k}}{\rho_k} \right) \quad (89)$$

The right term of the right side of equation 89 shows the net production of each bacterium (eq.90) corrected for dilution by other bacteria, whereby ε_l represents the water content of the film (eq. 91).

$$r_{X,i} = \left(\frac{dC_{X,i}}{dt} \right)_{\text{growth}} + \left(\frac{dC_{X,i}}{dt} \right)_{\text{decay}} \quad (90)$$

$$\varepsilon_l = 1 - \sum_{i=1}^{n_X} \frac{C_{X,i}}{\rho_i} \quad (91)$$

The left term of the right side of equation 89 describes the change of biomass concentration due to a shift by growth of underlying bacteria layers, whereby u_F represents the velocity of the shift (eq. 92) and z the spatial coordinate beginning with zero at the base of the biofilm.

$$u_F = \int_0^z \left(\frac{1}{1 - \varepsilon_l} \cdot \sum_{k=1}^{n_X} \frac{r_{X_k}}{\rho_k} \right) dz \quad (92)$$

No attachment of biomass to the film is taken into account but a detachment rate was applied (eq. 93, [m h⁻¹]) in order to restrict the biofilm thickness to reasonable values.

$$u_{detach} = 3 \cdot (d_{film})^2 \quad (93)$$

With this empirical detachment rate, the film thickness could be kept in a reasonable range (around 0.001 m). The thicker the film grows, the higher the detachment rate becomes.

The balance of dissolved components is given in eq. 94.

$$\frac{\partial C_i}{\partial t} = D_{eff} \cdot \frac{\partial^2 C_i}{\partial z^2} + \frac{1}{\varepsilon_l} \cdot r_i + \frac{1 - \varepsilon_l}{\varepsilon_l} \cdot u_F \cdot \frac{\partial C_i}{\partial z} + \frac{1}{\varepsilon_l} \cdot \sum_{k=1}^{n_x} \frac{r_{X,i}}{\rho_k} \cdot C_i \quad (94)$$

The first term describes the transport in the biofilm according to the Flick's law, the second represents the net production (eq. 95).

$$r_i = \left(\frac{dC_i}{dt} \right)_{hydrol} + \left(\frac{dC_i}{dt} \right)_{conv} + \left(\frac{dC_i}{dt} \right)_{growth} + \left(\frac{dC_i}{dt} \right)_{decay} \quad (95)$$

The remaining two terms of eq. 94 are of minor importance, but are necessary for compensation of a change of the biofilm in order to meet the balance. The former term is due to the transport of liquid inside shifting bacteria (due to expansion of the biofilm), the latter is due to uptake of water by growing bacteria.

3.6.4.5 Fluxes between compartments

Fluxes are illustrated in Figure 29 on page 79 and in Figure 30 on page 80.

Dosage of lye occurs, if the pH value decreases below the setpoint. The pH values for both reactors are adjusted in the model using a very fast proportional controller (eq.96). Volume of lye is not taken into account, hence $Q_{L1} = 0$ and $Q_{L2} = 0$.

$$\left(\frac{dC_b}{dt} \right)_{in} = \max(1000 \cdot (pH_{set} - pH), 0) \quad (96)$$

Inflow into any compartment is given in eq.97. The flux Q_1 into the acidification is a combination of any linear functions depending on the time and can be defined arbitrarily. However, Q_1 is limited by the boundary condition $V_1 \leq V_{1,max}$. Any of the substances C_i defined in the simulation system can be added to the inflow water. For the flow between two compartments, also the outflow has to be taken into account (eq. 98).

$$\left(\frac{dC_{i,2}}{dt}\right)_{in} = \frac{Q_{12}}{V_2} \cdot C_{i,1} \quad (97)$$

$$\left(\frac{dC_{i,1}}{dt}\right)_{out} = -\frac{Q_{12}}{V_1} \cdot C_{i,1} \quad (98)$$

The circulation Q_{2circ} can also be arbitrarily defined. However, for Q_{12} the boundary condition $V_2 \geq V_{2,min}$ must be fulfilled. A back-feed into the acidification was not taken into account ($Q_{21} = 0$). Now, water flow between the two compartments of the methane reactor results from the other flows:

$$Q_{2m} = Q_{12} + Q_{L2} + Q_{2circ} - Q_{21} \quad (99)$$

At last, the gas flows Q_{1G} and Q_{2uG} are modelled according to eq. 100.

$$Q_{cG} = \sum -\left(\frac{dC_i}{dt}\right)_{gas} \cdot V_c \cdot V_{mol}, \quad \text{with } V_c = V_l, V_{2u} \quad (100)$$

Loss of water with gas flow is not taken into account, as it is assumed to be only minor. Concentration of gases in the head space of both reactors is limited to the molar gas volume (eq. 101) using a very fast (therefore factor 10^5) dynamic process, whereby the gases ($C_i = C_{h2}, C_{ch4}, C_{co2}$) are removed proportionally to their fraction (equivalent to Q_{1GO} and Q_{2GO}). The mol volume V_{mol} (ideal gas law, eq. 102) as well as the moisture assuming 100 % humidity (eq. 103; Reid et al, 1987), depends on the temperature T ($^{\circ}C$) and the pressure p (1 bar).

$$\left(\frac{dC_i}{dt}\right)_{out} = \frac{C_i \left(C_{h2} + C_{ch4} + C_{co2} + C_{h2o} - \frac{1}{V_{mol}} \right) \cdot 10^5}{(C_{h2} + C_{ch4} + C_{co2} + C_{h2o})} \quad (101)$$

$$V_{mol} = \frac{8.3145 \cdot 10^{-5} \cdot (273 + T)}{p} \quad (102)$$

$$C_{h2o} = \frac{1}{V_{mol}} \cdot 6.107 \cdot 10^{\left(\frac{7.5T}{235+T}\right)} \quad (103)$$

3.6.5 Validation of the Model

The model was evaluated twofold, with experimental data (section 3.6.5.1) and by the use of sensitivity analysis (section 3.6.5.2).

3.6.5.1 Experimental Validation

Prior to simulations of the reactor as described in chapter 2.4, two one stage batch experiments (suspended biomass) as described by Kalyuzhnyi and Davlyatshina (1997) were simulated (simulations SK5 and SK7). In these experiments, glucose (66 mol C m^{-3}) was degraded at pH 5 and 7. For the simulation of the batch experiments all the acetogens were assumed to be present in the same concentrations as butyrate degraders ($0.13 \text{ mol C m}^{-3}$). Simulations without any parameter fitting already showed similar qualitative behaviour (data not shown). In particular, the heights of the hydrogen (7 mol m^{-3} in the gas in both, simulation and experiment at pH 5; 0.08 and 0.05 mol m^{-3} (= 15000 and 10000 ppm) at pH 7) and acetate peaks (26 and $31 \text{ mol C acetate m}^{-3}$ at pH 5 and 22; 25 at pH 7) were similar. Although the shape of the concentration curves were similar, there were large deviations in time scale (up to 4fold), which are due to the fact that biomass concentrations was uncertain and no parameter fitting was applied. In the experiment at a pH value of 5, there was also some ethanol formation which was not modelled. In both, experiment and simulation, acetate production compared to glucose uptake was delayed, which was due to lactate formation in the model and not investigated in the experiment. As experiments and simulations showed similar qualitative behaviour, results were regarded as being satisfying and thus the model was applied to the reactor configurations as used in this work.

The biofilm reactor system (chapter 2.4) was simulated using

- (a) the methane reactor be composed of two biofilm compartments switched in series and a recirculation (0.5 h^{-1}) loop (Figure 30a) and
- (b) one biofilm compartment for the methane reactor with ideally mixed bulk liquid, thus circulation rate was infinitely large (Figure 30b).

The pH value was set constant (5.5 in the acidification and 6.7 in the methane reactor). Details of the substrate composition used in the experiments and in the simulations are given in chapter Materials and Methods. Figure 34 shows hydrogen and methane concentrations of the experiment E0 versus simulations S0. Feed rates and effluent concentrations are given in Table 17. Additionally measured concentrations of volatile fatty acids are presented in the Appendix.

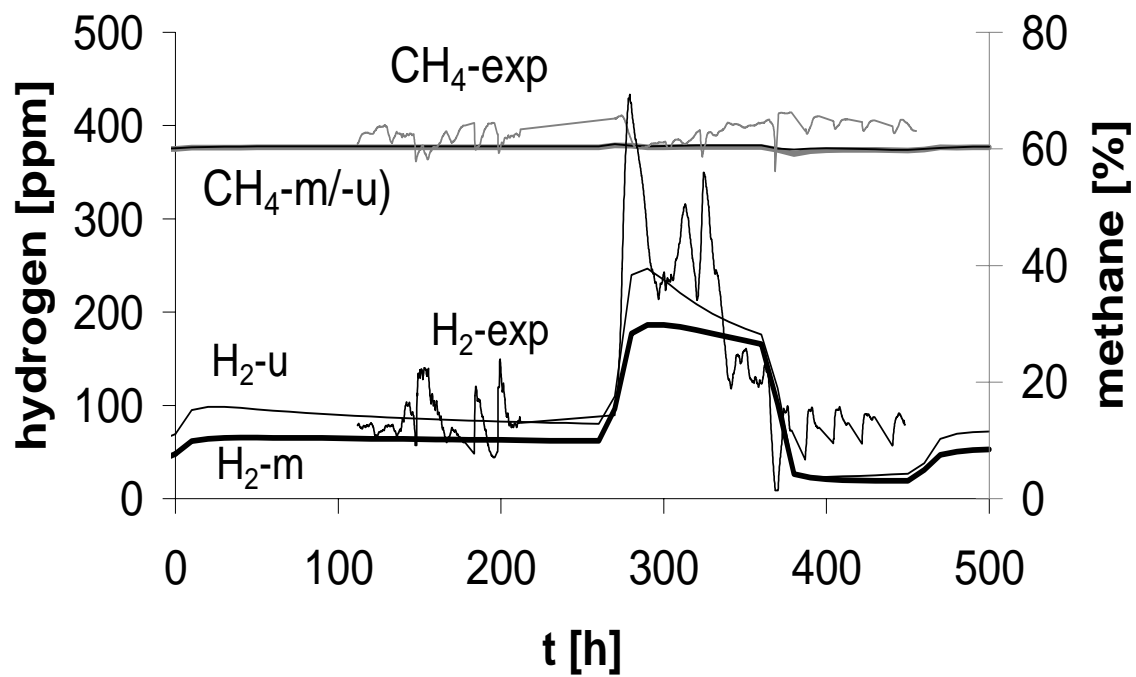


Figure 34. Hydrogen and methane concentrations in the experiment E0 versus simulations S0. exp: measured concentrations of experiment E0; m: simulated concentrations of the methane reactor consisting of one compartment (S0b); u: upper compartment of the methane reactor consisting of two compartments in series (S0a).

Table 17. Feed rate (d^{-1}), influent and effluent conc. ($kg\ COD\ m^{-3}$) of the experiments (E0, E1) and simulations (S0, S1) at different times (h). The feed rate is expressed as the volumetric flow into the acidification buffer tank per unit of volume of the methane reactor. Type: P: wastewater from potato processing, M: mash from pectin production, C: complex carbohydrates and protein, G: complex carbohydrates, glucose and protein. Influent concentration: Into acidification. Effluent concentration: From methane reactor; time when sample was taken in brackets (h).

Exp.	Time	Feed rate	Type	Influent conc.	Effluent conc. (time)
(E0)	0-270	0.6	P	3 – 4	0.28 (270)
	270-370	1.2	P	3 – 4	0.84 (320)
	370-460	0.3	P	3.5– 5	0.16 (460)
	460-500	0.6	P	3.5 – 5	0.46 (465)
(S0)	0-270	0.6	C	3.6	0.39-0.44
	270-370	1.2	C	3.6	0.43 – 0.57
	370-460	0.3	C	3.6	0.32 – 0.35
	460-500	0.6	C	3.6	0.35 – 0.42
(E1)	0 – 2	0			
	2 – 3	0 - 4	P	3 – 4	
	3 – 5.5	1-1.5	P	3 - 4	0.61(5.5)
	5.5 - 10	1-1.5	M	28	7.4 (10)
(S1)	0 – 2	0			≤ 0.02
	2 – 3	0 - 4	C	3.6	≤ 0.05
	3 – 5.5	1.2	C	3.6	0.59 (5.4)
	5.5 - 15	1.2	G	29	2.2 (10)

In both experiment and simulations hydrogen raised after an increase of the feed rate (which was identical for the acidification and methane reactor and thus filling level was constant). Vice versa it decreased after lowering of the feed. The fluctuations in the experiment arise from the feed, which was made in portions in the experiment but was steady in the simulations. In the simulation using two compartments (S0a), the hydrogen was higher and more correct than in the one compartment reactor (S0b), while methane and COD were identical. COD in the experiment and the simulations is given in Table 17. However, for further simulations the latter model was used as the same qualitative behaviour was achieved and computation time was considerably faster (more than two decades) due to the avoiding of back coupling.

3.6.5.2 Sensitivity Analysis

Every parameter (or function) p was changed by 1/1000 and the relative sensitivity was calculated by dividing the maximal deviation $\max(\partial y)$ during the simulation run (compared with the unchanged parameter) by the maximum value $\max(y)$ of acetate or hydrogen concentration and scaling with p according to eq. 104.

$$\delta = \frac{\max(\partial y)}{\partial p} \cdot \frac{p}{\max(y)}, \text{ with } \partial p = \frac{p}{1000} \quad (104)$$

Eq. 104 can be interpreted as the relative change of y per 100 % change of the parameter p (assuming linearity).

Table 18 shows all the parameters with sensitivities to acetate and hydrogen more than 10 % in the simulations SK, S5, K77, and S0.

Sensitivity analysis of the simulations show, that the most sensitive parameters influence mainly the pH value. As $\text{pH}_{\text{ac,hi}}$ is part of the pH dependency of acetate degrading methanogens, influence on acetate is clearly higher than on hydrogen, opposite is true for the pH dependency of hydrogen-consuming methanogens ($\text{pH}_{\text{h2,lo}}$). pH_{ini} represents the initial pH in the batch experiments of Kalyuzhnyi and Davlatshina. $K_{\text{a,ac}}$ is the dissociation constant of acetic acid, which has no effect in the experiment S0, as the pH was kept constant, and on experiment SK7 as pH was far beyond the value of $\text{p}K_{\text{a,ac}}$. C_{p04} represents the buffer capacity and thus influences the pH, too.

The diffusion constants D_i and the mass transfer coefficients $k_{\text{Lgas},i}A$ and $k_{\text{Lfilm},i}A$ show virtually no influence. As one could expect, the initial concentrations and the initial biofilm thickness showed also no influence in the experiment with the biofilm reactor, because the simulation was brought to steady state before beginning of the simulation experiments.

Table 18. Sensitivity analysis. Relative sensitivity δ of the concentrations of acetate (ac) and hydrogen (h2) to the parameters in the simulations SK5, SK7, and S0. in descending order. All parameters with sensitivities > 0.1 are shown. SK5: Batch experiment degrading glucose at pH 5, SK7: pH 7; S0: the two stage biofilm reactor system as used in this work.

	ac (SK5)	ac (SK7)	ac (S0)	h2 (SK5)	h2 (SK7)	h2 (S0)
pH _{ac,hi} *	-0.03	2.71	21.56	0.01	0.00	0.85
pH _{ini}	-1.20	-2.62		-18.72	-8.64	
K _{a,ac}	0.01	0.00	0.00	5.96	0.00	0.00
pH _{h2,lo} *	-0.01	0.00	-0.03	5.86	0.00	0.00
f _T *	0.14	1.76	-3.97	-1.78	-2.27	1.31
pH _{gluc,hi} *	-0.24	0.00	-0.12	-3.49	0.00	-0.81
C _{po4,in}	-0.14	0.21	0.00	-2.52	0.91	0.00
k _{ac}	-0.01	-0.57	-2.52	0.00	0.00	0.21
C _{gluc,in}	0.14	1.10	0.00	2.22	0.91	0.00
T	-0.04	0.81	-1.98	-1.10	-1.82	-1.04
Y _{ac}	0.00	-0.24	-1.78	0.00	0.00	0.04
pH _{gluc,lo} *	-0.13	0.00	0.00	-1.68	0.00	0.00
k _{gluc}	0.07	0.10	-0.01	0.96	1.36	0.00
C _{ch2o,in}			0.84			-1.28
K _{a2,po4}	-0.07	0.05		-1.28	0.00	
C _{h,c2}			1.24			0.24
pH _{h2,hi} *	-0.02	0.00	-0.02	-1.17	0.00	0.05
C _{X,h2,ini}	0.03	0.12		-1.14	-0.91	
k _{h2}	0.04	0.19	0.29	-1.11	-0.91	-0.85
Q ₁			0.75			1.08
k _{lac}	0.05	0.95	0.14	0.02	-0.45	0.01
C _{X,in}			-0.18			-0.93
Y _{gluc} *	0.06	-0.29		0.82	0.91	
K _{gluc}	0.00	0.00	0.01	-0.03	0.00	0.86
ρ_X			-0.73			0.25
Y _{lac} *	0.03	0.71		0.01	-0.45	
α			-0.10			0.71
K _{I,gluc,ac_but_lac}	0.05	0.05	-0.01	0.61	0.45	0.70
Y _{prop}	0.00	0.05	0.13	0.00	0.00	-0.70
H _{h2} *	0.05	0.00	0.00	-0.62	0.00	0.00
pH _{ac_lo} *	0.04	0.60	0.11	0.01	0.00	-0.03
K _{I,lac,ac_pro}	0.03	0.57	0.12	0.02	-0.45	0.08
K _{h2}	0.00	-0.12	-0.24	0.02	0.45	0.54
k _{ch2o}			0.10			-0.50
K _{ac}	0.01	0.14	0.49	0.00	0.00	-0.14
C _{X,gluc,ini}	0.01	0.02		0.17	0.45	
Z _{h2factor} *	-0.04	-0.10	-0.24	0.43	-0.45	-0.35
Y _e			0.10			0.39
C _{X,ac,ini}	-0.01	-0.33		0.00	0.00	
k _{pro}	0.00	0.12	0.28	0.01	0.00	-0.13
C _{ac_in}			0.26			-0.25
K _{val}	0.00	0.00	0.01	0.02	0.00	0.26
Y _{h2}	0.00	0.05	0.09	-0.23	0.00	0.13

*: result of function instead of parameter

Apparently, also the temperature dependency f_T , the temperature T , the specific acetate uptake rate k_{ac} , the biomass yield on acetate Y_{ac} and acetate production (depending on k_{gluc}) have relative high influence on the system.

However, results of sensitivity analysis always have to be interpreted with care, as they are only valid for the specific simulated experiment. The low influence of the mass transfer parameters is due to the assumed well mixed bulk liquid and the high surface to volume ratio due to the small reactor volume. In big scale applications with poor mixing, mass transfer might become more important.

3.6.6 Conclusions

The simulation model was able to predict experiments satisfactorily. In particular, the key parameters hydrogen concentration in the gas phase and the pH value can be simulated well. However, for simulation of the pH value, the composition or the buffer capacity of the wastewater has to be known or estimated. If the pH is set constant, the pH dependency of the microorganism is still important. Sensitivity analysis showed, that neglecting of some aspects of mass transfer, which is often done, would have been justified for the investigated reactor configuration. The mass transfer coefficients did not play any important role in the investigated configuration. The simulation model will be applied for validation of the control system (subchapter 3.6), where the model is further validated.

3.7 Validation by Simulation

As the fuzzy system as well as the simulation model could be validated using experimental data, ideally the fuzzy system should be able to give reasonable results by interacting with the simulation, too. First, the state detection of the fuzzy system is tested by simulation of experiment E1. After this, the output of the fuzzy controller is applied to the simulation model. At last, different wastewaters are applied to the control system.

3.7.1 Simulation of the Overload Experiment

In the experimental validation of the control system (subchapter 3.6.5.1), an experiment (E1) was made, whereby the conditions were kept constant but the state of the system was predicted by the fuzzy logic system (Figure 25 on page 67). This experiment was simulated (S1, see Figure 35). Like in the experiment, an overload was detected after an increase of the loading. In both experiment and simulation the methane concentration did not decrease much. A slight shortage was detected at the beginning of the experiment, due to the pH rules and the low gas production rate, as no gas measurement was available, because not enough gas had flushed the gas test point at that time. In the simulation, also a slight shortage was detected but superposed by detection of normal state, as gas values were always available in the simulation.

In addition, a simulation was made, whereby the output values of the fuzzy logic were used as setpoint values during the simulation (SC). As the COD in the methane reactor (which is the effluent assuming ideal mixing) was rather high, the fuzzy sets normal and high were modified in order to achieve a change in transition from normal to high from 200 .. 500 ppm to 150 .. 200 ppm. Simulation results (SC) with the original and modified fuzzy sets are shown in Figure 36. As in the right column (Figure 36) overload was reached at lower hydrogen levels (compare graphs b and c), feed into the methane reactor was less (a), resulting in a much better effluent (e). Overall gas production was higher in the second experiment (d) as substrate was better utilised. Hence, those modified fuzzy sets were used for subsequent simulations.

As the control system showed very similar behaviour on the simulation model compared to real experiments, the model can be used for simulation of advanced situations.

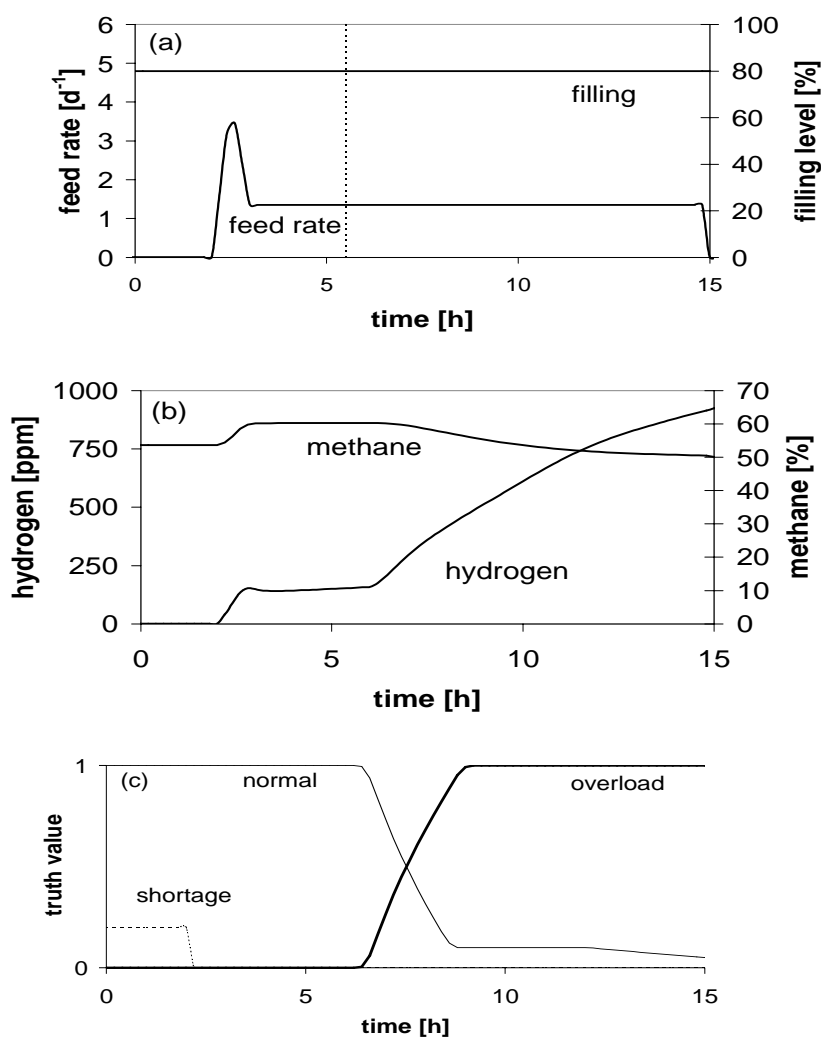
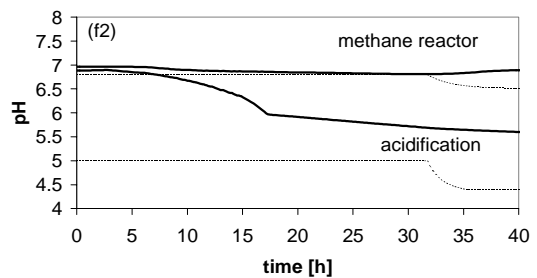
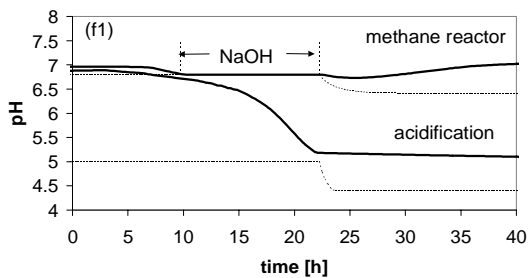
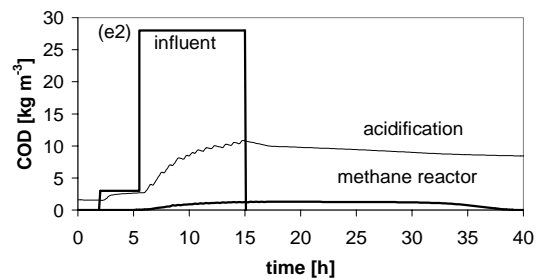
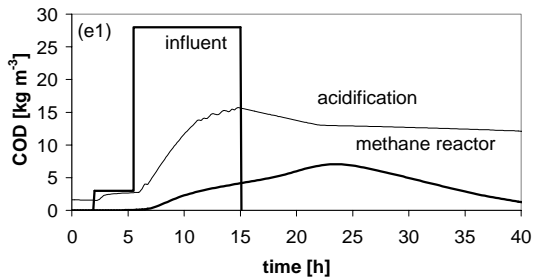
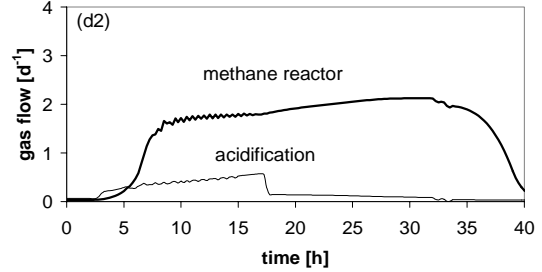
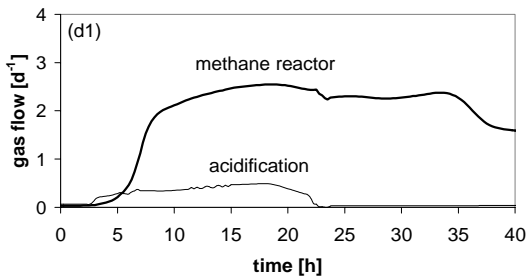
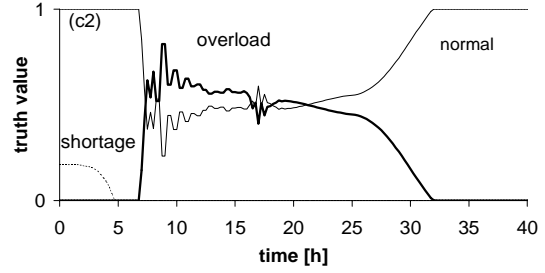
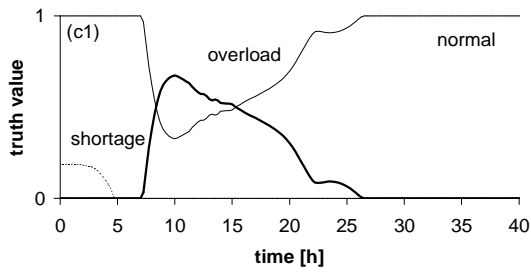
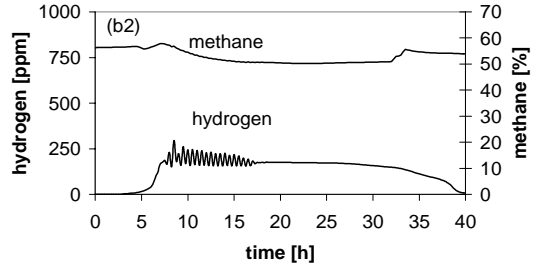
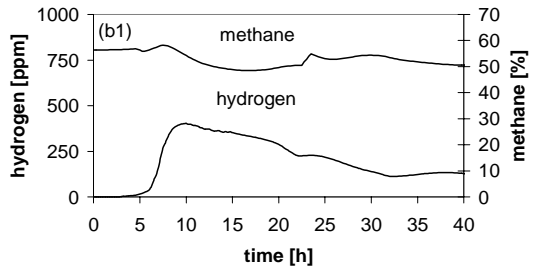
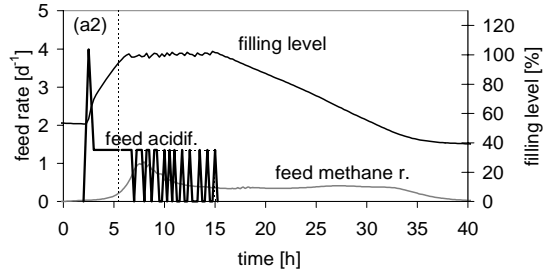
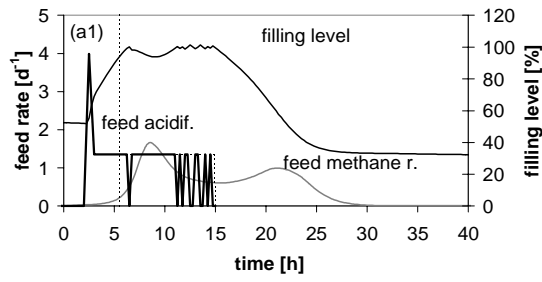


Figure 35. Simulation of the overload experiment without control. (a) shows the feed (volumetric flow into the acidification buffer tank per unit of volume of the methane reactor (d^{-1})) and the filling level of the acidification buffer tank (%). Begin of dosage of the higher concentrated wastewater (28 g/l COD) is indicated with a dotted line. (b) shows the concentrations of hydrogen (ppm) and methane (%) in the off-gas of the methane reactor. (c) shows truth values (degree of membership) of the fuzzy sets of the state variable for the methane reactor. Overload is indicated with a thick line, normal with a smaller line and shortage with a dotted line.

Next page:

Figure 36. Simulation and CONTROL of the overload experiment. Graphs on the right side (a2, b2 etc.) show simulations performed with changed sets of the hydrogen variable. (a) shows the feed rate into the acidification buffer tank normalised with the volume of the methane reactor per hour and the fill level of the acidification buffer tank. Begin of dosage of the higher concentrated wastewater (28 g/l COD) is indicated with a dotted line. (b) shows the concentrations of hydrogen (ppm) and methane (%) in the off-gas of the methane reactor. (c) shows truth values (degree of membership) of the fuzzy sets of the state variable for the methane reactor. Overload is indicated with a thick line, normal with a smaller line and shortage with a dotted line. (d) shows the gas production rates and (e) the COD in the inflow, acidification buffer tank and the methane reactor.



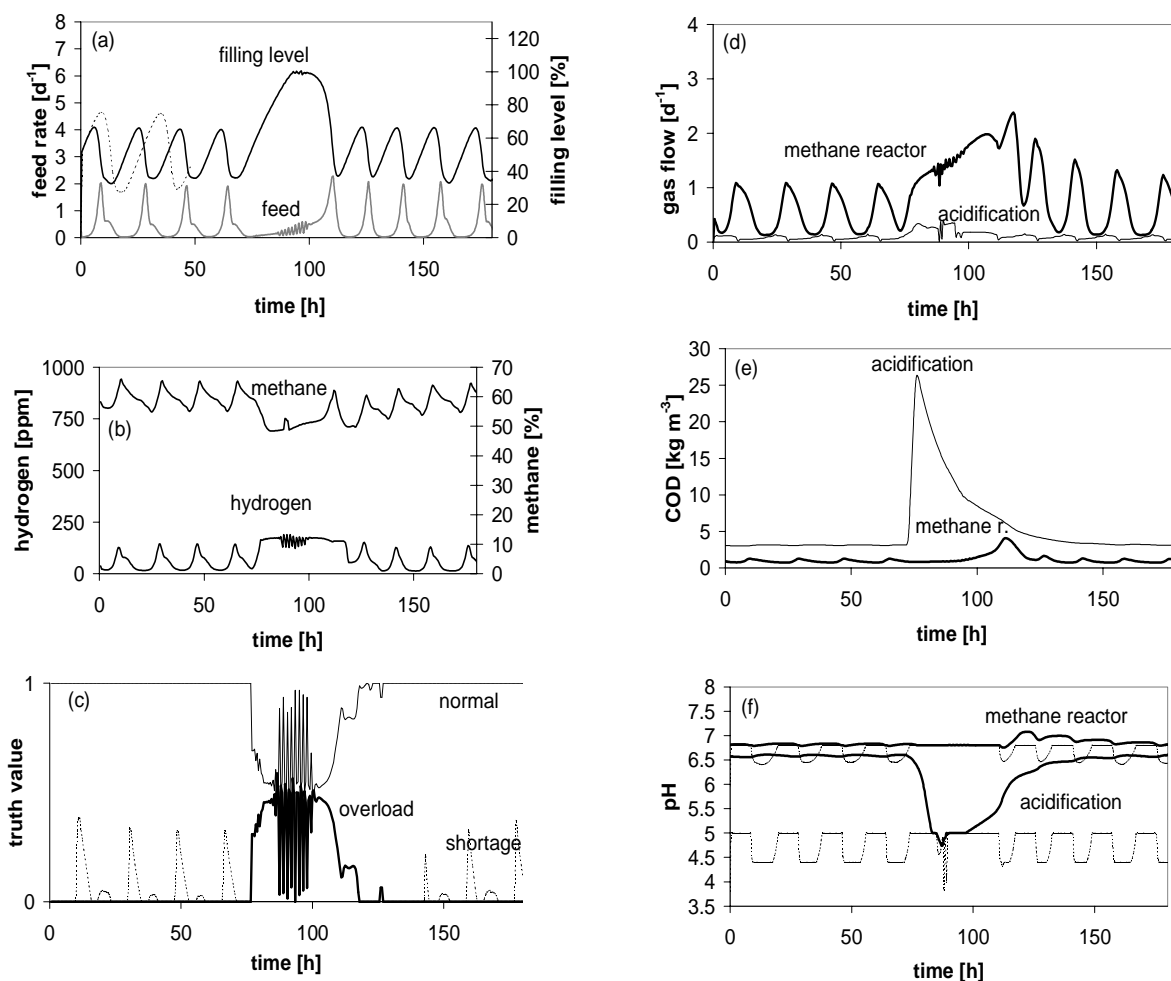


Figure 37. Simulation of COD pulse. At 72.5 hours COD in the influent was increased from 3 to 130 g l^{-1} for 3 hours. Sampling rate: 0.5 h^{-1} . (a) Filling level (acidification) and feed rate into methane reactor. Dotted line shows filling level when sampling rate was changed to 1 h^{-1} . (b) methane and hydrogen in the off-gas of the methane reactor. (c) detected states of the methane reactor. (d) flow rates normalised with methane reactor volume. (e) calculated COD in both reactors. (f) pH setpoints (thin lines) and calculated values (thick lines).

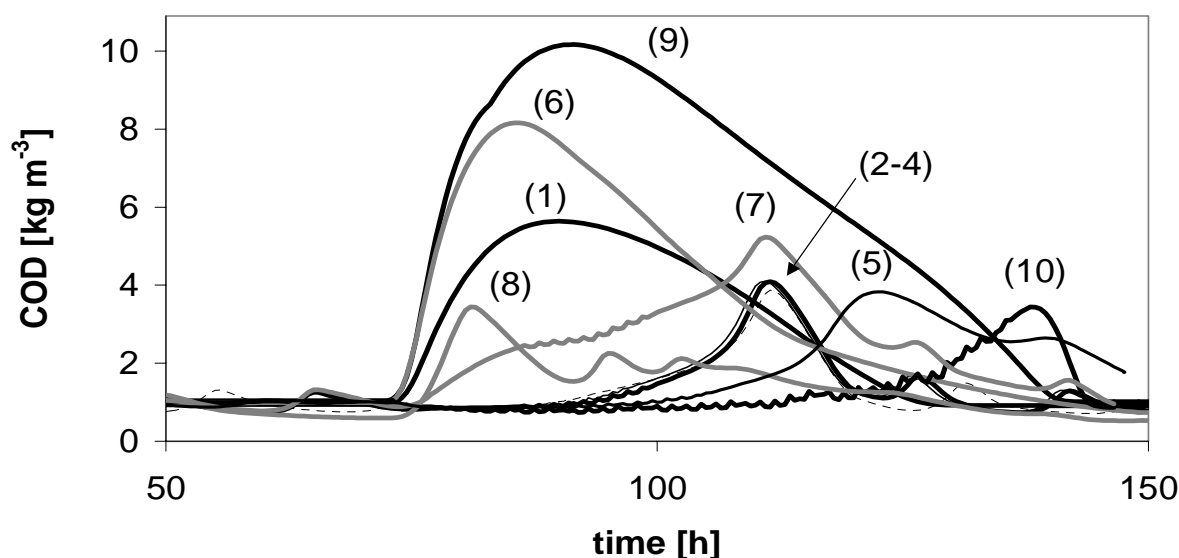


Figure 38. Simulation of pulses – COD in the methane reactor. At 72.5 hours COD in the influent was increased for 2.5 hours. Pulse of carbohydrates ($4000 \text{ C-mol m}^{-3}$): (1) not controlled, (2) controlled (thick line), (3): changed fuzzy set for feed (dotted line, see text), (4): glucose instead of complex carbohydrates (thin unbroken line), (5) controlled but not the pH. Pulse of proteins ($4000 \text{ C-mol m}^{-3}$): (6): not controlled, (7): controlled, (8): controlled but not the pH. Pulse of ethanol ($4000 \text{ C-mol m}^{-3}$): (9) not controlled, (10) controlled.

3.7.2 Prediction of More Extreme Process Variations

Experiments with extreme loadings were not carried out in real experiments to a greater extent because of the risk of a substantial overload, which could halt the treatment system for weeks. Moreover, experiments take much time and cannot be carried out in high numbers. Therefore several pulses of common substrates were simulated.

Simulations were carried out, whereby the influent COD was increased considerably for 3 hours. Figure 37 shows a simulation, whereby the carbohydrates in the influent were raised from 90 to $4000 \text{ C-mol m}^{-3}$ at 72.5 hours. Before the pulse, the filling level of the acidification buffer tank oscillated around 50 % because feed rate into the methane reactor was oscillating, too. The reason for this was the long sampling rate (exchange of values between simulation and fuzzy controller) of 0.5 h^{-1} which was chosen due to performance reasons and which made the controller slow - the dotted line in Figure 37a shows the filling level after a further decrease of the rate to 1 h^{-1} . Nevertheless, after the pulse a partial overload was detected (Figure 37c) and subsequently feed was lowered and hence the filling level of the acidification buffer tank went full (Figure 37a). As the tank was full, there was no feed into the acidification for some hours. Compared to the high COD concentration during the pulse, the effluent could be kept relatively low during the simulation experiment (Figure 37e) due to lowered feed and control of both, pH (Figure 37f) and

temperature. Temperature of the methane reactor (not shown) was already at the optimum before the pulse but of the acidification it was increased as the buffer tank filled up.

Simulations, as described before, but with glucose, protein and ethanol (each with 4000 C-mol m⁻³) respectively, had similar results. COD of the controlled pulse experiment is compared with the particular uncontrolled simulation experiment (Figure 38). In all these cases, COD of the methane reactor could be kept lower using the controller. In these simulations, a hydraulic residence time (HRT) of 1.1 days was applied (methane reactor) except for the protein, whereby a HRT of 2.2 was used. Although fat could be handled successfully (with 4 days HRT), results are not shown as the concentration of long chain fatty acids increased up to 25 C-mol m⁻³ which is inhibitory but not accounted for in the model. As there was still a COD peak in the controlled simulations, the set “more” of the output variable “feed_setp” (change of the feed into methane reactor) was changed that way the center of gravity became 1.5 instead of 2.0. Though feed was not doubled in case of 100 % “more” feed, but increased by 50 %, results were similar (compare Figure 38, curves (2) and (3)). In all cases, an overload could be detected which, as one can expect, was stronger in the uncontrolled simulations (truth value of the set “overload” of 100 %) than in the controlled ones (truth value 50 %, like in Figure 37c).

However, the system would not detect an overload if pure acetate was added as no hydrogen is formed in that case.

A further experiment was carried out, whereby pure water instead of wastewater was added after 72.5 hours for 3 hours. Subsequently shortage was detected and therefore feed into the methane reactor was increased, resulting to a lower filling level (Figure 39). Although COD decreases in the acidification, it was kept relatively constant in the methane reactor due to increased throughput.

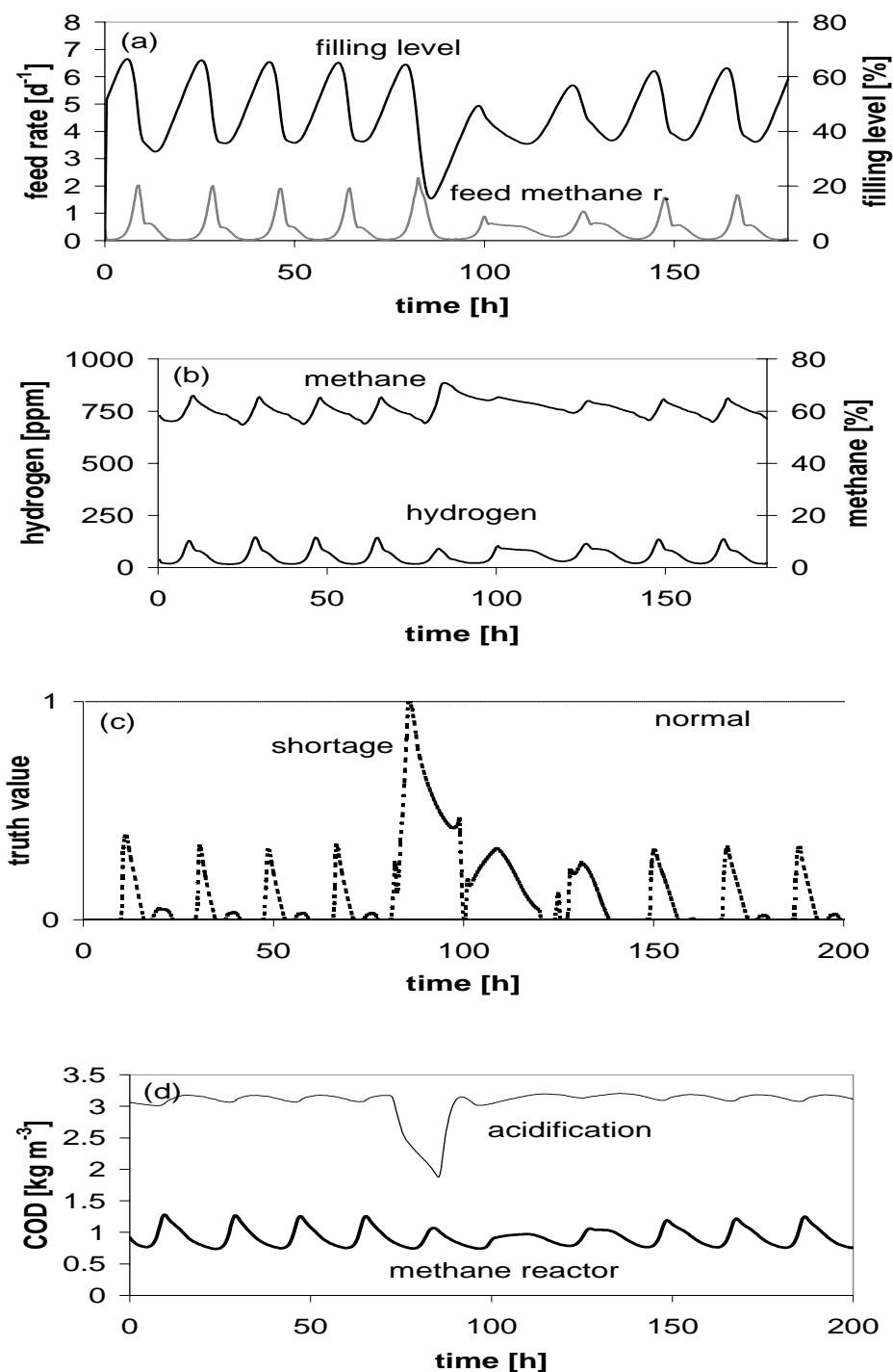


Figure 39. Simulation of a water pulse. At 72.5 hours water was added for 3 hours. (a) filling level of acidification buffer tank and feed into methane reactor (normalised with methane reactor volume). (b) methane and hydrogen concentrations of methane reactor. (c) detected states of methane reactor. (d) COD of both reactors.

3.7.3 Conclusions

Experimental results using the fuzzy logic control system designed for prevention of overloads could be validated by simulation. The model was able to predict both, non-controlled and controlled experiments.

Effluent quality could be improved considerably in the simulations by changing the transition from “high” to “normal” in the fuzzy variable “hydrogen” to lower values. A change of “more” feed into the methane reactor from twofold to 1.5fold had no effect.

In the simulation model, more extreme wastewater variations could be applied than in the experiment. Although pulses of different substrates could be detected, pure acetate would not have been detected as no hydrogen was formed then. However, hydrogen inhibition would be absent too in this case. Not only peaks with high COD, but also dilution with pure water, was controlled in order to keep the effluent quality relatively steady.

However, although the effluent increased considerably in the simulations where the controller was switched off, the system always recovered which not only might be due to the higher robustness because of the biofilm, but also because irreversible inhibitions are not included in the simulation model.

4 Conclusions and Outlook

With the fuzzy-logic system presented, a two stage laboratory scale anaerobic wastewater treatment plant was controlled that an heavy overload could always be avoided. Its overload state could be recognized by the measurement of hydrogen, methane, pH, and the gas rate, whereof economical sensors are available. Very strong fluctuations in the loading are handled automatically, even a restart of the feeding with very high COD loading (> 100 g/l) after several days of stand-by was possible, whereas in conventional plants already a doubling of the feed can halt the system, presumed the system runs near the performance limit. Moreover, measurement of the wastewater concentration (COD, TOC etc.) was not necessary in order to obtain low effluent concentrations. The adjustment of optimal conditions in respect to avoid an overload leads evidently to a good treatment efficiency. With the dynamic simulatin model, the control system showed identical behaviour as in the experiments. However, effluent quality was less in the simulations with the original fuzzy sets, compared to experiments, but could be improved considerably by changing of only two sets of the fuzzy variable “hydrogen”.

At times where low loading occurs, the reactor conditions are lowered in order to safe resources and to avoid methane production in the acidification buffer tank, while lye is only added, when an overload occurs and the buffer is full at the same time.

Though the control system was developed for and tested with an fixed bed reactor, the control strategy presented can certainly be adapted to other reactor configurations, too.

An anaerobic wastewater treatment system which is controlled this way is certainly very suitable for applications, where strong variations in volume or concentration of the wastewater occur or where an additional feed can be utilized in order gain additional biogas, because in both cases overloads occur often.

Further research should be carried out in order to evaluate and improve the detection of inhibition due to toxic substances. For these investigations, the dynamic simulation model presented in this thesis could be used, if inhibition by toxic substances was included. Moreover, it would be possible to test the control system with different reactor configurations by adaption of the model.

5 Materials and Methods

5.1 Reactor

A fully automated two-stage lab-scale wastewater treatment system was constructed (cf. P&ID - Figure 7 on page 25). The reactors were constructed by means of a transparent PVC pipe ($\varnothing_i = 150$ mm, $L = 250$ mm, $s = 5$ mm), which were connected with the head, the intermediate and the bottom by means of thread-rods ($\varnothing 10$ mm) and nuts (Figure 40).

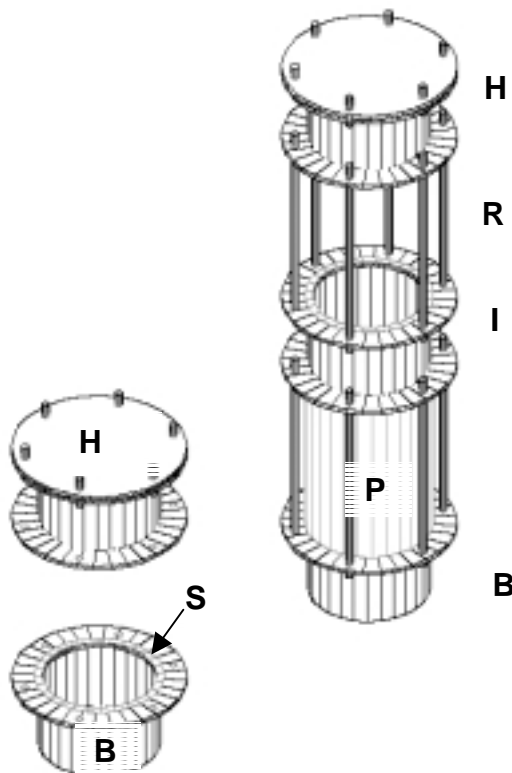


Figure 40. Sketch of the components of the reactors. H = head, B = bottom, I = intermediate ring, P = pipe (transparent PVC), S = seal, R = rod.

The head, the intermediate ring and the bottom was made of a stainless steel pipe ($\varnothing_i = 150$ mm, $L = 100$ mm, $s = 4$ mm) with one (bottom) or two (head and intermediates) flanges. The flanges ($\varnothing_o = 230$ mm, $s = 4$ mm) had 6 holes $\varnothing = 10$ mm, which were arranged symmetrically ($= 60^\circ$) at the radius $R = 100$ mm. The bottom was not closed with a flange but welded together with a steel plate (4 mm). Furthermore, there were sealing disks made of rubber ($\varnothing_i = 150$ mm, $\varnothing_o = 165$ mm) between the PVC pipes and the steel parts.

The 8 l acidification reactor (acidification buffer tank) was equipped with a pH sensor (with Teflon diaphragm from Jumo, Germany), a temperature sensor (Pt 100 equipped with 4..20 mA transmitter; Endress & Hauser, Germany), fuel level sensors

(hydrostatic; Endress & Hauser, 0..0.15 bar, 4..20 mA transmitter) and a stirrer (Heidolph Germany).

Heating for both reactors was achieved by the use of heating tapes (350 W, from Watlow, Germany), which were stuck on the bottom and the intermediate ring of the reactors by means of a special glue (Watlow).

The methane reactor was a fixed bed reactor with circulation and had a volume of 15 l. The pH and temperature was controlled, too. The fixed bed was a rolled web made of coconut fibres (section 5.2).

The reactors were connected with PVC pipes ($\varnothing_i = 10$ mm).

Pumping was done by means of two peristaltic pumps (Heidolph PD 5106), whereby a tube ($\varnothing_i = 8$ mm), made of Tygon, was used. The speed of the pumps was controlled by a 4..20 mA signal from the PLC. Magnetic valves (24 V DC) with checkback signal (Bürkert, Germany: Type 121, $\varnothing_{\min} = 8$ mm) were used for the liquid and also the gas pipings. Flexible PVC tubes ($\varnothing_i = 4$ mm) were used for the biogas piping. A small peristaltic pump (Möller, Fulda, Germany, SPR-66, 24 V DC) was used for dosage of lye.

Substrate was kept in a refrigerator and pumped automatically into the acidification buffer tank by use of the peristaltic pump. Using appropriate valves, the circulation pump of the methane reactor was also be used for recirculation of substrate back to the acidification tank and for feed into the methane reactor. Feed from the acidification buffer tank into the methane reactor was done in portions of 300 ml (2 % of methane reactor volume) with a maximum frequency of 12 times per hour. In the pipe, after the circulation pump, sensors for pH, ORP (oxidation reduction potential, from Jumo), and conductivity (four sensor electrode from Orion, USA) were placed enabling to measure these values from both reactors.

Off-gas of both reactors could interchangeably be switched on the installation for gas measurement. The gas was cooled to 15°C at the outlet of the reactors in order to condense water.

The cooler (Figure 41) was a 30 x 50 x 10 mm box, made of stainless steel, with a chamber milled into it. The chamber was filled with splinters made of stainless steel. The chamber was closed by means of a seal, a metal plate and screws. A peltier element (0..24 V), a cooler (as they were used in 486-personal computers) and a CPU fan were mounted at the opposite side of the seal and the steel plate. A tube was connected on the top and on the bottom via a nozzle.

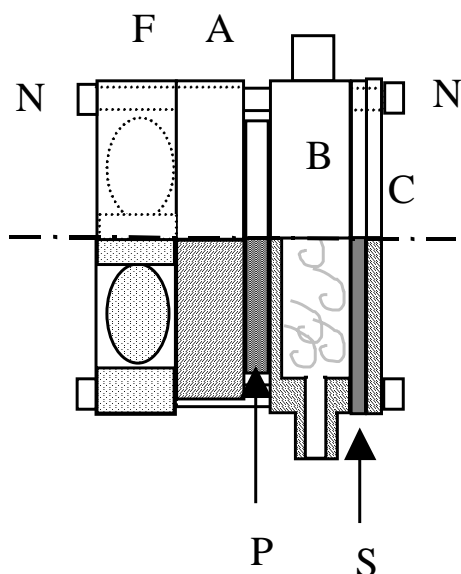


Figure 41. Sketch of the gas cooler. N = nut and screw, F = fan, A = aluminium block cooler, P = peltier element, B = gas cooler block, S = seal, C = plate.

Gas flow was measured by the thermal conductivity method (Kobold, Germany), hydrogen and hydrogen sulphide by electrochemical sensors (City technology, London), methane by measurement of infrared absorbance (Pewatron, Switzerland). As the flow of the gas to the sensors was not supported by a pump, measured values were rejected until 0.3 l or 0.05 l (after restart and short term interruption resp.) of gas flushed the installation. Switching of the valves and the subsidiary controllers were done on a PLC (Siemens S 7-314IFM), while the human-machine-interface (WinCC) and the fuzzy logic controller were running on a PC (Windows NT).

5.2 Fixed Bed

The fixed bed was a coconut fibre mat, which represented a 15 x 15 mm grid of cords with a varying diameter of 5 to 8 mm. Each cord was a netting of two thinner cords (2 to 3 mm diameter). For the two parts of the fixed bed 0.95 x 0.75 m of the mat was used. The surface of the rope ($L = 97$ m, $d = 6.5$ mm) would be 2.0 m². The volume was 0.0013 m³.

5.3 Analytical Methods

Chemical oxygen demand (COD) was measured using test kits LCK 514 and LCK 014 of Dr. Lange, Düsseldorf, Germany. If not mentioned otherwise, samples were filtered. Usually unfiltered values were 10 to 35 % higher.

Fatty acids were analysed using GC Analyses (Grepmeier, 2002).

5.4 Experiments and Simulations

Experiments with different types of wastewater (from potato processing, from a pectin factory, from a brewery) and different loads (0 to more than 100 kg COD m⁻³) were made. Some of these experiments were simulated. Concentrations of organic compounds are given in mol carbon m⁻³ or kg compound m⁻³.

5.4.1 Experiment E0

Wastewater from a potato-processing factory (Heigl, Abensberg, Germany) was added at different rates after a start-up phase of more than 1000 hours. The Fuzzy controller was not present at this time.

The pH value of the substrate was pH 6.5 ± 0.5. The pH value in the acidification buffer tank was in the range of 5 to 6 and in the methane reactor it was 6.4 to 7.5. Temperature was 30 °C in the acidification buffer tank (with short term decrease to 20 °C due to substrate addition) and 35 ± 1 °C in the methane reactor. COD concentrations and flow rates are given in Table 17 on page 99.

5.4.2 Experiments E1, E2, E3

Effluent from potato processing industry was used in the experiments E1 and E2 at the beginning (3.3 g and 4.5 g COD l⁻¹ filtered and unfiltered, resp.). The composition was similar to that of experiment E0, as it was from the same factory but at different times. COD varied from 3 to 4 g COD l⁻¹.

During the experiments, the wastewater was switched to a concentrated effluent from the production of pectin (mash from citrus fruits and apples in the ratio 3:2), which was diluted with water to 28 g COD l⁻¹. In Experiment E2, the wastewater was switched several times. Beer (13 % extract, 5 % alcohol, 120 g COD l⁻¹) was used in experiment E3.

Concentrations and flow rates of these experiments are given in Table 17 on page 99.

The pH value was set to 5.5 and 7 for the acidification and the methane reactor in experiment E1, while the temperature was set to 30 and 37 °C respectively. In the other experiments (subchapter 3.7.2), pH and temperature was automatically controlled by the fuzzy logic expert system.

5.4.3 Simulations S0, S1 and Substrate Peaks

If not mentioned otherwise, for the simulations 10, 20 and 92 C-mol m⁻³ fat, protein and complex carbohydrates were used. In order to achieve a suitable buffer capacity, 17 mol ammonia m⁻³ and 114 mol phosphate m⁻³ were added to the influent. The pH of the influent into the acidification was adjusted to 7.0 by addition of

cations. Hence, pH in the reactors was a result of the conversions or of the settings of the pH controllers. In simulation S0, the pH of the acidification was set to 5.5 and for the methane reactor a setpoint of 6.7 was used. For the simulation S1, the pH was set to 5.5 and 7 respectively. In the simulations of peak additions, either pH was controlled by the fuzzy logic expert system or not set at all (see description of results in Chapter 3). Temperature was set to 30 and 35 °C in S0, and 30 and 37 °C in S1. Temperature and pH value were controlled by the fuzzy logic expert system in the other simulations (subchapter 3.7.2). In these simulations, the same wastewater composition as for S1 was used, except for the period of 72.5 to 75.5 hours, where different substrate peaks were applied.

5.4.4 Experiments K5, K7 and Simulations SK5, SK7

The experiments K5 and K7 were not conducted by the author of this thesis. Results were taken from Kalyuzhnyi and Davlatshina (1997). They used a synthetic base medium consisting of 2 kg m⁻³ (37.4 mol m⁻³) NH₄Cl, 3.6 kg m⁻³ (15.8 mol m⁻³) K₂HPO₄*3H₂O, 2.8 kg m⁻³ (20.5 mol m⁻³) KH₂PO₄, 0.3 kg m⁻³ (1.47 mol m⁻³) MgCl₂ * 6 H₂O, 0.08 kg m⁻³ Na₂S * 9 H₂O. Experiments were conducted in a 525ml-flask containing 200 ml of base medium, 0.04 g sludge as an inoculum and varying amounts of substrate. Experiments K7 and K5 were started with a substrate concentration of 11 mol m⁻³ glucose (C-mol).

For the simulations, 37.4 mol m⁻³ NH₄⁺, 37.8 mol m⁻³ PO₄³⁻, 11 mol m⁻³ glucose were applied. pH was adjusted by addition of strong anions or cations. Initial biomass concentrations were used as given by Kalyuzhnyi (1997): 0.44 mol m⁻³ acidogens, 0.084 mol m⁻³ ethanol degraders, 0.13 mol m⁻³ butyrate degraders, 0.19 acetoclastic methanogens and 0.30 mol m⁻³ hydrogenotrophic methanogens. The concentration of the other acetogens, which were not taken into account by Kalyuzhnyi, was assumed to be as high as for the acetogenic butyrate degraders (0.13 mol m⁻³).

For the liquid to gas mass transfer coefficient, the $k_{Lg}A$, a value of 650 h⁻¹ was applied for the methane ($D_{ch_4} = 2 \cdot 10^{-4} \cdot 3600$ [m² h⁻¹]), which was calculated from the equations given in section 3.6.4.3 assuming that the flask was a half-sphere ($V = 0.0002$ m³, $d = 0.115$ m). Mass transfer for the other gases was calculated according to eq. 77.

5.5 Online-Measurements and Data Logging

5.5.1 Calibration

Calibration gas from Linde, Munich, was used for calibration of the gas sensors,. The 10 l gas cylinder (50 bar) contained synthetic biogas with a concentration of 80,0 ± 0.8 % methane, 19,9 ± 0.2 % carbon dioxide, and 1000 ± 10 ppm hydrogen.

Calibration buffer solutions from Merck (pH 4.00 and 7.00) were used for calibration of the pH sensors.

Cold (12 °C) water and hot (60 °C) water was used for calibration of the temperature sensors. Temperature of the sensors was adjusted by comparison with a calibration thermometer (± 0.1 °C).

5.5.2 Measurement Value Processing and Logging

The signals (4..20 mA) were scaled to physical values on the PLC. Signals for gas flow and feed rates were added to a counter. Measured values and counters were collected by the PC every minute and handed over to a particular DLL (dynamic link library), which was developed by the author of this thesis using C++ (<http://www.lfp.blm.tu-muenchen.de/pa/Software/sonstiges/messStat.htm>).

At initialisation time, the DLL had created a matrix, where the columns represented the sensors and counters and the rows the particular measurements (one per minute). In order to calculate statistics over one hour, the matrix consisted of 60 rows, which however could be changed during run-time. In particular, the DLL was needed in order to calculate the average feed rates and gas production rates over one hour by calculation of the second derivative a of the counters x according to

$$y = a \cdot x^2 + b \cdot x + c \quad (105)$$

The change of the pH value in the acidification was calculated in a similar way. As a change in the pH value could have been due to substrate addition, the pH change (difference of the current value and the old value one minute ago) was added to a fictive pH value every minute, when no feed into the acidification was active. From this fictive pH value x the first derivative b (eq. 106) was used as input variable “d_pH” for the fuzzy system. Consequently, “d_pH” represents the change of the pH due to the activity of microorganisms.

$$y = b \cdot x + c \quad (106)$$

All the measured values and the input variables for the fuzzy logic system were logged to a log file (tabulator separated text file with date and time in the first column) every 5 minutes. Additional data logging was done by use of the HMI software.

5.6 Implementation of the Human Machine Interface

The HMI was developed by the use of the software Siemens WinCC and was designed using a top-down approach, whereby the user interface was defined first.

Colors of the user interface were chosen according to Charwat (1996a-c). The start screen shows a graphical overview of the plant (light grey background). Menus, states and error messages are arranged on the borders (dark grey background).

Inactive components (valve closed, motor off) are shown in dark grey color on a light grey background. Active components (valve open, motor on) are shown in green. Errors and dangerous situations are indicated red, while warnings are yellow and other messages are white. Measured values are shown in a dark grey box if they are OK, otherwise the box becomes red. Setpoint values are in a blue box.

If an error occurs, a flag is set by the PLC or by the PC. Errors are shown in the alarm logging window. All relevant states and variables, in particular the measured values, are logged by the HMI and can be shown graphically by opening a new window on the screen.

There were several scripts (ANSI C) implemented by the author of this thesis, which were executed cyclic. Data processing (a DLL) was called every minute and data were logged every 5 minutes (subchapter 5.5.2). Fuzzy logic, which is an independent computer program (subchapter 5.7), was called every minute via OLE Automation. Here, some plausibility checks had been calculated before values were used as input values for the fuzzy system and before output values of the fuzzy system were used as setpoint values for the subsidiary controllers. In case on non-plausibility, the values were not used and an error flag was set, which lead to an error message on the screen.

Output values were only transferred to the PLC as new setpoint values if the fuzzy control button had been activated, otherwise values set by the human operator were used instead.

Time of averaging could be changed for each of the measured values.

The counter for substrate addition was calculated by an Microsoft Excel spreadsheet cyclic and transferred every five seconds to the HMI, from where it was transferred to the PLC.

5.7 Implementation of the Fuzzy Logic Software

The program “LFP-Fuzzy”, which was originally developed by Dr. Thomas Becker, was extended. Completely written in C++, the functionality, which includes all important methods for fuzzification, inference and defuzzification as well as an unlimited number of variables, rules and rulebases is encapsulated in a core which is device independent. The user interface was programmed for 32bit-Windows. Data exchange is done by COM-Automation.

With this work, more fuzzy methods were introduced into the Fuzzy core. However, for the thesis presented, standard definitions were sufficient and therefore used (cf. subchapters 2.3.3 and 3.4). A rule parser was programmed, which makes it possible to use the Fuzzy rules in the well known IF...THEN formate. Finally, the device independend code was embeded into a graphical user interface and equipped

with the COM automation interface in order to beeing able to exchange data online with other programs, respectively the WinCC HMI interface.

How the fuzzy logic software works, is outlined in the following.

5.7.1 Rule parser

A rule is splitted into premise and conclusion by searching the keyword “THEN”. A function “LeftParse” is called with the premise (without the IF) as parameter. LeftParse calls itself recursively until the function returns zero. It only returns zero if the term is solved.

LeftParse performses these tasks in that order:

- Removal of the outer brackets
- Looking for an operator which is outside the brackets. In case it finds one, it stores the operator in a command stack and calls itself two times – with the term left and right of the operator.
- If no operator and no brackets are found, the term is solved: the fuzzy variable and set is stored in the command stack.

Example, how LeftParse resolves the premise of the rule:

“IF conditions(1) = keep AND (pH(1) = optimal OR pH(1) = high) THEN pH_setp(1) = optimal”

- LeftParse is thus first called with “conditions(1) = keep AND (pH(1) = optimal OR pH(1) = high)”. It first searches an operator which is outside of brackets and finds the “AND”. The “AND” is stored in the command stack and LeftParse is called A) with “conditions(1) = keep” and B) with “(pH(1) = optimal OR pH(1) = high)” as parameter.
- When LeftParse is called with (A), the fuzzy variable “conditions” and the set “keep” is appended to the command stack. Here, the function returns with zero as this term is already solved. Therefore thread (A) is already finished.
- When LeftParse is called with (B), it removes the brackets from “(pH(1) = optimal OR pH(1) = high)” and calls itself again with “pH(1) = optimal OR pH(1) = high”.

- Now, it finds the OR as it is not inside brackets. Thus, OR is added to the command stack and LeftParse is called two times, C) with “pH(1) = optimal” and D) with “pH(1) = high”.
- Now, the fuzzy variable “pH(1)” and the set “optimal” is added to the command stack (C) and LeftParse returns with zero.
- Afterwards, the fuzzy variable “pH(1)” and the set “high” is added to the command stack (D) and this thread returns with zero, too.

At the end, the command stack looks like:

operator	AND
variable and set	conditions = keep
operator	OR
variable and set	pH(1) = optimal
variable and set	pH(1) = high

The parsing has only to be calculated at the beginning. The conclusion is treated similarly (RightParse).

5.7.2 Fuzzy inference

The fuzzy inference has always to be called, if an input value changes. Fuzzification, inference and defuzzification was implemented as described in subchapter 2.3.3. In the following, it is presented, how a rule, which had already been parsed, is evaluated:

- **Fuzzification** calculates the membership value of each set of each input variable (cf. subchapter 2.3.3.2).
- **Aggregation:** The command stack of each rule is evaluated by searching the operators beginning at the bottom (the youngest entry). In the present example no operator is found at the bottom and thus the read-pointer is moved

upwards until the operator “OR” is found. As the “OR” needs two parameters, the two lower entries are used: the membership value (e.g. 0.7) of the set “optimal” of the variable “pH(1)” is combined with the membership value (e.g. 0.4) of the set “high” of the variable “pH(1)” using the MAXIMUM. The result (0.7) is written at the place, where the operator is and all entries are moved down 2 rows. The command stack looks now like:

operator	AND
variable and set	conditions = keep
intermediate membership value	0.7

- When the next operator is searched, “AND” is found and the two rows below are combined with the “AND” operator: MINIMUM. Like before, the operator is replaced by the new membership value (e.g. 0.3) and the entries are moved down two rows. Hence, the command stack looks like:

intermediate membership value	0.3
-------------------------------	-----

- **Activation:** As there is only one entry left in the command stack, this entry is the result of the rule. Hence the rule fires with 0.3.
- **Accumulation:** The set in the conclusions part is activated with the membership value of 0.3, if it was not already activated higher by another rule in that calculation cycle.
- **Defuzzification:** One crisp value is calculated from every fuzzy output variable taking into account all the sets of this variable (cf. subchapter 2.3.3.4).

At the beginning of each inference cycle, the membership values of the sets of the output variables are set to zero and a copy of the command stack is made, as it is modified during the calculations.

5.8 Implementation and Tuning of the Controllers

5.8.1 Adaptive pH Controller for the Acidification Buffer Tank

Ladder logic (LD, LAD - IEC-1131) was used for programming of the PLC. However, the pH Controller was programmed in instruction list (IL, STL - IEC-1131), because much calculations have to be made. It is encapsulated into a particular function block (FB) and represents an own operational state. Request, entrance and exit of the state are handled as it is outlined in chapter 3.1 (Overall Concept).

The Settings for the controller are given in Table 19. The controller was tested with 0.2 % acetic acid (667 mol/m^3), which was set to the desired pH value by addition of sodium hydroxyde (NaOH, 10000 mol/m^3 and 1000 mol/m^3). For the controller, a NaOH solution with 1000 mol/m^3 was used as dosing agent.

Table 19. Settings of the pH controller of the acidification buffer tank and other relevant values.

Parameter	Symbol	Value	Unit
Concentration of the lye	C_{lye}	1000	mol/m^3
Maximum amount of lye to be added at once		0.020	m^3
Flow of the lye pump		0.0009	m^3/h
Max. Volume of the acidification buffer tank		0.0085	m^3
ratio fuel level to max. volume of the tank	h	0.5	
Initial volume of lye for changing the pH for 1 unit	$V_{\text{lye_rel}}$	$5 \cdot 10^{-6}$	m^3
	f	0.0008	$\text{m}^3/(\text{pH})$
death width (hysteresis for pH controller)		0.1	(pH)
response time of pH sensor		20/3600	h
delay time after taking the pH value, after switching of valves		120/3600	h
mixing time in the acidification buffer tank		< 20/3600	h
time for reinitialisation of $V_{\text{lye_rel}}$		1	h
flow rate of circulation pump		0.03	m^3/h

The response time of the pH sensor was tested by immersing it from a buffer with a pH of 4,0 into one with a pH of 7,0. The measured values were recorded and the response time was evaluated graphically, see Figure 42 in the appendix on page 127.

The flow of the lye pump was evaluated on the ready laboratory scale plant (inlet 0.8 m beneath pump, outlet into circulation pipe 0.2 m beneath pump level) with water. Mixing time of the acidification buffer tank was evaluated graphically after adjusting the stirrer to 80 rpm by adding lye with the lye pump and measuring of the pH value. It was 14 seconds at a flow rate of 0.060 m³/h of the circulation pump (Figure 43 on page 127).

5.8.2 PID Controller for the pH of the Methane Reactor

The pH controller for the methane reactor was implemented in the PLC as an own function block (FB) which calls the internal PID block of the PLC every two minutes. As no separate operational state (chapter 3.1) was assigned to it, the controller is always active, if it is switched on and if substrate of the methane reactor circulates through the test point in the circulation pipe.

Acetic acid and NaOH was also used for tuning of the controller. PID-Parameters were estimated using the method of Takashi, which is the adapted method of Ziegler and Nichols for digital controllers (Olsson and Piani, 1993). The equations are given in the appendix on page 126.

The response to the jump function after dosage of NaOH was recorded for circulation rates of 0.030 and 0.060 m³/h (see Figure 44 and Figure 45 in the appendix on page 128), the latter one was used for estimation of the PID parameters.

The settings for the controller and other values, which were relevant for the tuning, are given in Table 20.

Table 20. Settings of the pH controller of the methane reactor and other relevant values.

<i>Parameter</i>	<i>Symbol</i>	<i>Value</i>	<i>Unit</i>
Concentration of the lye	C_{lye}	1000	mol m ⁻³
Maximum runtime of lye pump in relation to whole time		1/6	
Flow of the lye pump		0.0009	m ³ h ⁻¹
relative buffer capacity of the substrate	f_{buff}	1	
flow rate of circulation pump		0.060	m ³ h ⁻¹
dead time, taken from Figure 45	T_u	7/60	h
slope, taken from Figure 46	\dot{x}_a	1.728	h ⁻¹

The controller was tested with 0.2 % acetic acid (667 mol/m³), which was set to the desired pH value by addition of sodium hydroxyde (NaOH, 10000 mol/m³ and 1000 mol/m³). For the controller, a NaOH solution with 1000 mol/m³ was used as dosing agent. Disturbances were applied by feeding 0.2 % acetic acid, which was set to pH 4 with NaOH (10000 mol/m³) with a period of 5 and 10 seconds of every 180 seconds respectively (pumpe rate was also 0.060 m³/h).

5.8.3 PID Controllers for the Temperature

The Temperature controllers for both reactors were implemented in the PLC as function blocks (FB), which call the internal PID block of the PLC every second. Heating is applied if the stirrer is on (acidification buffer tank) or the substrate is circulated (methane reactor).

PID-Parameters were estimated using the method of Ziegler-Nichols (Mann et al, 1997). The input variable of the PID controller is the temperature and the output variable is the fraction of the max. heater power. The response to the jump function showed a small lag time (Figure 46 in the appendix on page 129). Hence, the controlled systems represents a P-T₂ element (lag time of second order), which is typical for temperature control. Thereofre, a PID controller is will be used (Mann et al, 1997).

According to Ziegler-Nichols, a P-controller was first applied whereby the proportional action coefficient was increased, until oscillation occurred. The frequency T_{krit} and the proportional action coefficient K_{pkrit} are given in Table 21. From these, the PID settings were calculated from eqs. 107 - 109.

$$K_p = 0.6 \cdot K_{pkrit} \quad (107)$$

$$T_n = 0.5 \cdot T_{krit} \quad (108)$$

$$T_v = 0.125 \cdot T_{krit} \quad (109)$$

Table 21. Settings of the temperature controllers of both reactors and other relevant values.

Parameter	Symbol	Value for acidification	Value for methane reactor	Unit
max. heater power		350	700	W
Stirring		30	-	rpm
fuel level		50	100	%
flow rate of circulation pump		-	0.030	m ³ /h
Kp when oscillation occurred	K_{pkrit}	42		°C ⁻¹
frequency of oscillation	T_{krit}	0.10	0.20	h
Parameters used:				
proportional action coefficient	K_p	25	15	°C ⁻¹
integral action time	T_n	2/60	6/60	h
derivative action time	T_v	0.5/60	1.5/60	h

APPENDIX

Derivation of the modified PID controller

$$y = K_p \cdot \left(e + \frac{1}{T_n} \cdot \int e \cdot dt + T_v \cdot \dot{e} \right) \quad (110)$$

$$K_p = \frac{0,4}{T_U \cdot K_S} \quad (111)$$

$$K_S = \frac{\dot{x}_a}{y_a} \quad (112)$$

$$f_C = \frac{C}{C_a} \quad (113)$$

$$f_{\dot{V}} = \frac{\dot{V}}{\dot{V}_a} \quad (114)$$

$$K_p = \frac{0,4 \cdot f_{\text{puffer}} \cdot f_{\dot{V}}}{T_U \cdot K_S \cdot f_C} = \frac{0,4 \cdot f_{\text{puffer}} \cdot x \cdot \dot{V} \cdot C_a}{T_U \cdot \dot{x}_a \cdot \dot{V}_a \cdot C} \quad (115)$$

$$K_p = 5,509 \cdot 10^3 \cdot \frac{f_{\text{puffer}} \cdot \dot{V}}{C} \left[\frac{\text{mol} \cdot \text{h}}{\text{m}^6} \right] \quad (116)$$

$$T_n = \frac{3,2 \cdot T_u}{f_{\dot{V}}} = \frac{3,2 \cdot T_u \cdot \dot{V}_a}{\dot{V}} \quad (117)$$

$$T_n = \frac{22,4}{\dot{V}} \left[\frac{\text{l}}{\text{h}} \cdot \text{h} \right] \quad (118)$$

$$T_v = 0,8 \cdot T_u \quad (119)$$

$$T_v = \frac{0,8 \cdot T_u}{f_{\dot{V}}} = \frac{0,8 \cdot T_u \cdot \dot{V}_a}{\dot{V}} \quad (120)$$

$$T_v = \frac{5,6}{\dot{V}} \left[\frac{\text{l}}{\text{h}} \cdot \text{h} \right] \quad (121)$$

Additional Figures

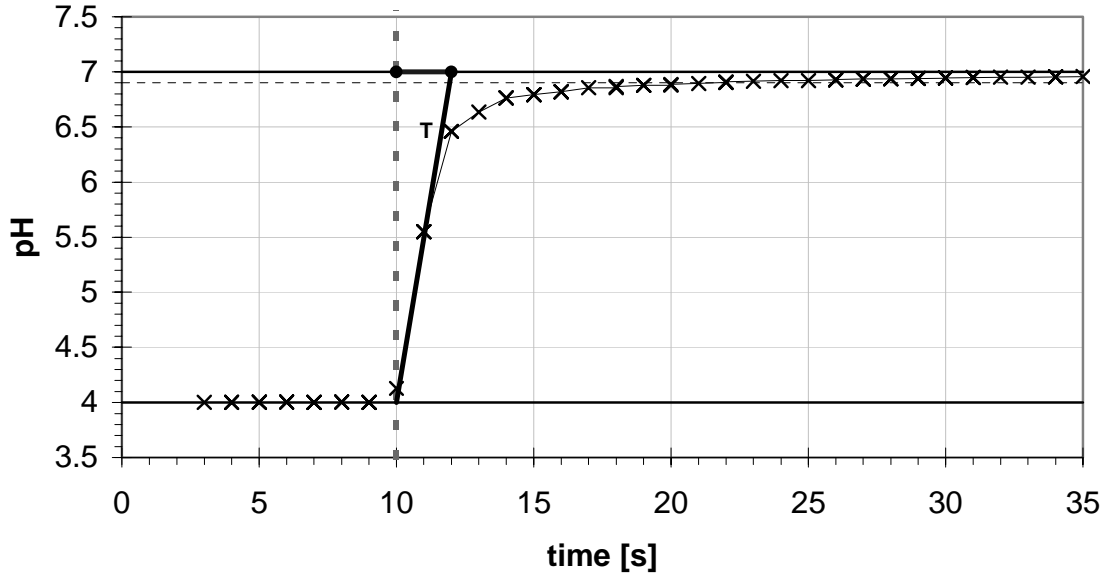


Figure 42 response to the jump function of a pH sensor (with PTFE diaphragma, from Jumo, Germany). At time 10 seconds (indicated with a dotted line) it was immersed out of buffer pH 4 into buffer pH 7. The tolerable pH of 6.9 (assuming a set point of 7.0) is indicated with a dotted horizontal line.

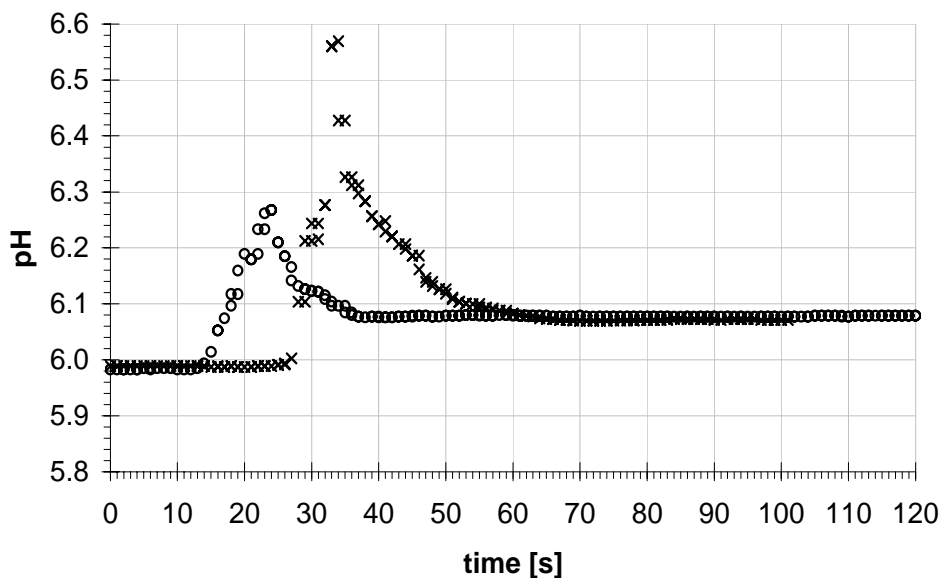


Figure 43 Mixing response of the acidification buffer tank. The pH is plotted against the time after dosage of NaOH (1000 mol/m^3) for 10 s ($0.0009 \text{ m}^3/\text{h}$) at a flow rate of the circulation pump of 0.060 (ooo) and $0.030 \text{ m}^3/\text{h}$ (xxx).

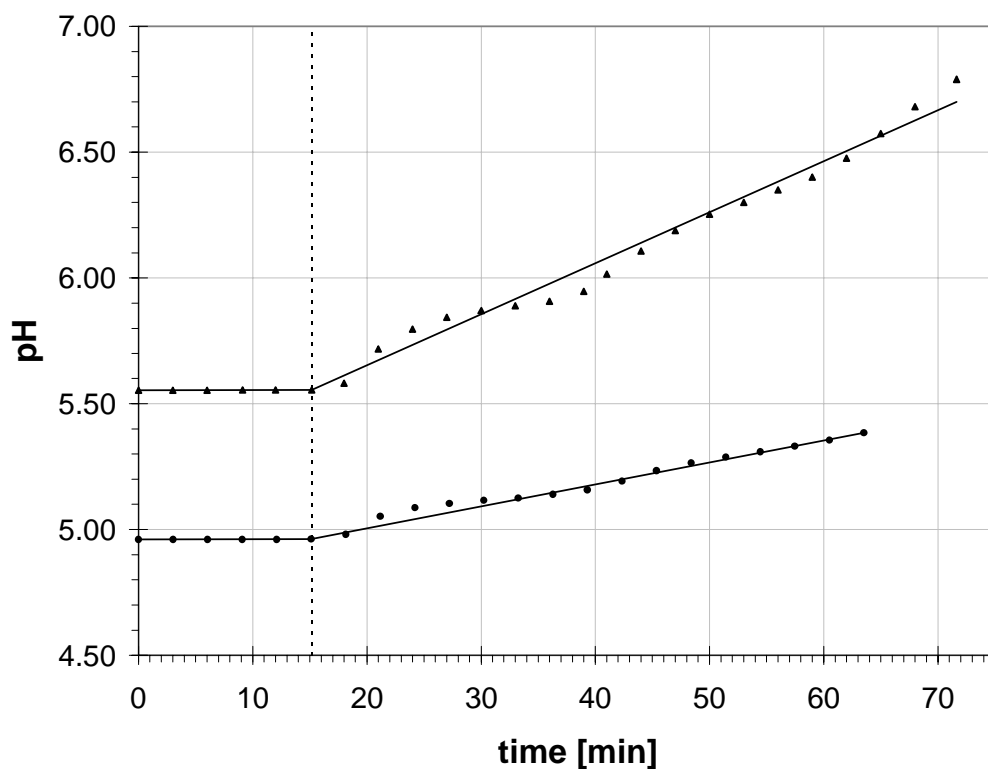


Figure 44 Response to the jump function of the methane reactor. Circulation rate was $0.030 \text{ m}^3/\text{h}$. Substrate: 0.2% Acetic acid ($667 \text{ mol}/\text{m}^3$) adjusted to the start pH using NaOH. Running time of the lye pump was 30 s every 180 s.

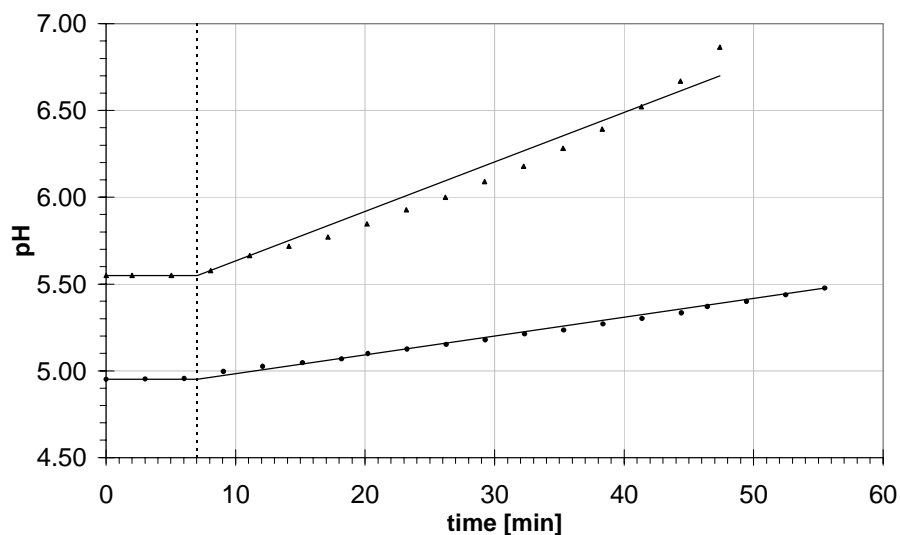


Figure 45 Response to the jump function of the methane reactor. Circulation rate was $0.060 \text{ m}^3/\text{h}$. Substrate: 0.2% Acetic acid ($667 \text{ mol}/\text{m}^3$) adjusted to the start pH using NaOH. Running time of the lye pump was 30 s every 180 s.

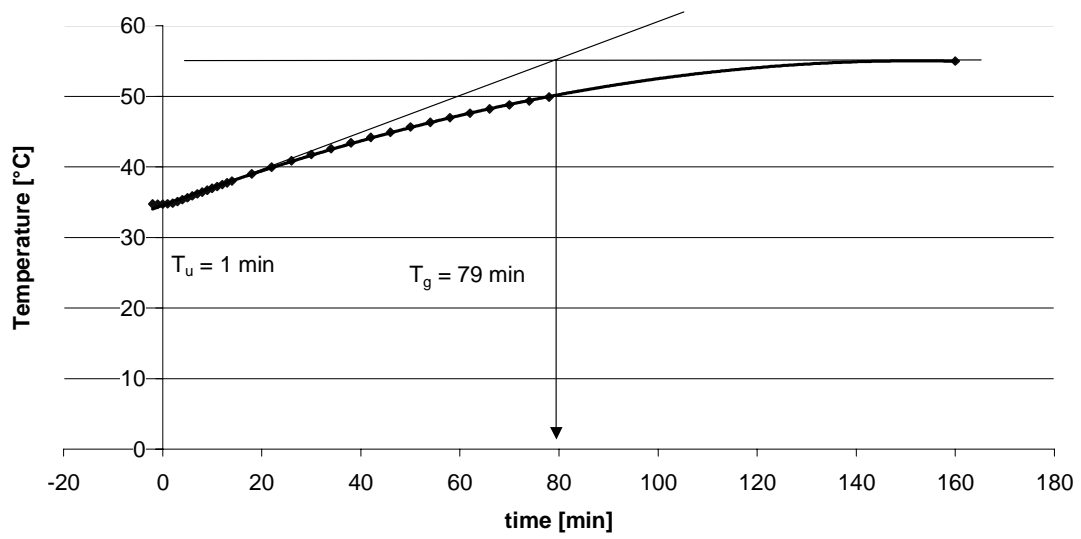


Figure 46 Response to the temperature jump function of the acidification buffer tank. Fill level was 50 %, stirring was switched on (30 rpm). Heating power was changed from 22.5 % to 27.5 % (of 350 W) at time 0.

Simulation of pH-Step Function-Response of the Methane Reactor

The pH step function response of the experiment was simulated:

Circulation rate: $0.030 \text{ m}^3 \text{ h}^{-1}$; Substrate: $667 \text{ C-mol acetate l}^{-1}$; NaOH dosage: 1000 mol m^{-3} with a flow rate of $0.00015 \text{ m}^3 \text{ h}^{-1}$.

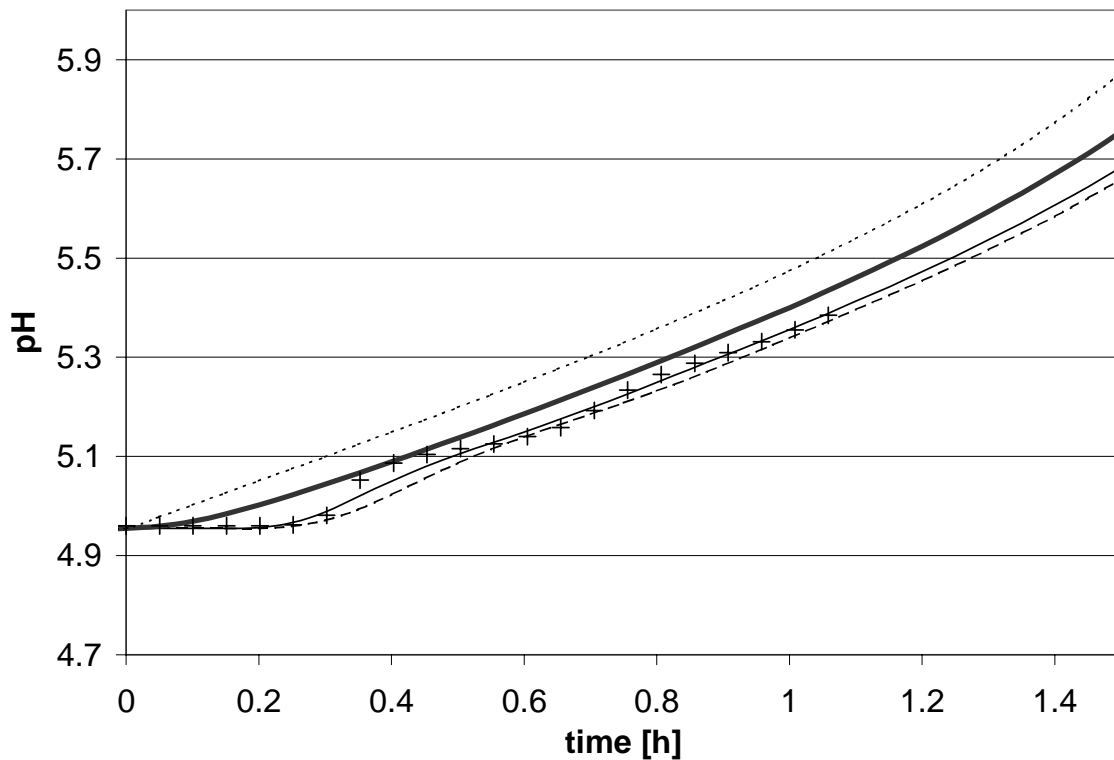


Figure 47. pH step function response of the methane reactor. Experiment (+) versus simulation. Dotted line : reactor consisting of one CSTR; thick line: two CSTR compartments of equal volume; thin line: CSTR and PFR of equal volume; broken line: CSTR (1/4 volume) – PFR (1/2) – CSTR (1/4).

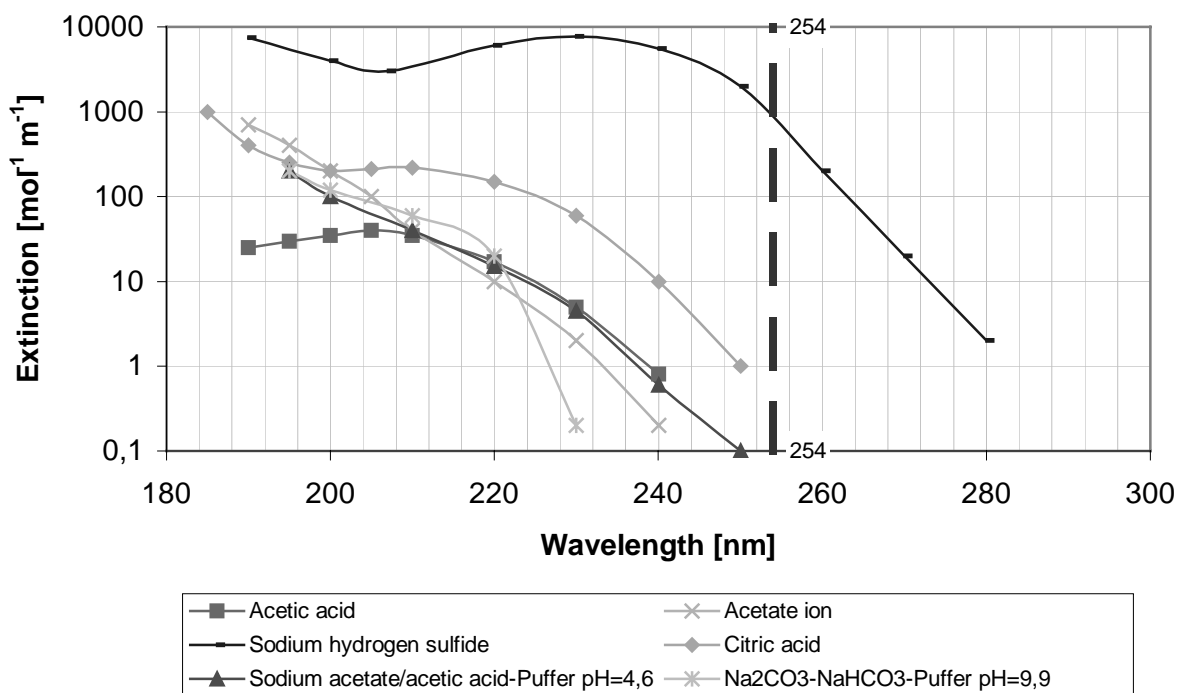


Figure 49. Comparison of the absorbance of some common substances. The ordinate is shown logarithmically.

(B) Measurement of density was taken into account as a replacement method for COD or TOC. Theoretical considerations and practical experiments showed, that the density cannot be used as a replacement for TOC or COD at such low concentrations of some kg per m³. For measurement of the density, a device of Anton Paar, Austria, was used. The accuracy of the device ($\pm 0.1 \text{ kg m}^{-3}$) seemed to be sufficient. However, due solid particles and gas bubbles, the repeatability of the density measurement of wastewater was not better than $\pm 1 \text{ kg m}^{-3}$, which is in the range of a temperature difference of 5 °C or a concentration difference of 5 kg m⁻³ for many substances. As the concentration of degradable organic compounds was around 5 kg m⁻³, density cannot be used as a replacement for TOC or COD measurement.

(C) A device (Elox 100) from LAR, Germany, which oxidised the pollutants in the wastewater by the use of hydroxyl ions, was also tested. This device produces OH-radicals as the oxidizing agent on an electrode, by an electrical current. However, acetate, a main component in anaerobic digestion produced a signal less than 10 % of glucose. Also ethanol delivered only small signals. Therefore, COD measurement with hydroxyl ions instead of chromate ions in hot acid solution (the standard COD measurement method) cannot be used for anaerobic digestion as common substance are not detected sufficiently.

Conductivity, pH and Volatile Fatty Acid Concentrations

Acetate and other volatile fatty acids are produced from the undissociated starch and other, low conductive, organic compounds. For a constant wastewater composition, the pH value could be used for the estimation of the amount of acids formed. However, due to adjustment of the pH by means of sodium hydroxide, the pH is altered but the conductivity increases. Thus, the pH value together with conductivity measurement is considered theoretically in the following.

Using a model system of e.g. known amounts of acetic acid and sodium hydroxide, the degree of dissociation can be calculated. From the degree of dissociation and the concentrations, the pH value and the conductivity can be calculated.

The specific conductivity decreases at higher concentrations, because the ions interfere the mobility.

Therefore, the concentration is multiplied by an activity coefficient f_m which depends on the compound and its concentration C , in order to get the real activity a of the ions.

$$a = f_m * C \quad (122)$$

The average activity (f_m) depends on the overall amount of ions in the solution, the ion-strength. For ion-strengths more than 10 mol m^{-3} the extended Debye/Hückel equation can be used (Näser, Lempe, Regen, page 307):

$$\lg f_m \approx \frac{-A * z_+ * z_- * \sqrt{J}}{1 + \sqrt{J}} \quad (123)$$

The constant A depends on the solvent and is $A = 0.509$ for water at $25 \text{ }^\circ\text{C}$. z represents the ion charge and J is the ion-strength (the sum of all ions in mol m^{-3}).

The number of ions can be calculated from the law of mass action with the use of the dissociation constant K_a . For



it can be written :

$$K_a = \frac{C_A^x * C_K^y * f_m^{x+y}}{C_{AK} * f_{AK}} \quad (125)$$

For acetate: $K_a = 1,8 * 10^8 \text{ mol m}^{-3}$ ($25 \text{ }^\circ\text{C}$). Propionic and butyric acid is similar: $1,4 * 10^8$ und $1,5 * 10^8$ (Atkinson). The – in case of acetic acid – produced acetate ion binds with hydrogenium ions (and is thus a base):



Combination of the introduced equations gives:

$$pH = pK_a + \lg C_A/C_{AK} \quad (127)$$

Finally, the ion concentrations are multiplied with the particular specific equivalent conductivity, which is 40.9 S cm mol⁻¹ for acetate, 349.8 for hydronium (H₃O⁺) and 50.1 for the sodium ion. For other ions, it is mostly between 40 and 80 (all at 25 °C) (Kunze, 1986).

Figure 50 shows calculated conductivities for acetate and chloride at different pH values.

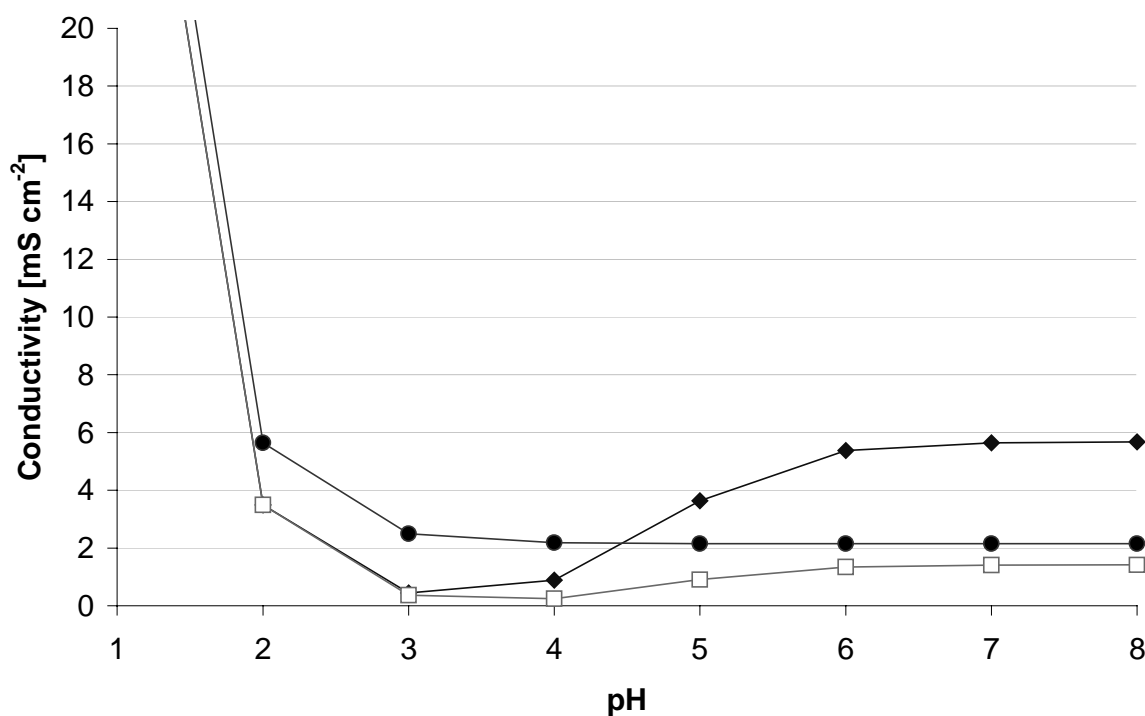


Figure 50. Calculated Conductivity of 4 (◆) and 1 (□) kg acetic acid m⁻³ and 1 kg hydrochloric acid m⁻³ (●) - all adjusted to the particular pH value by the use of sodium hydroxyde.

At pH values less than 2, the conductivity is dominated by the hydroxylum ion – the acetic acid is not dissociated. Above 6, acetic acid is nearly fully dissociated and, thus, conductivity results from the sodium, chlorid and acetate ions. At pH values of $pK_a \pm 1$ (for acetic acid: 3.75 – 5.75 ($-\log[mol l^{-1}] = 0.75 - 2.75$ ($-\log[mol m^{-3}]$)), the dissociated as well as the undissociated part of the acetic acid had to be taken into account.

When substrate acidifies, acetic acid is formed. According to eq. 127 the pH value decreases somewhat. The conductivity, however, remains constant as no additional

counterions are added and the pH does not change much. When the pH is adjusted with aid of sodium hydroxide, pH increases due to the sodium ions and the same amount of newly formed acetate from acetic acid.

Knowing the concentration of the other - in the considered pH range fully dissociated - ions, the concentration of volatile fatty acids could roughly be estimated from conductivity and pH value ($\text{pH} > 3$) as pK_a values do not differ much. However, at pH values around 7 the hydrogen-carbonate puffer-system (pK_a of $\text{H}_2\text{CO}_3 = 6.37$ calculated from $[\text{mol l}^{-1}]$) has to be taken into account.

Conversion of units

For convenience, in order to beeing able to compare simulation results with measured data, conversion functions are integrated into the simulation model.

Gas concentrations can be measured with or without removing the moisture prior to measurement.

$$\%_{i, humid} = \frac{C_i \cdot 100}{C_{h_2} + C_{ch_4} + C_{co_2} + C_{h_2o}} \quad (128)$$

$$\%_{i, dry} = \frac{C_i \cdot 100}{C_{h_2} + C_{ch_4} + C_{co_2}} \quad (129)$$

As wastewater concentration often is specified in units of kg COD/m³, the conversion is given:

$$COD = \sum C_i \cdot cf_i \quad (130)$$

The conversion factors from C-mol/m³ to kg COD/m³ is given in Table 22.

Table 22 Conversion factors (cf) for the calculation of kg COD/m³ from C-mol/m³.

Substance	mol O ₂ /mol C	cf
gluc	1	32
ac	1	32
pro	3.5/3	37.33
but	5/4	40
val	6.5/5	41.6
et	1.5	
lac	1	
lcfa (n:ω)	(2+(n-2)*1.5-ω*0.5)/n	(2+(n-2)*1.5-ω*0.5)/n*32
h ₂	0.5	16
nh ₄	2	64
protein (CH _{6/7} O _{1/2} N _{1/7})	1.14	36.6 (Henze et al, 1995)
X	1.1	
e	1.1	

Volatile Fatty Acid Concentrations of Experiment E0

Table 23. Measured concentrations and feed rate of the acidification buffer tank.

time h	<i>Ac</i> mol C m ⁻³	<i>Pro</i> mol C m ⁻³	<i>But</i> mol C m ⁻³	<i>Val</i> mol C m ⁻³	<i>COD</i> kg m ⁻³
1000	<i>Q_I</i> set to 10 l/d				
1270	13.6	15.0	26.0	15.0	2.98
1270	<i>Q_I</i> set to 20 l/d				
1320	1.2	13.2	16.0	10.5	3.07
1370	<i>Q_I</i> set to 5 l/d				
1460	16.0	24.3	29.2	19.5	4.12
1460	<i>Q_I</i> set to 20 l/d				
1465	16.0	18.6	28.0	20.0	4.21

Table 24. Measured concentrations of the methane reactor.

time h	<i>Ac</i> mol C m ⁻³	<i>Pro</i> mol C m ⁻³	<i>But</i> mol C m ⁻³	<i>Val</i> mol C m ⁻³	<i>COD</i> kg m ⁻³
270	2.4	0	0	0	0.28
320	1.6	0	0	0	0.84
460	2.4	0	0	0	0.16
465	2.2	1.5	1.6	2.0	0.46

REFERENCES

- Angelidaki, I., Ellegaard, L., Ahring, B.K. (1993) A Mathematical Model for Dynamic Simulation of Anaerobic Digestion of Complex Substrates: Focusing on Ammonia Inhibition. *Biotechnology and Bioengineering*, Vol. 42, pp. 159-166
- Angelidaki, I., Ellegaard, L., Ahring, B.K. (1999) A Comprehensive Model of Anaerobic Conversion of Complex Substrates to Biogas. *Biotechnology and Bioengineering*, Vol. 63 (3), 363 – 372
- Araki, N. and Harada, H. (1994) Population dynamics of methanogenic biofilm consortium during a start-up period of anaerobic fluidized bed reactor. *Water Science and Technology*, Vol. 29, No 10 – 11, pp. 361 – 368
- Archer, D.B., Hilton, M.G., Adams, P., Wiecko, H. (1986) Hydrogen as a process control index in a pilot scale anaerobic digester. *Biotechnology Letters*. Vol. 8 (3)
- Assilian, S., Mamdani, E.H (1975) An experiment in Linguistic Synthesis with a Fuzzy Logic Controller. *Internat. J. Man-Machine Stud.* vol. 7, 1-13.
- Batstone, D. (2000) High-Rate Anaerobic Treatment of Complex Wastewater. PhD Thesis. University of Queensland, Australia.
- Batstone, D.J., Keller, J., Newell, R.B., Newland, M. (2000) Modelling Anaerobic Degradation of Complex Wastewater. I: Model Development. *Bioresource Technology*, Vol. 75, 67-75
- Batstone, D.J., Keller, J., Newell, R.B., Newland, M. (2000b) Modelling Anaerobic Degradation of Complex Wastewater. II: Parameter Estimation and Validation Using Slaughterhouse Effluent. *Bioresource Technology*, Vol. 75, 75-85
- Bishop, P.L., Gibbs, J.T., Cunningham, B.E. (1997) Relationship Between Concentration and Hydrodynamic Boundary Layers Over Biofilms. *Environ. Technol.* 18, 375 – 386
- Braun, R. (1982) *Biogas - Methangärung organischer Abfallstoffe*. Springer, Wien
- Buckley, J.J., Hayashi, Y., Czogala, E. (1993). On the equivalence of neural nets and fuzzy expert systems. *Fuzzy Sets and Systems*, Vol. 53, p. 129 - 134
- Charwat, H. J. (1996a) Farbkonzept für die Prozessführung mit Bildschirmen (Teil 1). *atp* 38 (5), 50 – 53
- Charwat, H. J. (1996b) Farbkonzept für die Prozessführung mit Bildschirmen (Teil 2). *atp* 38 (6), 58 – 63

- Charwat, H. J. (1996c) Farbkonzept für die Prozessführung mit Bildschirmen (Teil 3). *atp* 38 (7), 62 – 65
- Christensen, B.E., Charaklis, W.G. (1990) Physikal and Chemical Properties of Biofilms. 93 – 130. In: Charaklis, W.G., Marshall, K.C. (eds.), *Biofilms*. Jon Wiley & Sons, New York.
- Christensen, B.E., Charaklis, W.G. (1990) Physikal and Chemical Properties of Biofilms. 93 – 130. In: Charaklis, W.G., Marshall, K.C. (eds.), *Biofilms*. Jon Wiley & Sons, New York.
- Cordón, O., Herrera, F., Peregrín, A. (1997) Applicability of the fuzzy operators in the design of fuzzy logic controllers. *Fuzzy sets and systems*. Vol. 86, 15 – 41
- Cord-Ruwish, R., Mercz, T.I., Hoh, C.-Y., Strong, G.E. (1997) Dissolved Hydrogen Concentration as an On-Line Control parameter for the Automated operation and Optimization of Anaerobic Digesters. *Biotechnology and Bioengineering*, Vol. 56, 626 – 634
- Costello, D.J., Greenfield, P.F., Lee, P.L. (1991) Dynamic Modelling of a Single-Stage High-Rate Anaerobic Reactor – I. Model Derivation. *Water Research*, Vol 25 (7) 847-858.
- de Beer, D., Stoodley, P., Lewandowsky, Z. (1997) Measurement of Local Diffusion Coefficients in Biofilms by Microinjection and Confocal Microscopy. *Biotechnology and Bioengineering*, Vol. 53, 151-158
- Dochain, D.; Perrier, M. (1996) Dynamical Modelling, Analysis, Monitoring and Control Design for Nonlinear Bioprocesses. *Advances in Biochemical Engineering Biotechnology*. Vol. 56; 147-197
- Estaben, M., Polit, M., Steyer, J.P. (1997) Fuzzy Control for an Anaerobic Digester. *Control Engineering Practice*. Vol. 98, 303 – 1310
- Ghaly, A. E.; Pyke, J. B. (1991) Amelioration of methane yield in cheese whey fermentation by Controlling the pH of the Methanogenic Stage. *Applied Biochemistry and Biotechnology*, Vol. 27 (3), 217 – 237
- Ghaly, A.E. (1996) *Bioresource Technology*. A comparative study of anaerobic digestion of acid cheese whey and dairy manure in a two stage reactor. Vol. 58, 61-72
- Grepmeier, M. (2002) Experimentelle Untersuchungen an einer zweistufigen fuzzy-geregelten Abwasserreinigungsanlage mit neuartigem Festbettmaterial (Experimental investigations using a two-stage fuzzy-controlled wastewater treatment plant with novel fixed bed material). Thesis TU Munich. In preparation.

- Guwy, A.J., Hawkes, F.R., Hawkes, D.L., Rozzi, A. G. (1997). Hydrogen production in a High Rate Fluidised Bed Anaerobic Digester. *Water Research*. Vol. 31 (6), 1291 - 1298
- Harper, S. R., Pohland, F. G. (1986) Recent developments in hydrogen management during anaerobic biological wastewater treatment. *Biotechnology and Bioengineering*. Vol. 28, 585 – 602
- Heijnen (1994) Thermodynamics of Microbial Growth and its Implications for Process Design. *Trends in Biotechnology*, Vol. 12, 483 – 492.
- Henze, M., Harremoes, P., Jansen, J.C., Arvin, E. (1995) *Wastewater Treatment – Biological and Chemical Processes*. Springer-Verlag, Berlin.
- Kalyuzhnyi, S.V.(1997) *Bioresource Technology. Batch Anaerobic Digestion of Glucose and its Mathematical Modeling. II. Description, Verification and Application of the Model*, Vol. 59 , 249-258
- Kalyuzhnyi, S.V., Davlyatshina, M.A. (1997) *Bioresource Technology. Batch Anaerobic Digestion of Glucose and its Mathematical Modeling. I. Kinetic Investigations*, Vol. 56 , 73-80
- Kampè de, Fériet J. (1982) Interpretation of Membership Functions of Fuzzy Sets in Terms of Plausibility and Belief, in *Fuzzy Information and Decision Process*, M.M. Gupta and E. Sanchez (editors). North-Holland, Amsterdam. 93 - 98
- Kettunen, R.H., Rintala, J.A. (1997) The effect of low temperature (5-29°C) and adaption on the methanogenic activity of biomass. *Appl. Microbiol. Biotechnol*, Vol 48, 570 - 576
- Kiely, G., Tayfur, G., Dolan, C., Tanji, K. (1997) Physical and Mathematical Modelling of Anaerobic Digestion of Organic Wastes. *Water Research*, Vol. 31 (3), 534-540
- Kiendl, H. (1997) *Fuzzy Control methodenorientiert*. Oldenburg Verlag, München. 338 pages.
- Kissl, J.C. (1986) Modeling Mass Transfer in Biological Wastewater Treatment Processes. *Water Science and Technology*, Vol.18, 35-45
- Kiupel, N. (1997) *Fuzzy-logic-basierte Fehlerdiagnose am Beispiel eines anaeroben Abwasserreinigungsprozesses*. VDI-Verlag, Düsseldorf.
- Koch, M, Kuhn, Th, Wernstedt, J. (1996) *Fuzzy Control. Optimale Nachbildungen und Entwurf Optimaler Entscheidungen*. Oldenburg. München.
- Kunze, U.R., Schwedt, G. (1996) *Grundlagen der qualitativen und quantitativen Analyse*. Thieme Verlag, Stuttgart, Germany.

- Kus, F. (1993) Kinetik des anaeroben Abbaus von Essig- und Propionsäure in Bioreaktoren mit immobilisierten Bakterien. Dissertation, Technische Universität Berlin
- Lide and Frederikse (1995) CRC Handbook of Chemistry and Physics, 76th Edition, D. R. Lide and H. P. R. Frederikse, ed(s)., CRC Press, Inc., Boca Raton, FL, 1995.
- Mann, H., Schiffelgen, H., Froriep, R. (1997) Einführung in die Regelungstechnik - anlage und digitale Regelung, Fuzzy-Regler, Regler-Realisierung, Software. Hanser-Verlag, München, Wien, 7. Auflage
- Mitchell, P. (1966) Chemiosmotic coupling in oxidative and photosynthetic phosphorylation. *Biological Reviews* 41, 445-502
- Mosey, F.E. (1983). Mathematical Modeling of the Anaerobic Digestion Process: Regulatory Mechanisms for the Formation of Short Chain Volatile Acids from Glucose. *Water Science and Technology* 15
- Müller, A., Marsili-Libelli, S., Aivasidis, A., Lloyd, T., Kroner, S., Wandrey, C. (1997) Fuzzy control of disturbances in a wastewater treatment process. *Water Research*. Vol 12, 3157-3167
- Murnleitner, E., Becker, T.M., Delgado, A. (2001) State Detection and Control of Overloads in the Anaerobic Wastewater Treatment Using Fuzzy Logic. *Water Research*. Accepted.
- Murnleitner, E., Kuba, T., van Loosdrecht, M.C.M. and Heijnen, J.J. (1997) An integrated metabolic model for the aerobic and denitrifying biological phosphorus removal. *Biotechnology and Bioengineering*. Volume 54 (5), 434-450
- Näser, K-H., Lempe, D., Regen, O. (1990) *Physikalische Chemie für Techniker und Ingenieure*. Dt. V. Grundstoffindustrie.
- Ndon, U. J., Dague, R. R. (1997) Effects of Temperature and Hydraulic Retention Time on Anaerobic Sequencing Batch Reactor Treatment of Low-Strength Wastewater. *Water Research* Vol. 31, No.10, pp. 2455-2466
- Olsson, G., Piani, G. (1993) *Steuern, Regeln, Automatisieren - Theorie und Praxis der Prozeßleittechnik*. Hanser-Verlag und Prentice-Hall International, Wien, London
- Parekh, M, Desai, M., Li, H., Rhinehart, R. R. (1994) In-line control of nonlinear pH neutralization based on fuzzy logic. *IEEE Transactions on Components, Packaging and Manufacturing Technology, Part A – Volume 17, No. 2, June 1994*

- Pauss, A., Guiot, S., Dochain, D., Perrier, M. (1993) Hydrogen as a key-parameter for the monitoring and control of methane producing processes. Proceedings Workshop on Modelling, Monitoring and Control of Wastewater Treatment Processes. Vol. 58, 2011 – 2017
- Pfeiffer, B.-M. (1995) Einsatz von Fuzzy-Logik in lernfähigen digitalen Regelsystemen. VDI Fortschrittberichte, Reihe 8 Nr. 500
VDI-Verlag, Düsseldorf
- Ramsay (1997) Modelling and Control of High Rate Anaerobic Wastewater Treatment Systems. PhD thesis. Chemical Engineering. The University of Queensland, Brisbane: 270
- Reichert, P. (1994) Concepts Underlying a Computer Program for the Simulation of Aquatic Systems. Schriftenreihe der EAWAG No. 7, Switzerland.
- Reid, R.C., Prausnitz, J.M., Poling, B.E. (1987) The Properties of Gases and Liquids. 4th Edition. McGraw-Hill, New York.
- Romli, M. (1993) Modelling and Verification of a Two-Stage High-Rate Anaerobic Wastewater Treatment System. PhD thesis. Chemical Engineering. The University of Queensland, St. Lucia: 206
- Sillen, L. G. and Martel, A. E. (1964) Stability Constants of Metal Ion Complexes. The Chemical Society, London.
- Snoeyink, V. L. and Jenkins, D. (1980) Water Chemistry. 3rd ed John Wiley and Sons, New York.
- Stumm, W. and Morgan, J.J. (1988). Aquatic Chemistry: An introduction emphasizing chemical equilibria in natural waters, 2nd ed, John Wiley and Sons, New York
- Tartakovsky, B., Guiot, S.R. (1997) Modeling and optimization in anaerobic bioconversion of complex substrates to acetic and butyric acids. Biotechnology and Bioengineering. Wiley. Vol. 54, 122 - 130
- Vavilin, V.A., Lokshina, L.Y. (1996). Modeling of volatile fatty acids degradation kinetics and evaluation of microorganism activity. Bioresource Technology 57 (1996), 69 - 80
- Whitmore, T.N., Lloyd, D., Jones, G., Williams, T.N. (1987) Hydrogen-dependent control of the continuous anaerobic digestion process. Applied Microbiology and Biotechnology. Vol. 26, 383 - 388
- Wolin, M. J. (1976) Interactions Between H₂-Producing and Methane-Producing Species. IN: Microbial production and utilisation of gases (H₂, CH₄, CO), Goltze, Göttingen, 141 – 150,

Xing, J., Criddle, C., Hickey, R. (1997). Effects of a long-term periodic substrate perturbation on an anaerobic community. *Water Research*. Vol. 31 (9), 2195 – 2204.

Zadeh, L(1965) Fuzzy Sets. *Information and Control*. Vol. 8, 338-353.

Zell, A. (1994) *Simulation Neuronaler Netze*. Addison-Wesley-Verlag, Bonn, 1994

Curriculum Vitae of Ernst Murnleitner

- 1967 Born on 25th January in Kufstein, Austria, as the eldest of three sons of Johanna and Erich Murnleitner. Mother tongue german.
- 1973 Primary school until 1982.
- 1982 Apprenticeship laboratory technician at Biochemie GmbH, Kundl, until 1986.
- 1984 Courses of anti radiation precaution and breathing protection as voluntary member of the fire brigade of Biochemie GmbH.
- 1986 Laboratory technician at Biochemie GmbH until 1990.
- 1987 Foundation-member of a computer club in Wörgl, Austria.
- 1987 Development of the shareware computer program "Mauspaint".
- 1987 Secondary school Handelsakademie in Wörgl, Austria, in evening courses, until 1991.
- 1991 Study of Food Science and Biotechnology at the University of Agriculture in Vienna, Austria, until 1996.
- 1991 Development of several computer programs in Basic, Modula-2, Pascal, C and C++, up to now.
- 1994 Study and Master thesis at the Technical University of Delft, the Netherlands, until 1995 (for 9 months). Author and Co-author of scientific publications:
 Murnleitner, E., Kuba, T., van Loosdrecht, M.C.M. and Heijnen, J.J. (1997) An integrated metabolic model for the aerobic and denitrifying biological phosphorus removal. *Biotechnology and Bioengineering*. Volume 54, Number 5, Pages 434-450
 Kuba, T., Murnleitner, E., van Loosdrecht, M.C.M. and Heijnen, J.J. (1996) A Metabolic model for the biological phosphorus removal by denitrifying organisms. *Biotechnology and Bioengineering*, 52, pp 685 - 695.
 Kuba, T., van Loosdrecht, M.C.M., Murnleitner, E. and Heijnen, J.J. (1997) Kinetics and stoichiometry in the biological phosphorus removal process with short cycle times. *Water Research*. Vol. 31, 4, 1997, p. 918-928.
- 1995 Internship at R&D Department at DSM Chemie Linz, Austria (2 months).
- 1996 Advanced course on microbiological physiology and fermentation technology at Delft University of Technology.
- 1996 Degree "Diplom-Ingenieur" at University of Agriculture in Vienna.
- 1996 Civil service at the Red Cross organisation in Wörgl and Kufstein as an ambulance man until 1997 (11 months).
- 1997 Doctoral thesis at Technical University of Munich, Germany, at the Chair of Fluid Mechanics and Process Automation, until 2001.
 Murnleitner, E., Becker, T., Delgado, A.: State Detection and Control of Overloads in the Anaerobic Wastewater Treatment using Fuzzy Logic. *Water Research* (2001), Vo. 36 (1), 201 - 211
 Optimisation and Validation of a Fuzzy-Based Closed-Loop Control Strategy Using a Dynamic Simulation Model. *Biotechnology and Bioengineering*. submitted.
- 1997 Network administrator at the Chair of Fluid Mechanics and Process Automation until 2001.
- 2000 Foundation of Awite Bioenergie, Grepmeier and Murnleitner GbR, in Langenbach, Germany.
- 2002 Degree "Dr.-Ing." at Technical University of Munich.